

2015

Variations in selenium concentrations by photochemical and temperature-controlled iron cycles

Kendi L. Waltemyer

Follow this and additional works at: <https://researchrepository.wvu.edu/etd>

Recommended Citation

Waltemyer, Kendi L., "Variations in selenium concentrations by photochemical and temperature-controlled iron cycles" (2015). *Graduate Theses, Dissertations, and Problem Reports*. 6893.
<https://researchrepository.wvu.edu/etd/6893>

This Thesis is protected by copyright and/or related rights. It has been brought to you by the The Research Repository @ WVU with permission from the rights-holder(s). You are free to use this Thesis in any way that is permitted by the copyright and related rights legislation that applies to your use. For other uses you must obtain permission from the rights-holder(s) directly, unless additional rights are indicated by a Creative Commons license in the record and/ or on the work itself. This Thesis has been accepted for inclusion in WVU Graduate Theses, Dissertations, and Problem Reports collection by an authorized administrator of The Research Repository @ WVU. For more information, please contact researchrepository@mail.wvu.edu.

**VARIATIONS IN SELENIUM CONCENTRATIONS BY PHOTOCHEMICAL AND
TEMPERATURE-CONTROLLED IRON CYCLES**

Kendi L. Waltemyer

**Thesis submitted
to the Eberly College of Arts and Sciences
at West Virginia University
in partial fulfillment of the requirements
for the degree of**

**Master of Science
in
Geology**

**Dorothy Vesper, Ph.D., Chair
Louis McDonald, Ph.D.
Helen Lang, Ph.D.**

Department of Geology and Geography

**Morgantown, West Virginia
2015**

Keywords: geochemistry, diel, cycles, iron, Fe, selenium, Se

Copyright 2015 Kendi L. Waltemyer

ABSTRACT

Variations in Selenium Concentrations by Photochemical and Temperature-Controlled Iron Cycles

Kendi L. Waltemyer

Selenium (Se) concentrations in natural waters may vary over a 24-hour (diel) period in response to temperature changes. Diel cycles of Se have not been reported in coal mine drainage (CMD) waters, and understanding the mechanisms of Se concentration variations in CMD is important for predicting Se fate and mobility. Iron (Fe) is often associated with CMD, and diel cycles of dissolved Fe species concentrations and/or the formation of Fe oxyhydroxide minerals may impact Se mobility. Experiments were conducted in a laboratory setting between July 2014 and April 2015 to determine if selenite (Se^{IV}) concentration changes could be detected in the same experiments with solid 2-line ferrihydrite (a synthesized Fe oxyhydroxide mineral) and dissolved Fe species concentration changes. Light and temperature controls were used to drive Fe species and Se^{IV} concentration changes. Each experiment differed in solution type (Fe-only, Se-only, or Fe-Se combined), length, temperature, and light conditions. Samples were collected and analyzed for Se^{IV} , total Se, Fe^{II} and total Fe. Se^{IV} concentration changes were found to be directly correlated with temperature in both Se-only and Fe-Se solutions. The cycles were more pronounced in the presence of 2-line ferrihydrite. Temperature-dependent sorption of Se^{IV} onto 2-line ferrihydrite was the likely cause of Se^{IV} cycles. Se^{IV} did not cycle with temperature in vessel solutions with pH values greater than 3, indicating that pH is a critical factor in Se^{IV} cycling. The experiments were completed at pH values around 3, underwent significant temperature changes ranging from 2.2°C to 36.5°C, and contained solid Fe oxyhydroxide (2-line ferrihydrite). These conditions are known to exist in some CMD waters, suggesting that Se^{IV} diel cycles may exist in these settings.

ACKNOWLEDGEMENTS

I would like to thank the faculty at WVU who have helped to further my education in the geosciences. A special thanks goes to my advisor, Dorothy Vesper; Ph.D., and my committee members, Louis McDonald; Ph.D. and Helen Lang; Ph.D., for their support and guidance both in and out of the classroom. I would also like to thank Cecil Slaughter from the Office of Surface Mining Reclamation and Enforcement (OSMRE) for providing funding for this project through the OSM-WV Acid Drainage Technology Initiative (ADTI) cooperative agreement. Special thanks also goes to Lisa Lohr, my “selenium buddy”, for spending countless hours working with me in the lab and always keeping a smile on my face. I would also like to thank Habib H. Bravo Ruiz, R. Christopher Nicholson, and Derek Weicht for their help with running the temperature control system for my experiments. Thanks also go to my parents and grandparents for always believing in me and supporting my academic goals. Lastly, a huge thank you goes to my fiancé, Derek Weicht, for his encouragement, love, and support throughout my graduate school career.

TABLE OF CONTENTS

1	INTRODUCTION	1
2	BACKGROUND.....	2
2.1	Se speciation in natural waters	2
2.2	Se diel cycles.....	2
2.3	Se sorption onto ferrihydrite	9
2.4	Ferrihydrite solubility.....	10
2.5	Fe diel cycles.....	11
2.5.1	Light cycles	11
2.5.2	Temperature cycles	14
3	PURPOSE AND OBJECTIVES	15
4	METHODS.....	16
4.1	Experimental overview and layout	16
4.2	Materials	20
4.2.1	2-line Ferrihydrite	20
4.2.2	Solutions	22
4.3	Data logging and meter measurements.....	22
4.4	Sampling and analysis.....	25
4.4.1	Fe sampling and analysis.....	25
4.4.2	Se sampling and analysis.....	27
4.5	Data analysis	33
4.6	Quality Control Assessment	33
4.6.1	Filtering experiment for Fe analysis	34
4.6.2	Evaporation experiment	38
4.6.3	Se ^{IV} loss from sorption to glass	39
4.6.4	Se ^{IV} desorption from glass.....	39
5	RESULTS.....	42
5.1	Cycle 1: 7/22-23/2014.....	42
5.2	Cycle 2: 10/17-18/2014.....	46
5.3	Cycle 3: 10/25/2014.....	50
5.4	Cycle 4: 12/09/2014.....	58
5.5	Cycle 5: 1/29/2015.....	58
5.6	Cycle 6: 2/28/2015.....	67
5.7	Cycle 7: 4/26/2015.....	75
6	DISCUSSION.....	82
6.1	Comparison of similar cycles	82
6.1.1	Fe-only cycles	82
6.1.2	Se-only cycles	84
6.1.3	Fe-Se combined cycles.....	84
6.2	Evaluation of mechanisms	87
6.2.1	Light.....	87
6.2.2	Temperature	88
6.2.3	Se sorption onto 2-line ferrihydrite	89
6.2.4	pH	90
6.2.5	Oxidation-reduction reactions	91

7	CONCLUSIONS.....	94
8	FUTURE WORK.....	95
	REFERENCES.....	96
	APPENDICES	99

List of Tables

Table 4-1. Experiment vessel solutions.....	23
Table 4-2. Measured parameters and instrumentation.....	24
Table 4-3. Ferrozine method sample to solution ratios for Fe ^{II} and Fe(total) analysis	28
Table 4-4. Ratios of sample, DI water, and 6 M HCl prepared for Se ^{IV} HG-ICP-OES analysis.....	29
Table 4-5. HG-ICP-OES Se ^{IV} analysis parameters	30
Table 4-6. Filtering experiment for Fe analysis: A comparison of unfiltered and filtered samples	35
Table 4-7. Evaporation experiment K ⁺ results	40
Table 5-1. Summary of light and temperature cycle experiments	43
Table 5-2. Cycle 1 (7/22-23/2014) parameter variability	45
Table 5-3. Cycle 2 (10/17-18/2014) parameter variability	49
Table 5-4. Cycle 3 (10/25/2014) parameter variability	53
Table 5-5. Se ^{IV} versus temperature linear regression results	55
Table 5-6. Conditional Enthalpies of Sorption for Cycle 3	57
Table 5-7. Cycle 4 (12/9/2014) parameter variability	61
Table 5-8. Conditional Enthalpies of Sorption for Cycle 4	64
Table 5-9. Cycle 5 (1/29/2015) parameter variability	68
Table 5-10. Cycle 6 (2/28/2015) parameter variability	71
Table 5-11. Conditional Enthalpies of Sorption for Cycle 6	74
Table 5-12. Cycle 7 (4/26/2015) parameter variability	78
Table 5-13. Conditional Enthalpies of Sorption for Cycle 7	81
Table 6-1. Summary of cycles by group (Fe-only, Se-only, and Fe-Se combined)	83
Table 6-2. Comparison of Se-only and Fe-Se cycles	85

List of Figures

Figure 2-1.	Redox potential-pH diagram for a dissolved Se species concentration of 10^{-6} M at 1 atm and 25 °C. Figure modified from Reddy and DeLaune, 2008.	3
Figure 2-2.	Selenite ion speciation plot, where Se^{IV} concentration equals 3.80×10^{-6} M (300 µg/L), temperature equals 25°C, and ionic strength equals 0.1 M. Figure constructed using Visual MINTEQ, version 3.1 (Allison et al., 1991).	4
Figure 2-3.	Selenate ion speciation plot, where Se^{VI} concentration equals 3.80×10^{-6} M (300 µg/L), temperature equals 25°C, and ionic strength equals 0.1 M. Figure constructed using Visual MINTEQ, version 3.1 (Allison et al., 1991).	5
Figure 2-4.	Summary of Dicataldo et al. (2011) results for Se diel cycles in a freshwater wetland of the Great Salt Lake, Utah. The gray shaded areas indicate nighttime hours (dark conditions). Figure modified from Dicataldo et al., 2011.	6
Figure 2-5.	Summary of Carling et al. (2011) results for Se diel cycles in two freshwater wetlands (ADC-1 and ADC-2) of the Great Salt Lake, Utah. The gray shaded areas indicate nighttime hours (dark conditions). Figure modified from Carling et al., 2011.	8
Figure 2-6.	(a) Solubility curves for 0.5 g of ferrihydrite, $\text{Fe}(\text{OH})_3$, at 10 °C, 25°C, and 35 °C showing Fe(total) concentrations and (b) Solubility diagram for 0.5 g of ferrihydrite at 25°C showing all Fe species, where ionic strength equals 0.1 M. Figure constructed using Visual MINTEQ, version 3.1 (Allison et al., 1991).	12
Figure 2-7.	Redox potential-pH diagram for the Fe-O-H ₂ O system for a dissolved Fe species concentration of 10^{-6} M at 1 atm and 25 °C. Figure modified from Drever, 1997.	13
Figure 4-1.	Schematic of temperature control system. Arrows indicate water flow direction.	17
Figure 4-2.	Photograph of completed temperature and light control systems. RT is room temperature. V1, V2, V3, and V4 are the vessel numbers.	18
Figure 4-3.	Schematic of light control system.	19
Figure 4-4.	Synthesis of 2-line ferrihydrite. (a) 40 grams $\text{Fe}(\text{NO}_3)_3 \cdot 9\text{H}_2\text{O}$ dissolved in 500 mL DI water; (b) 300 mL KOH added to solution; (c) Solid solution soaking in dialysis membrane tubing; (d) Solid drying in crucible; (e) Dried 2-line ferrihydrite crushed with mortar and pestle; and (f) 2-line ferrihydrite sieved through a 125 µm sieve.	21
Figure 4-5.	Ferrozine method calibration samples for Fe^{II} analysis. Fe^{II} concentrations decrease from left to right as indicated by the different shades of purple.	26
Figure 4-6.	Multimode sample introduction system (MSIS) using vapor generation mode (modified from Marathon Scientific, 2007).	31
Figure 4-7.	Photograph of the filtering experiment for Fe analysis. Vessels are numbered 1 through 6 from left to right. Vessels 1 and 6 are beakers, and vessels 2 through 5 are jacketed reaction vessels.	36
Figure 4-8.	Results of the filtering experiment for Fe analysis showing the comparison between unfiltered and filtered samples analyzed for Fe^{II} and Fe(total). Standard deviations are represented by error bars for six replicate samples.	37

Figure 5-1.	Cycle 1 (7/22-23/2014) results. A single vessel was set up for this experiment containing Fe-only solution. The straight, solid line indicates the MDL for Fe ^{II} analysis (0.02 mg/L Fe ^{II}) on the HACH DR2800 Spectrophotometer. The gray shaded areas indicate when the light was turned off (dark conditions).....	44
Figure 5-2.	Cycle 2 (10/17-18/2014) results with all vessels (V1-V4) graphed together. All vessels contained Fe-only solutions. The solid red lines indicate the MDL for Fe ^{II} analysis (0.02 mg/L Fe ^{II}) on the HACH DR2800 Spectrophotometer. Fe(total) is equal to the sum of Fe ^{II} and Fe ^{III} species. Standard deviations are represented by error bars for triplicate samples. The gray shaded areas indicate when the light was turned off (dark conditions).	47
Figure 5-3.	Cycle 2 (10/17-18/2014) results with all vessels (V1-V4) graphed separately. All vessels contained Fe-only solutions. The solid red lines indicate the MDL for Fe ^{II} analysis (0.02 mg/L Fe ^{II}) on the HACH DR2800 Spectrophotometer. Fe(total) is equal to the sum of Fe ^{II} and Fe ^{III} species. Standard deviations are represented by error bars for triplicate samples. The gray shaded areas indicate when the light was turned off (dark conditions). Note that the pH was adjusted in Vessel 3 during hour 13.	48
Figure 5-4.	Cycle 3 (10/25/2014) results with all vessels (V1-V4) graphed together. All vessels contained Fe-Se solutions. The solid red line indicates the MDL for Fe ^{II} analysis (0.02 mg/L Fe ^{II}) on the HACH DR2800 Spectrophotometer. Fe(total) is equal to the sum of Fe ^{II} and Fe ^{III} species. Standard deviations are represented by error bars for triplicate samples. The gray shaded area indicates that the light was turned off for this experiment (dark conditions).....	51
Figure 5-5.	Cycle 3 (10/25/2014) results with all vessels (V1-V4) graphed separately. All vessels contained Fe-Se solutions. The solid red lines indicate the MDL for Fe ^{II} analysis (0.02 mg/L Fe ^{II}) on the HACH DR2800 Spectrophotometer. Fe(total) is equal to the sum of Fe ^{II} and Fe ^{III} species. Standard deviations are represented by error bars for triplicate samples. The gray shaded area indicates that the light was turned off for this experiment (dark conditions).....	52
Figure 5-6.	Cycle 3 (10/25/2014) relationship between Se ^{IV} concentrations and temperature. The start and end of each cycle is labeled next to the corresponding data symbol (red square). Red squares represent the temperature increasing series, whereas the blue circles represent the temperature decreasing series. Solid red lines are linear regression lines for the temperature increasing series. Solid blue lines are linear regression lines for the temperature decreasing series. The black dashed lines indicate the order in which samples were collected over time. The gray shaded area indicates that the light was turned off for this experiment (dark conditions).....	54
Figure 5-7.	Enthalpy of sorption plot for Cycle 3 (10/25/2014). Increasing temperature series (solid symbols and lines) and decreasing temperature series (open symbols and dashed lines) data are plotted separately for each vessel. Vessel numbers are labelled V1 through V4.	56
Figure 5-8.	Cycle 4 (12/09/2014) results with all vessels (V1-V4) graphed together. Vessels 1 and 2 contained Fe-only solutions, whereas Vessels 3 and 4 contained Fe-Se solutions. The solid blue lines indicate the MDL for Se ^{IV} analysis (5 µg/L Se ^{IV}) on the Perkin Elmer Optima 2100 DV ICP-OES. Standard deviations are represented by error bars for triplicate samples.	59

Figure 5-9.	Cycle 4 (12/09/2014) results with all vessels (V1-V4) graphed separately. Vessels 1 and 2 contained Fe-only solutions, whereas Vessels 3 and 4 contained Fe-Se solutions. The solid blue lines indicate the MDL for Se^{IV} analysis ($5 \mu\text{g/L Se}^{\text{IV}}$) on the Perkin Elmer Optima 2100 DV ICP-OES. Standard deviations are represented by error bars for triplicate samples.	60
Figure 5-10.	Cycle 4 (12/9/2014) relationship between Se^{IV} concentrations and temperature. The start and end of each cycle is labeled next to the corresponding data symbol (red square). Red squares represent the first temperature increasing series, blue circles represent the temperature decreasing series, and green triangles represent the second temperature increasing series. Solid red lines are linear regression lines for the first temperature increasing series. Solid blue lines are linear regression lines for the temperature decreasing series. The black dashed lines indicate the order in which samples were collected over time.	62
Figure 5-11.	Enthalpy of sorption plot for Cycle 4 (12/9/2014). The increasing temperature series 1 (solid symbols and solid lines), decreasing temperature series (open symbols and dashed lines), and increasing temperature series 2 (patterned symbols and solid lines) data are plotted separately for each vessel. Vessel numbers are labelled V3 and V4.	63
Figure 5-12.	Cycle 5 (1/29/2015) results with all vessels (V1-V4) graphed together. All vessels contained Se-only solutions. Standard deviations are represented by error bars for triplicate samples.	65
Figure 5-13.	Cycle 5 (1/29/2015) results with all vessels (V1-V4) graphed separately. All vessels contained Se-only solutions. Standard deviations are represented by error bars for triplicate samples.	66
Figure 5-14.	Cycle 6 (2/28/2015) results with all vessels (V1-V4) graphed together. Vessels 1 and 2 contained Fe-only solutions, whereas Vessels 3 and 4 contained Fe-Se solutions. The solid red line indicates the MDL for Fe^{II} analysis ($0.02 \text{ mg/L Fe}^{\text{II}}$) on the HACH DR2800 Spectrophotometer. The solid blue line indicates the MDL for Se^{IV} analysis ($5 \mu\text{g/L Se}^{\text{IV}}$) on the Perkin Elmer Optima 2100 DV ICP-OES. Standard deviations are represented by error bars for triplicate samples. The gray shaded area indicates that the light was turned off for this experiment (dark conditions).	69
Figure 5-15.	Cycle 6 (2/28/2015) results with all vessels (V1-V4) graphed separately. Vessels 1 and 2 contained Fe-only solutions, whereas Vessels 3 and 4 contained Fe-Se solutions. The solid red lines indicate the MDL for Fe^{II} analysis ($0.02 \text{ mg/L Fe}^{\text{II}}$) on the HACH DR2800 Spectrophotometer. The solid blue lines indicate the MDL for Se^{IV} analysis ($5 \mu\text{g/L Se}^{\text{IV}}$) on the Perkin Elmer Optima 2100 DV ICP-OES. Standard deviations are represented by error bars for triplicate samples. The gray shaded area indicates that the light was turned off for this experiment (dark conditions).	70

Figure 5-16.	Cycle 6 (2/28/2015) relationship between Se^{IV} concentrations and temperature. The start and end of each cycle is labeled next to the corresponding data symbol (red square). Red squares represent the first temperature increasing series, blue circles represent the temperature decreasing series, and green triangles represent the second temperature increasing series. Solid red lines are linear regression lines for the first temperature increasing series. Solid blue lines are linear regression lines for the temperature decreasing series. The black dashed lines indicate the order in which samples were collected over time. The gray shaded area indicates that the light was turned off for this experiment (dark conditions).....	72
Figure 5-17.	Enthalpy of sorption plot for Cycle 6 (2/28/2015). The increasing temperature series 1 (solid symbols and solid lines), decreasing temperature series (open symbols and dashed lines), and increasing temperature series 2 (patterned symbols and solid lines) data are plotted separately for each vessel. Vessel numbers are labelled V3 and V4.....	73
Figure 5-18.	Cycle 7 (4/26/2015) results with all vessels (V1-V4) graphed together. All vessels contained Se-only solutions. Standard deviations are represented by error bars for triplicate samples.....	76
Figure 5-19.	Cycle 7 (4/26/2015) results with all vessels (V1-V4) graphed separately. All vessels contained Se-only solutions. Standard deviations are represented by error bars for triplicate samples.....	77
Figure 5-20.	Cycle 7 (4/26/2015) relationship between Se^{IV} concentrations and temperature. The start and end of each cycle is labeled next to the corresponding data symbol (red square). Red squares represent the first temperature increasing series, blue circles represent the temperature decreasing series, and green triangles represent the second temperature increasing series. Solid red lines are linear regression lines for the first temperature increasing series. Solid blue lines are linear regression lines for the temperature decreasing series. Solid green lines are linear regression lines for the second temperature increasing series. The black dashed lines indicate the order in which samples were collected over time.	79
Figure 5-21.	Enthalpy of sorption plot for Cycle 7 (4/26/2015). Increasing temperature (solid symbols and lines) and decreasing temperature (open symbols and dashed lines) data are plotted separately for each vessel. Vessel numbers are labelled V1 through V4.	80
Figure 6-1.	Gibbs Free Energy (ΔG_R) calculated using thermodynamic data from Stumm and Morgan (1996) for $[\text{Se}^{\text{IV}}] = [\text{Se}^{\text{VI}}] = 3.8 \times 10^{-6} \text{ M}$ and $[\text{Fe}^{\text{III}}] = [\text{Fe}^{\text{II}}] = 9 \times 10^{-6} \text{ M}$. Activity-concentration corrections not included. Modified from the final OSMRE report (Vesper et al., 2015).	93

List of Appendices

Appendix A. X-ray diffraction (XRD) results.....	100
Appendix B. Fe Colloid Experiment Data	102
Appendix C. Diel Cycle Data	103
Appendix C-1. Cycle 1 (7/22/2014) Data.....	103
Appendix C-2. Cycle 2 (10/17-18/2014) Data	104
Appendix C-3. Cycle 3 (10/25/2014) Data.....	110
Appendix C-4. Cycle 4 (12/9/2014) Data.....	113
Appendix C-5. Cycle 5 (1/29/2015) Data.....	118
Appendix C-6. Cycle 6 (2/28/2015) Data.....	120
Appendix C-7. Cycle 7 (4/26/2015) Data.....	124

List of Acronyms and Abbreviations

CMD	Coal mine drainage
DI water	Deionized water
HFO	Hydrous ferrous oxides
HG	Hydride Generation
HX	Hydroxylamine hydrochloride
ICP-OES	Inductively Coupled Plasma – Optical Emission Spectroscopy
LOD	Limit of detection
MDL	Method detection limit
MSIS	Multimode Sample Introduction System
pH_{PZC}	Point of zero charge
RSD	Relative standard deviation
RT	Room temperature
USEPA	United States Environmental Protection Agency
XRD	X-ray diffraction
ΔG_R	Gibbs free energy of reaction
ΔH_{ads}	Conditional enthalpy of sorption

List of Chemical Species

Fe^{II}	Ferrous iron, Fe in the +II oxidation state, including both dissolved and colloidal species unless specified otherwise in text.
Fe^{III}	Ferric iron, Fe in the +III oxidation state, including both dissolved and colloidal species unless specified otherwise in text.
Fe(total)	Total iron, including both dissolved and colloidal Fe ^{II} and Fe ^{III} species unless specified otherwise in text.
Se^{IV}	Selenite, Se in the +IV oxidation state, including protonated and deprotonated Se ^{IV} species (H ₂ Se ^{IV} O ₃ , HSe ^{IV} O ₃ ⁻ , and Se ^{IV} O ₃ ⁻²)
Se^{VI}	Selenate, Se in the +VI oxidation state, including protonated and deprotonated Se ^{VI} species (HSe ^{VI} O ₄ ⁻ or Se ^{VI} O ₄ ⁻²)
Se(total)	Total dissolved selenium, including both Se ^{IV} and Se ^{VI} species

1 INTRODUCTION

Selenium (Se) is a naturally occurring element found in the Earth's crust. Leaching of Se into the natural environment occurs from anthropogenic processes like coal mining, the combustion of coal, and the use of Se-enriched agricultural products (Lenz and Lens, 2009). High concentrations of Se are often reported in coal mine drainage (CMD) and may be present at levels above the United States Environmental Protection Agency (USEPA) stream water standard of 5 $\mu\text{g/L}$ (2013). Compared to other rock types, coal can contain up to 300 times more Se (Coleman et al., 1993).

Recent research has demonstrated that Se concentrations in natural waters may vary over a 24-hour (diel) period in response to light and temperature changes (Carling et al., 2011; Dicataldo et al., 2011; Nimick et al., 2011). Understanding the mechanisms of variations in Se concentrations is important for predicting the mobility of Se in the natural environment. Se mobility may be influenced by the presence of other dissolved species and/or mineral formation and dissolution. For example, iron (Fe) is often associated with CMD, and dissolved Fe species and/or the formation of Fe oxyhydroxide minerals may impact Se mobility. Fe associated with CMD is commonly released by the dissolution of pyrite (FeS_2) (Younger, 2002), and Fe concentrations are known to cycle over a diel period. A few processes that control the diel cycling of Fe include mineral dissolution and formation, sorption processes, changes in pH, changes in redox state, photochemical reactions, photosynthesis, microbial-mediated reactions, and variations in stream flow (Gammons et al., 2005a; Gammons et al., 2005b; Kimball et al., 1992; McKnight et al., 2001; McKnight et al., 1988; Nimick, 2003). The presence of Fe minerals and the processes that control the diel cycling of dissolved Fe species may directly impact Se concentrations and cycling. It is well established that selenite (Se^{IV}) and selenate (Se^{VI}), the two more oxidized forms of Se, sorb to Fe^{III} oxides and hydroxides, such as hematite, goethite, and ferrihydrite (Balistrieri and Chao, 1987; Duc et al., 2006; Parida et al., 1997; Rovira et al., 2008). However, diel fluctuations in Se concentrations related to sorption or the relationship between Se concentration variations and Fe diel cycles has not been studied extensively.

2 BACKGROUND

2.1 Se speciation in natural waters

Four different oxidation states of Se exist: selenide (Se^{II}), elemental Se (Se^0), selenite (Se^{IV}), and selenate (Se^{VI}) (Balistreri and Chao, 1987). Under oxidizing conditions, Se forms oxyanions in water. $\text{HSe}^{\text{IV}}\text{O}_3^-$ and $\text{Se}^{\text{VI}}\text{O}_4^{2-}$ are the thermodynamically favored Se species under oxidizing conditions and in neutral pH ranges. The kinetics of Se^{IV} to Se^{VI} oxidation are very slow and are not favorable for Se^{IV} to Se^{VI} conversion (Torres et al., 2011). Therefore, Se^{IV} , in the form of $\text{H}_2\text{Se}^{\text{IV}}\text{O}_3$ is the dominant Se species in natural systems at pH values less than 2.62, and $\text{HSe}^{\text{IV}}\text{O}_3^-$, is the most dominant Se species between pH values of 2.62 and 8.32 (Figures 2-1 and 2-2) (CRC Handbook of Chemistry and Physics, 2003). The biological toxicity of Se^{IV} is greater than that of Se^{VI} , and in natural waters, Se^{VI} tends to be the dominant Se species in highly oxidizing conditions and neutral pH ranges (Das et al., 2013) (Figures 2-1 and 2-3).

The pH of the solution is critical for Se^{IV} and Se^{VI} acid protonation and deprotonation (Figures 2-1, 2-2, and 2-3). The following dissociation reactions may occur for Se^{IV} (Eq. 1 and 2) and Se^{VI} (Eq. 3) acids (CRC Handbook of Chemistry and Physics, 2003):



2.2 Se diel cycles

Dicataldo et al. (2011) reported diel cycles of Se during three sampling events (September 2005, May 2006, and August 2007) in a freshwater wetland of the Great Salt Lake in Utah (Figure 2-4). $\text{Se}(\text{total})$ (the sum of all dissolved Se species) concentrations displayed a different diel pattern for each sampling event. In September 2005, filtered $\text{Se}(\text{total})$ concentrations increased at night and decreased during the day, ranging from 0.9 to 1.3 $\mu\text{g/L}$. In May 2006, filtered $\text{Se}(\text{total})$ and unfiltered $\text{Se}(\text{total})$ concentrations had the opposite signal, decreasing at night and increasing during the day, with $\text{Se}(\text{total})$ concentrations ranging from

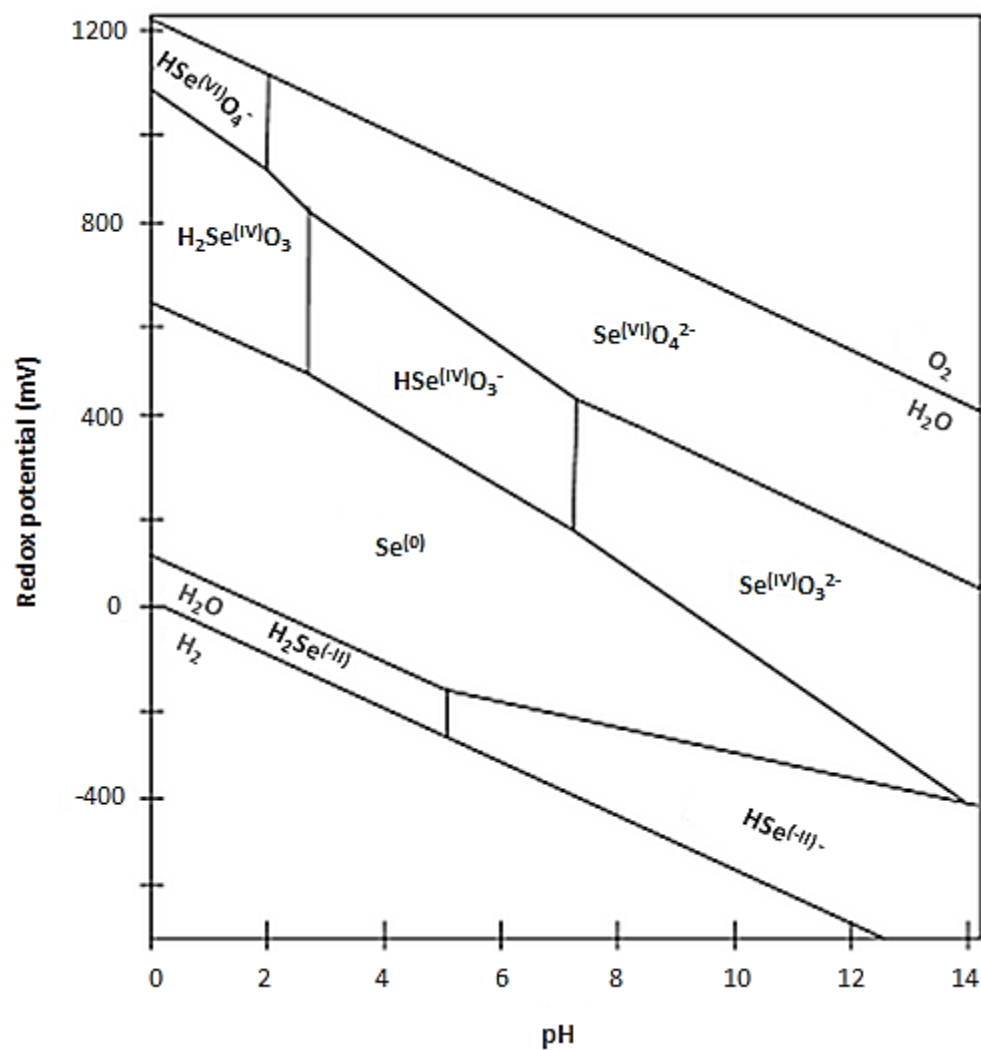


Figure 2-1. Redox potential-pH diagram for a dissolved Se species concentration of 10^{-6} M at 1 atm and 25 °C. Figure modified from Reddy and DeLaune, 2008.

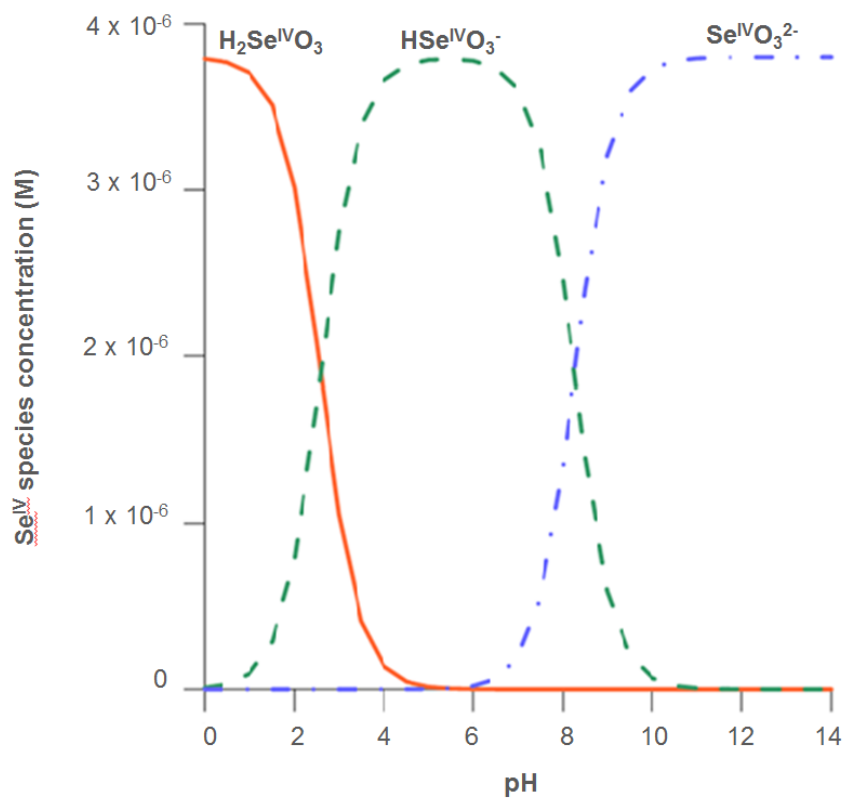


Figure 2-2. Selenite ion speciation plot, where Se^{IV} concentration equals 3.80×10^{-6} M ($300 \mu\text{g/L}$), temperature equals 25°C , and ionic strength equals 0.1 M. Figure constructed using Visual MINTEQ, version 3.1 (Allison et al., 1991).

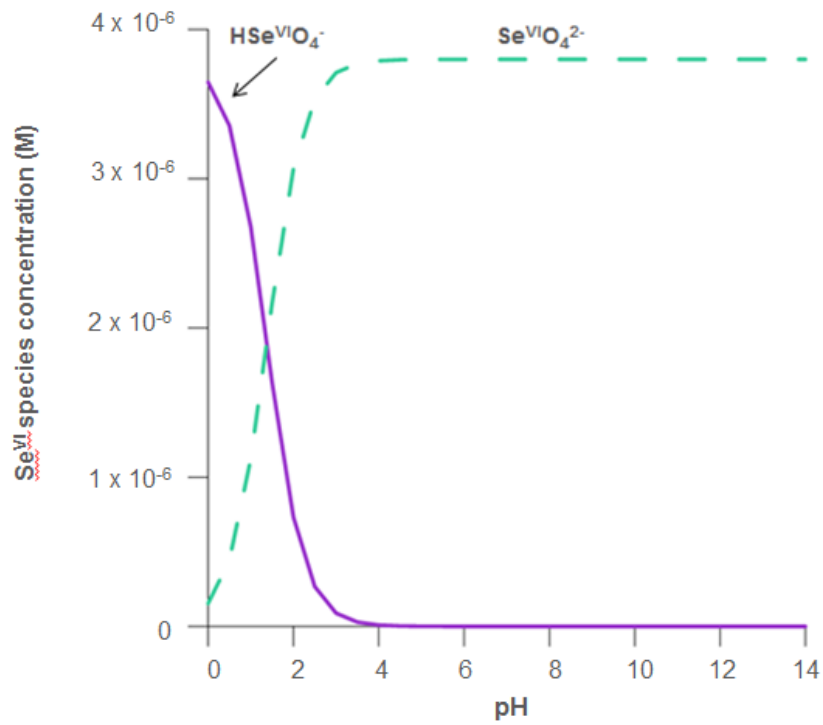


Figure 2-3. Selenate ion speciation plot, where Se^{VI} concentration equals 3.80×10^{-6} M (300 $\mu\text{g/L}$), temperature equals 25°C, and ionic strength equals 0.1 M. Figure constructed using Visual MINTEQ, version 3.1 (Allison et al., 1991).

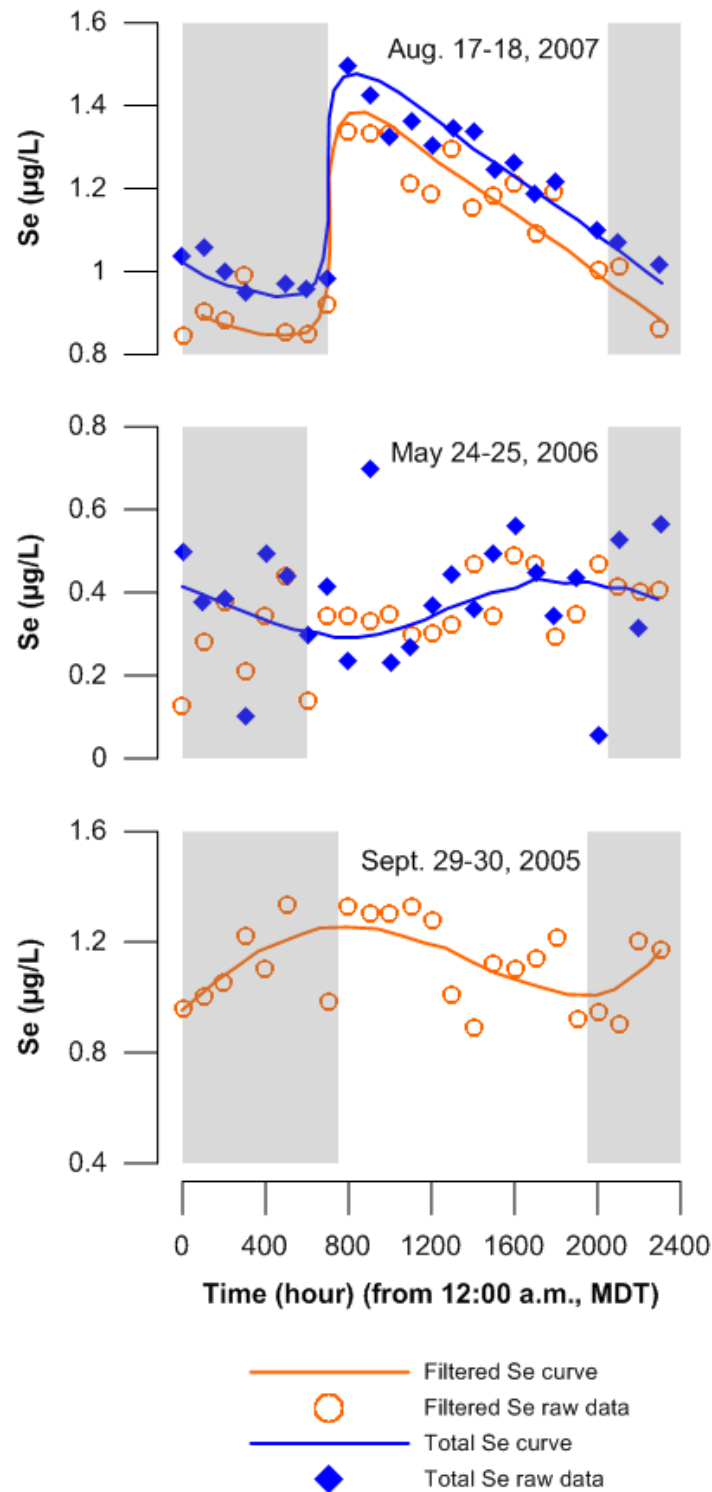


Figure 2-4. Summary of Dicaldo et al. (2011) results for Se diel cycles in a freshwater wetland of the Great Salt Lake, Utah. The gray shaded areas indicate nighttime hours (dark conditions). Figure modified from Dicaldo et al., 2011.

0.1 to 0.7 $\mu\text{g/L}$. Dicataldo et al.'s August 2007 sampling event resulted in maximum filtered Se(total) and unfiltered Se(total) concentrations at sunrise and decreasing concentrations throughout the remainder of the day and night, ranging from 0.7 to 1.5 $\mu\text{g/L}$. They found that Se(total) cycled in phase with pH, dissolved oxygen, and water temperature. It was hypothesized that the variation in Se(total) concentrations could have occurred due to Se species sorption onto metal oxyhydroxides. The sorption and desorption of Se species was likely controlled by changes in pH and redox conditions caused by photosynthesis.

Carling et al. (2011) reported diel cycles of Se(total) in two freshwater wetlands of the Great Salt Lake (Figure 2-5). They hypothesized that filtered Se(total) concentrations cycled due to pH-controlled sorption onto metal oxides during nighttime hours. The Se(total) concentrations increased during the day and decreased at night which was positively correlated with dissolved oxygen and temperature changes. In August 2008, Se(total) concentrations ranged from 1.2 to 1.7 $\mu\text{g/L}$ in both wetlands. In September 2009, the Se(total) concentrations ranged from 0.7 to 1.0 $\mu\text{g/L}$ in both wetlands. Diel cycles of Se have not been reported outside the wetland studies of the Great Salt Lake, Utah.

Although Se cycles have not been studied extensively, diel cycles of arsenic (As), another element that forms oxyanions in water, have been reported. Nimick et al. (1998) reported pH-controlled diel cycles of filtered As(total) (dissolved or particulate $<0.1\ \mu\text{m}$ in diameter, including both As^{III} and As^{V} species) at three of five sampling sites along the Madison and Missouri Rivers. Concentrations of As(total) increased as pH values increased, and decreased with decreasing pH. The As(total) concentrations cycled in the opposite phase of the cations in this study. The pH at their sampling sites ranged from 7.2 to 9.0, and speciation analysis indicated that As^{V} was the dominant species. The researchers concluded that As diel cycles were controlled by pH-dependent sorption onto hydroxide coatings and desorption from hydroxide coatings in river bed sediments. Additionally, for their sites that did not display an As diel cycle, they concluded the pH values were not high enough for cycling to occur. As pH decreases, the sorption of As oxyanions, such as arsenite ($\text{As}^{\text{III}}\text{O}_3^{3-}$) and arsenate ($\text{As}^{\text{V}}\text{O}_4^{3-}$), onto hydroxide coatings is more likely. Fuller and Davis (1989) and Nimick et al. (2005) also found that filtered As(total) concentrations cycled in phase with pH. The As cycle patterns during those studies were similar to those reported by Nimick et al. (1998).

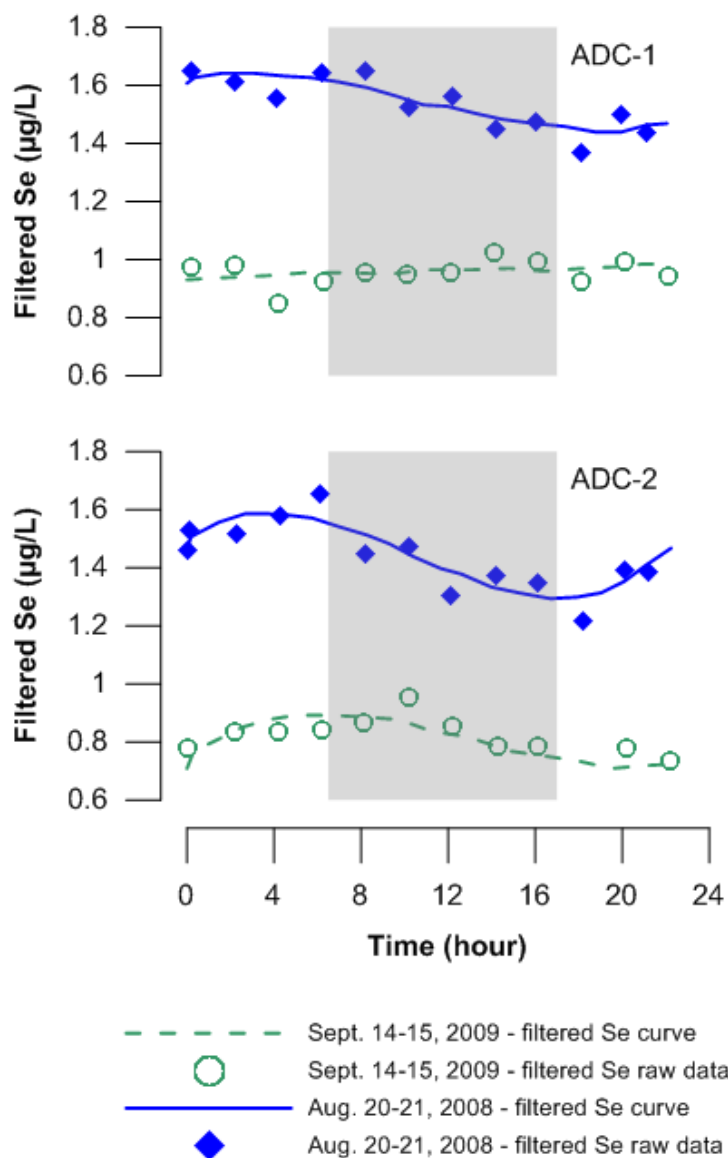


Figure 2-5. Summary of Carling et al. (2011) results for Se diel cycles in two freshwater wetlands (ADC-1 and ADC-2) of the Great Salt Lake, Utah. The gray shaded areas indicate nighttime hours (dark conditions). Figure modified from Carling et al., 2011.

2.3 Se sorption onto ferrihydrite

Ferrihydrite ($\text{Fe}(\text{OH})_3$) is a Fe^{III} hydroxide mineral with a large surface area ($>200 \text{ m}^2 \text{ g}^{-1}$) and a high affinity for sorption of Se^{IV} (Parida et al., 1997; Zhao et al., 1994). Se^{IV} is known to sorb more strongly to Fe oxide and oxyhydroxide surfaces than Se^{VI} , and sorption studies have concluded that ferrihydrite is the best Fe oxide/hydroxide for Se sorption under oxic and acidic conditions (Das et al., 2013). Se^{IV} sorption onto ferrihydrite is known to increase with decreasing temperature and pH (Balistrieri and Chao, 1990; Parida et al., 1997). Parida et al. (1997) also found that Se^{IV} sorption onto ferrihydrite reached equilibrium within two hours under various pH (3.5 to 9.5) and temperature conditions. They also concluded that the surface of ferrihydrite is heterogeneous based on calculated distribution coefficient (K_D) values from sorption experiments. At a pH of 3, the K_D increased as the Se^{IV} (adsorbent) concentration increased. Sorption of Se^{IV} can occur via the formation of two types of surface complexes: $\equiv\text{SeO}_3^-$ and $\equiv\text{HSeO}_3$, where \equiv represents the surface. The first is the formation of $\equiv\text{OH}_2^+ - \text{SeO}_3^{2-}$ and $\equiv\text{OH}_2^+ - \text{HSeO}_3^-$ outer sphere complexes, which are produced by the electrostatic attraction between the Se^{IV} aqueous species and surface hydroxyl groups. The second type of surface complex is an inner sphere complex resulting from the replacement of a water molecule with a Se^{IV} aqueous species on an active surface site resulting in $\equiv\text{SeO}_3^-$ or $\equiv\text{HSeO}_3^0$. Se^{IV} can also adsorb to ferrihydrite at pH values greater than the zero point of charge (pH_{PZC}), which is possible when Se^{IV} and ferrihydrite interactions are able to exceed electrostatic forces (Parida et al., 1997). Se^{VI} is known to sorb onto ferrihydrite as both monodentate and bidentate inner-sphere complexes (Das et al., 2013). Manceau and Charlet (1994) found that Se^{VI} sorbs to ferrihydrite via an inner-sphere binuclear complex in pH ranges of 3.5 to 6.7 whereas Se^{IV} sorbs via an inner-sphere bidentate complex at a pH of 3. Many factors may affect the sorption of Se species onto ferrihydrite, including solution ionic strength, pH, temperature, surface loading, Se species present, and timing (Sparks, 2003).

The conditional enthalpy for trace metal adsorption onto hydrous ferric oxides (HFO) can be calculated when temperatures and dissolved trace metal concentrations are known over time. Conditional enthalpies of adsorption (ΔH_{ads}) can be calculated using the following equation (Gammons et al., 2005b):

$$\Delta H_{ads} = \frac{2.303R \log(\frac{C_2}{C_1})}{(\frac{1}{T_2} - \frac{1}{T_1})} \quad [\text{Eq. 4}]$$

where R is the ideal gas constant, C_1 and C_2 are the dissolved trace metal molar concentrations at temperatures T_1 and T_2 (Kelvin). For a set of concentration and temperature data, the ΔH_{ads} can be calculated by plotting $1/T$ versus $\log C$, where T is temperature in Kelvin and C is the dissolved trace metal concentration. The slope of the line is then multiplied by 2.303R to get the ΔH_{ads} value (Gammons et al., 2005b):

$$\log C = \frac{\Delta H_{ads}}{2.303R} \left(\frac{1}{T}\right) + b \quad [\text{Eq. 5}]$$

This calculation assumes that a single trace metal is present in solution at a constant concentration, the sorbent concentration remains constant, and changes in dissolved trace metal concentrations are only due to adsorption/desorption with temperature. Machesky (1990) used a chemical modeling approach to calculate enthalpy of sorption values of Se^{IV} (specifically, the HSeO_3^- species) onto goethite. The resulting ΔH_{ads} values ranged from -82 kJ/mol to -22 kJ/mol. ΔH_{ads} values for Se^{IV} sorption onto HFO have not been reported in natural waters.

Many trace metals are present as cations in natural waters, and exhibit different sorption behavior than Se which forms an oxyanion. Laboratory studies suggest that adsorption of trace metal anions increases with decreasing temperature (Nimick et al., 2003); therefore, resulting in negative ΔH_{ads} values. Nimick et al. (2003) found that As adsorption increases with decreasing temperature. Since As forms oxyanions in water, it is likely that Se sorption will reflect similar sorption behavior in response to temperature changes.

2.4 Ferrihydrite solubility

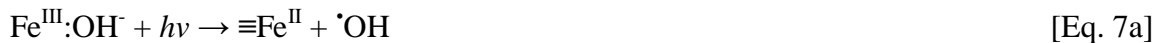
Fe^{III} oxyhydroxides have extremely low solubility (Schwertmann, 1991). The solubility product (K_{sp}) of ferrihydrite, $\text{Fe}(\text{OH})_3$, is 1×10^{-37} (Benjamin, 2002). At pH values less than four, Fe^{III} , $\text{Fe}(\text{OH})^{2+}$, and $\text{Fe}(\text{OH})_2^+$ are the dominant Fe species associated with the dissolution of ferrihydrite. Changes in temperature, pH, and oxidation-reduction potential may affect the

solubility of ferrihydrite (Figures 2-6 and 2-7). Ferrihydrite is likely to precipitate with increasing temperature and pH values around eight (Schwertmann and Cornell, 2007). Ferrihydrite solubility can also be affected by the presence of other ions in solution, such as chloride or sulfate. These ions may form surface complexes with hydrogen on the mineral surface and increase ferrihydrite solubility by weakening Fe-O bonds (Schwertmann, 1991). When submerged in water at low pH values, ferrihydrite can alter to hematite or goethite (Schwertmann and Cornell, 2007), which have a lower solubility and sorption capacity than ferrihydrite (Schwertmann, 1991).

2.5 Fe diel cycles

2.5.1 Light cycles

Photoreduction of ferric Fe (Fe^{III}) to ferrous Fe (Fe^{II}) occurs in the ultraviolet (UV) spectrum in a wavelength range from 360 to 450 nm and at an optimal pH range from 2 to 4 (Gammons et al., 2008; King et al. 1993; McKnight et al., 2001). In this pH range, in the presence of sunlight, the dissolution of HFO is favorable, and has been linked to increases in Fe^{II} and total dissolved Fe ($\text{Fe}(\text{total})$; including both dissolved Fe^{II} and Fe^{III} species) (Nimick et al., 2003). Fe^{III} photoreduction may occur via two chemical pathways as described by Kimball et al. (1992) in the equations below:



Where $\cdot\text{OH}$ is a hydroxyl radical, $h\nu$ the photon, and $\equiv\text{Fe}^{\text{II}}$ is a surface bound species. Equation 6 represents a homogeneous aqueous phase. The main aqueous species responsible for Fe^{III} photoreduction is $\text{Fe}(\text{OH})^{2+}$, which is typically the most abundant Fe^{III} species present at pH values between 2 and 4 (Kimball et al., 1992; King et al., 1993). Equations 7a and 7b represent a heterogeneous surface phase where a surface bound Fe^{III} species is reduced and then released. This process may occur at the surface of Fe^{III} oxyhydroxides (e.g. ferrihydrite).

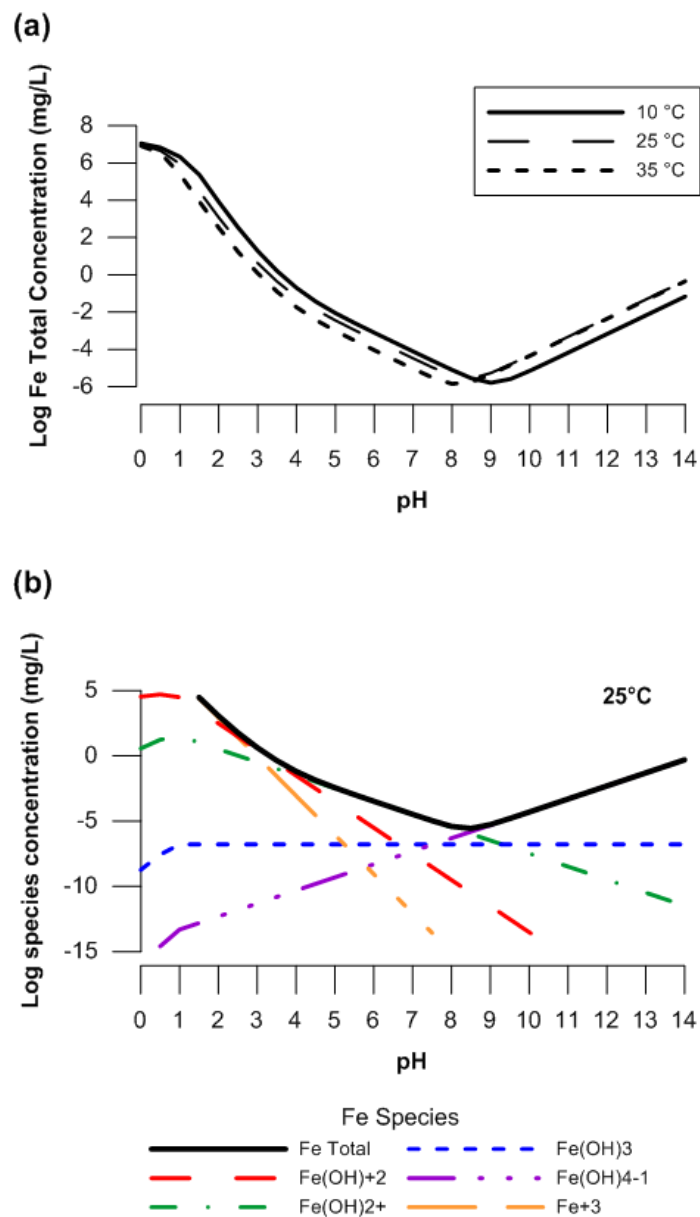


Figure 2-6. (a) Solubility curves for 0.5 g of ferrihydrite, $\text{Fe}(\text{OH})_3$, at 10 °C, 25 °C, and 35 °C showing Fe(total) concentrations and (b) Solubility diagram for 0.5 g of ferrihydrite at 25 °C showing all Fe species, where ionic strength equals 0.1 M. Figure constructed using Visual MINTEQ, version 3.1 (Allison et al., 1991).

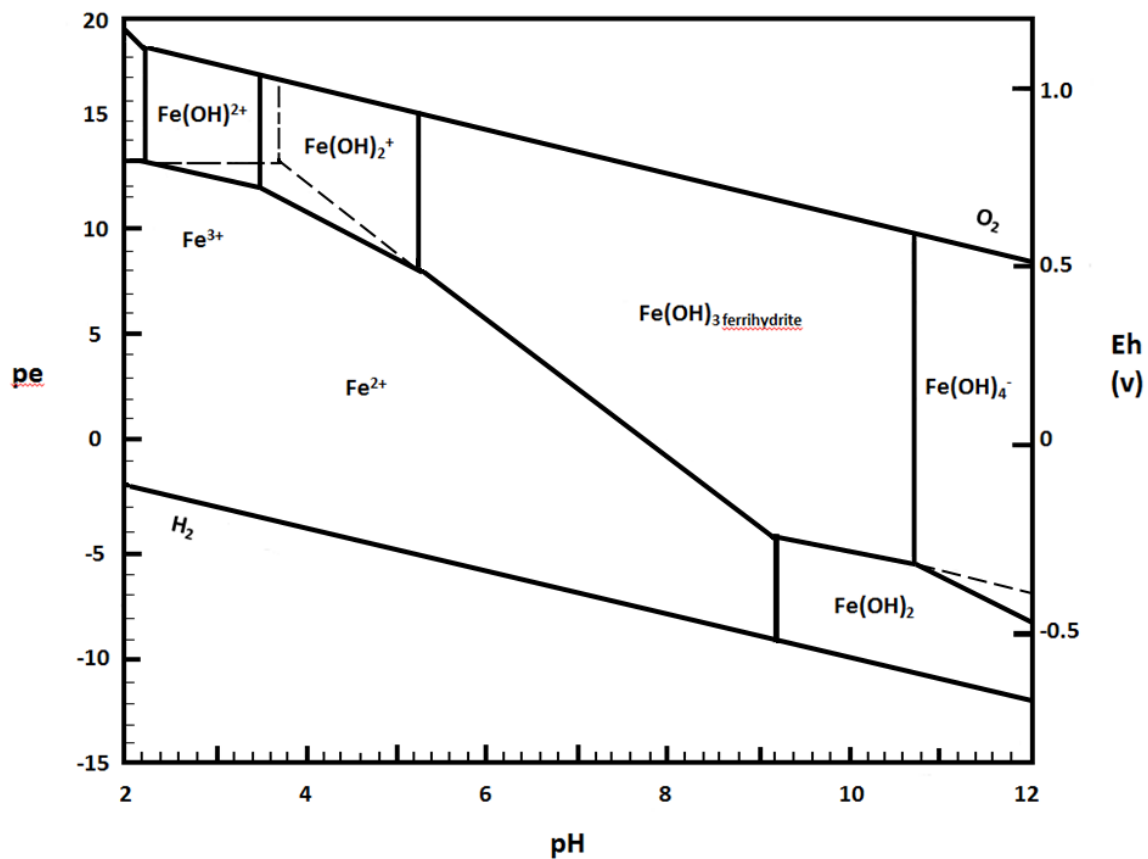


Figure 2-7. Redox potential-pH diagram for the Fe-O-H₂O system for a dissolved Fe species concentration of 10^{-6} M at 1 atm and 25 °C. Figure modified from Drever, 1997.

2.5.2 Temperature cycles

In nature, it is difficult to delineate the difference between the effects of temperature, pH, and solar input on Fe concentrations (Nimick, 2003). Temperature often cycles in phase with light intensity (i.e. temperature increases during the day and decreases at night). Temperature also creates a kinetic effect for Fe cycles by increasing Fe oxidation rates in warmer water (Wakao and Shiota, 1982). Parker et al. (2007) and Gammons et al. (2005a) found that (Fe(total)) and Fe^{II} both decreased with lower temperatures at night, and increased with higher temperatures during daytime hours. However, they determined that Fe cycles were likely influenced more by Fe^{III} photoreduction by solar input. They also concluded that as temperature increases, the solubility of HFO decreases, which could contribute to the change in Fe(total) concentrations.

3 PURPOSE AND OBJECTIVES

The purpose of this research was to test in a laboratory setting if Se^{IV} cycles exist in the presence of Fe cycles. The hypothesis was that Se^{IV} (including the protonated and deprotonated species) will cycle in phase with Fe due to Se^{IV} species sorption onto 2-line ferrihydrite (i.e. as Fe moves from the solid to the dissolved phase it will release the existing sorbed Se^{IV} species). Se^{IV} was chosen over Se^{VI} , because it has a greater affinity for sorption onto ferrihydrite. The oxidation of Se^{IV} to Se^{VI} is also kinetically slow; therefore, reducing the possibility of Se species conversion. The specific objectives of this project are outlined below.

- Objective 1: Generate Fe-only cycles (both Fe^{II} and Fe^{III} cycles) via temperature and light control experiments.
- Objective 2: Generate Se-only cycles via temperature and light control experiments.
- Objective 3: Generate combined Fe-Se cycles using temperature and light control experiments.
- Objective 4: Evaluate the relative effectiveness of temperature and light on creating Fe and Se^{IV} cycles.

4 METHODS

4.1 Experimental overview and layout

The experiments were conducted using temperature and light as potential drivers of Fe and Se cycles. A flow system was constructed to regulate temperature in four 1-liter water-jacketed vessels where the experiments were carried out (Figures 4-1 and 4-2). Three different controls were used to regulate water temperature of this system: ice water (ideally 0°C), room temperature (RT) water (21-23°C), and hot water (set to 35°C). Valves that connect the temperature baths to a mixing chamber were adjusted to achieve the desired temperature. Each temperature controlled cycle followed this general trend: started at room temperature, heated up slowly (35°C maximum), cooled down slowly to room temperature, continued to cool down slowly using ice water (3°C minimum), and finally heated back up to room temperature. All temperature control experiments were conducted in either light on or light off (dark) conditions.

Two standard full spectrum fluorescent bulbs (1.07 meters long) with a reflector were located 7.6 centimeters above the top of four water-jacketed vessels. The light was hung from a shelf, and its vertical position above the vessels was fixed by chains connected to the reflector (Figures 4-2 and 4-3). The full spectrum bulbs covered a wavelength range from 400 nm to 700 nm, which includes the optimum wavelength for photoreduction of Fe^{III} (Emmenegger et al., 2001). For each temperature control experiment, the light was either turned on or off throughout the duration of the experiment. For light control experiments, the light was turned on and off at specific intervals throughout the experiments. Temperature was not controlled during the light control experiments (the reaction vessel water jackets were filled with room temperature water). During dark cycles (light off), red light-emitting diode (LED) strip lights were used as a light alternative for vision purposes. Red LED lights were chosen, because they emit wavelengths less than the wavelength range needed for Fe^{III} photoreduction.

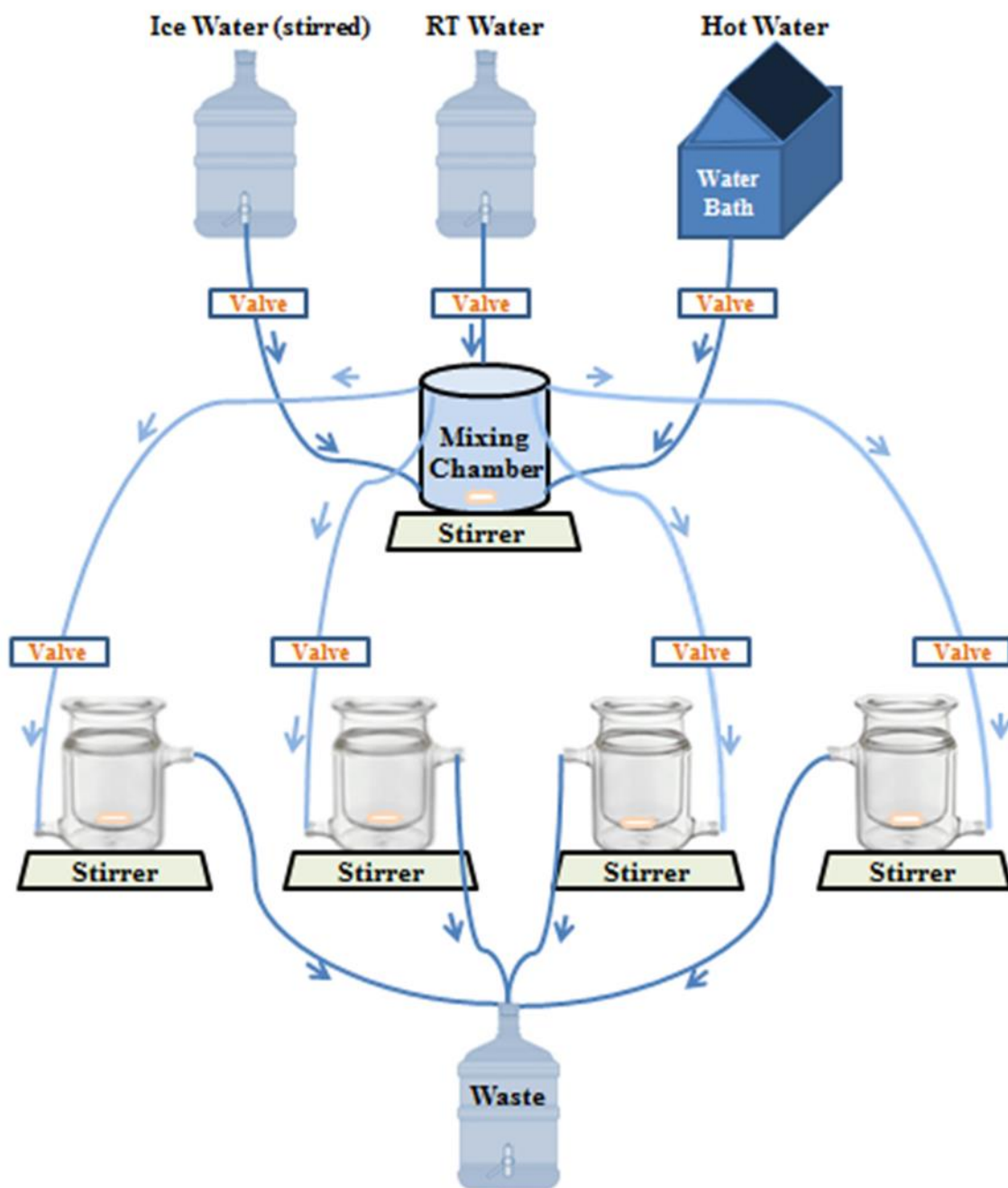


Figure 4-1. Schematic of temperature control system. Arrows indicate water flow direction.

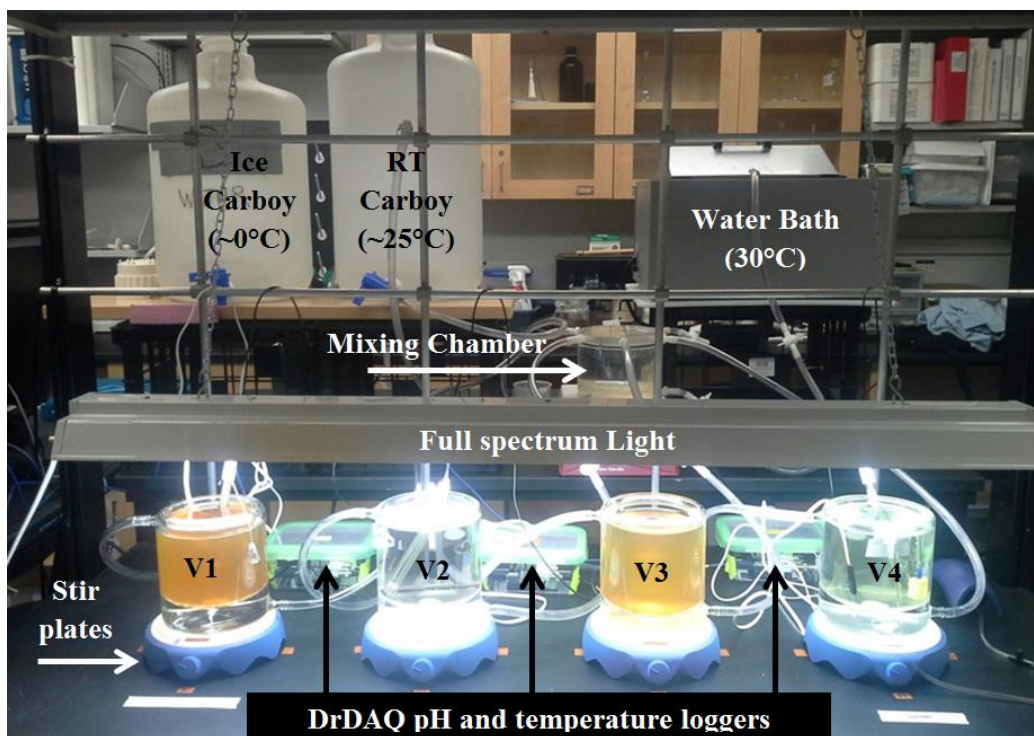


Figure 4-2. Photograph of completed temperature and light control systems. RT is room temperature. V1, V2, V3, and V4 are the vessel numbers.

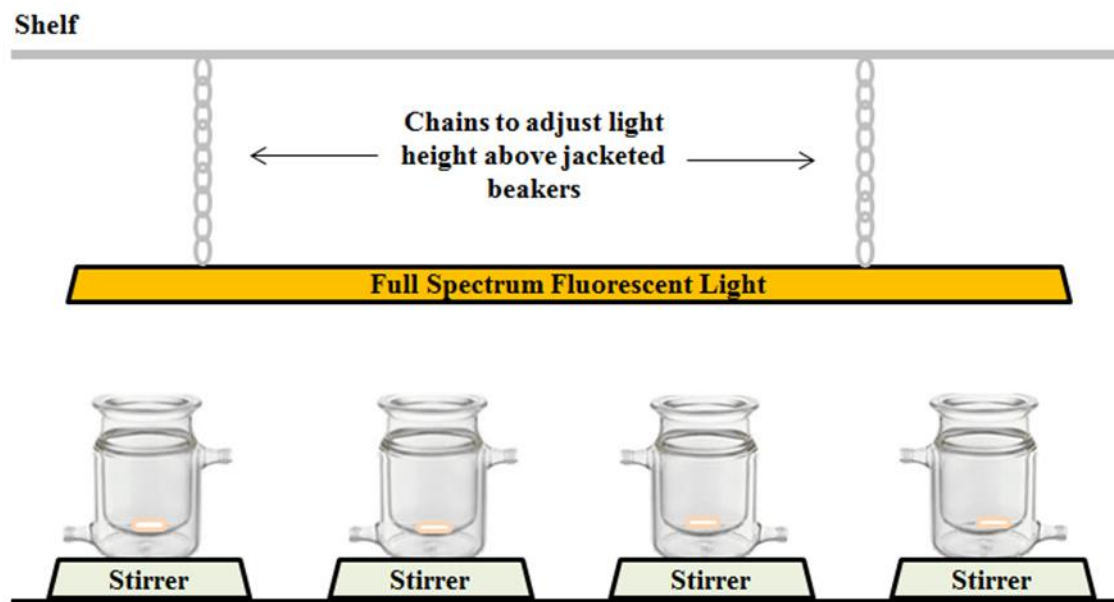


Figure 4-3. Schematic of light control system.

4.2 Materials

4.2.1 2-line Ferrihydrite

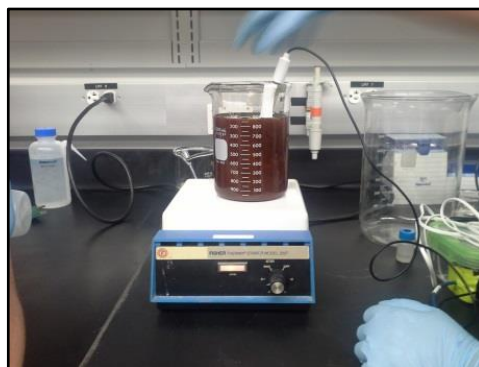
2-line ferrihydrite (a Fe oxyhydroxide mineral with two distinct x-ray diffraction (XRD) peaks) having an approximate chemical formula of $5\text{FeOOH}\cdot 2\text{H}_2\text{O}$ (Lee et al., 2014; Zhao et al., 1994), was synthesized using the method described by Schwertmann and Cornell (2007) with a few minor adjustments. First, Dry Spectra/Por® dialysis membrane tubing (Spectrum Laboratories, Inc., TX, USA) was soaked in deionized water (DI) water for 30 minutes. 40 grams of ferric nitrate nonahydrate ($\text{Fe}(\text{NO}_3)_3\cdot 9\text{H}_2\text{O}$) (Fisher Scientific, NJ, USA) was then added to 500 mL of DI water and was magnetically stirred until all of the solid dissolved. Approximately 300 mL of 1 N potassium hydroxide (KOH) (Fisher Scientific, NJ, USA) was then added to bring the solution pH between 7 and 8. The solution was stirred vigorously for several minutes and was then poured into 60 mL syringes. The syringes were stored tip down for 30 minutes until the solid settled. The solid was syringed into the dialysis membrane tubing and was soaked in DI water for 72 hours. The DI water was replaced periodically over the 72-hour period to maximize the removal of K^+ and NO_3^- ions from the solid 2-line ferrihydrite slurry. After the soaking period, the 2-line ferrihydrite was poured into crucibles and set in a laboratory hood for four days to air dry. Once dry, the 2-line ferrihydrite was ground into a fine powder using a mortar and pestle and sieved through a 125 μm sieve to obtain a consistent solid particle size. The solid was then stored in a glass container until use (Figure 4-4).

It was important to closely monitor the pH of the Fe solution once the KOH was added. If the solution exceeded a pH value between 8 and 9, it was likely for goethite or hematite to precipitate instead of 2-line ferrihydrite. To ensure that the proper chemical composition for 2-line ferrihydrite was achieved, a sample was sent for XRD analysis. The results confirmed that 2-line ferrihydrite was synthesized (Appendix A).

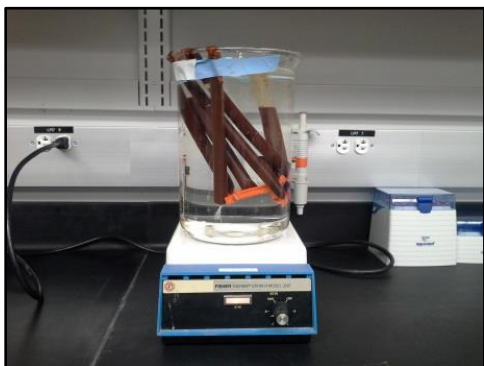
(a)



(b)



(c)



(d)



(e.)



(f.)

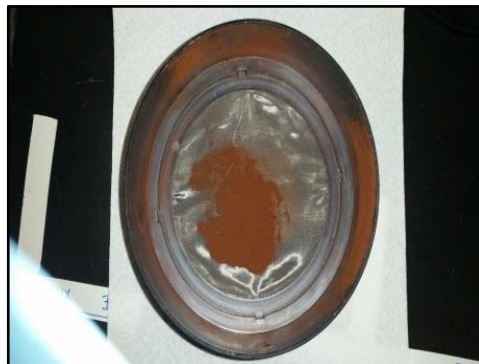


Figure 4-4. Synthesis of 2-line ferrihydrite. (a) 40 grams $\text{Fe}(\text{NO}_3)_3 \cdot 9\text{H}_2\text{O}$ dissolved in 500 mL DI water; (b) 300 mL KOH added to solution; (c) Solid solution soaking in dialysis membrane tubing; (d) Solid drying in crucible; (e) Dried 2-line ferrihydrite crushed with mortar and pestle; and (f) 2-line ferrihydrite sieved through a 125 μm sieve.

4.2.2 Solutions

All solutions were prepared in 1-liter water jacketed vessels, and contained the following components (Table 4-1):

- 1 liter of DI water.
- Potassium chloride (KCl) (Fisher Scientific, NJ, USA) – 7.45 g added to each beaker to a concentration of 0.1 M to fix the solution ionic strength. KCl was chosen, because K^+ and Cl^- are conservative ions and will not interfere with Fe or Se species in solution.
- Hydrochloric acid (HCl) (Fisher Scientific, NJ, USA) – the solution pH was adjusted to 3 using 10% (v/v) 12 N HCl.
- 2-line ferrihydrite – 500 mg was added to introduce Fe into solution for Fe-only and Fe-Se combined experiments. The 2-line ferrihydrite solid did not dissolve completely.
- Se^{4+} CertiPrep Spex standard (NJ, USA) – 300 μ L of a 1000 mg/L Se^{4+} CertiPrep Spex standard (containing 2% (v/v) nitric acid) was added to Se-only and Fe-Se combined experiments to a final concentration of 300 μ g/L (3.80 μ M) Se^{IV} . 3000 μ L of the 1000 mg/L Se^{4+} CertiPrep Spex standard was added to one Fe-Se combined cycle experiment (Cycle 3) to a final concentration of 3000 μ g/L (40.0 μ M) Se^{IV} .

Each vessel was placed on a magnetic stir plate and stirred at 400 rpm. The vessels equilibrated for 48 hours until Fe(total) concentrations were stable, which was confirmed by 48 hour sorption experiments.

4.3 Data logging and meter measurements

DrDAQ[®] temperature sensors and HOBO[®] Pendant light/temperature loggers (Table 4-2) were used to record temperature. DrDAQ[®] temperature sensors recorded in one second intervals and were displayed real-time during the experiments using PicoLog Recorder software. HOBO[®] Pendant light/temperature loggers were set to a five minute logging interval, and the data were retrieved after each experiment using HOBOWARE 2 software. Both instruments recorded temperature in degrees Celsius.

Table 4-1. Experiment vessel solutions

Solution component	Fe-Only Experiments	Se-Only Experiments	Fe-Se combined Experiments
DI water (L)	1	1	1
KCl concentration (M)	0.1	0.1	0.1
pH (standard units)	3	3	3
2-line ferrihydrite (g)	0.5	---	0.5
Se ^{IV} concentration (µg/L)	---	300	300 or 3000

Note: DI is deionized water. All experiments contained 300 µg/L Se^{IV}, except for Cycle 3 which contained 3000 µg/L Se^{IV}.

Table 4-2. Measured parameters and instrumentation

	Measured Parameters	Units	Instrumentation	Software
Continuous Monitoring	Temperature	°C	DrDAQ® USB temperature probes	PicoLog Recorder
	Temperature	°C	HOBO® Pendant light/temperature loggers	HOBOWARE 2
	Light Intensity	Lux	HOBO® Pendant light/temperature loggers	HOBOWARE 2
	Light Intensity	μMol/m ² s	AccuPAR Model LP-80 PAR/LAI ceptometer	N/A
	pH	Standard units	DrDAQ® USB pH probes	PicoLog Recorder
Fe Analysis	Dissolved Fe ^{II}	mg L ⁻¹	Hach® DR2800 Spectrophotometer (MDL = 0.02 mg L ⁻¹)	N/A
	Dissolved Fe(total)	mg L ⁻¹	Hach® DR2800 Spectrophotometer (MDL = 0.02 mg L ⁻¹)	N/A
Se Analysis	Dissolved Se ^{IV}	μg L ⁻¹	Perkin Elmer Optima 2100 DV ICP-OES (MDL = 5 μg L ⁻¹)	WinLab 32 ICP

Light intensity was monitored using HOBO[®] Pendant light/temperature loggers and an AccuPAR Model LP-80 PAR/LAI ceptometer (Table 4-2). The HOBO[®] Pendants measured light intensity in units of Lux (1 lumen/m²) and were set to a five minute logging interval. The AccuPAR ceptometer measured light intensity in units of $\mu\text{Mol/m}^2\text{s}$, and measurements were taken periodically throughout each experiment. Maximum light intensities were measured at 4168 Lux and 193 $\mu\text{Mol/m}^2\text{s}$ with the light located 3 inches above the top of each reaction vessel.

Solution pH was monitored using DrDAQ[®] pH probes. The pH was recorded in one second intervals and was displayed real-time during the experiments using PicoLog Recorder software. Before each temperature cycle, each probe was placed in a pH 4 buffer to correct for any differences in pH readings between the probes. The pH was recorded in standard units (Table 4-2).

4.4 Sampling and analysis

The volume of sample removed from each beaker did not exceed 10% of the total solution volume (one liter). This was to ensure that the solid to solution ratio was preserved.

4.4.1 Fe sampling and analysis

Unfiltered Fe^{II} and Fe(total) samples were collected for each experiment. Selected sets of Fe^{II} and Fe(total) samples were collected in triplicate to determine the error in the measurement. Fe^{II} and Fe(total) concentrations were determined by the ferrozine method (Stookey, 1970) using a Hach[®] DR 2800 Spectrophotometer (Table 4-2). A ferrozine solution was prepared containing HEPES buffer (OmniPur, NJ, USA), ferrozine (HACH, CO, USA), and NaOH (Fisher Scientific, NJ, USA). The ferrozine solution reacts with Fe^{II} in aqueous samples to form a purple colored complex (Figure 4-5) that can be analyzed spectrophotometrically at a wavelength of 562 nm. Fresh ferrozine reagent was made for each cycle to ensure proper chemical composition and the optimal pH range between 4 and 9 (Stookey, 1970).

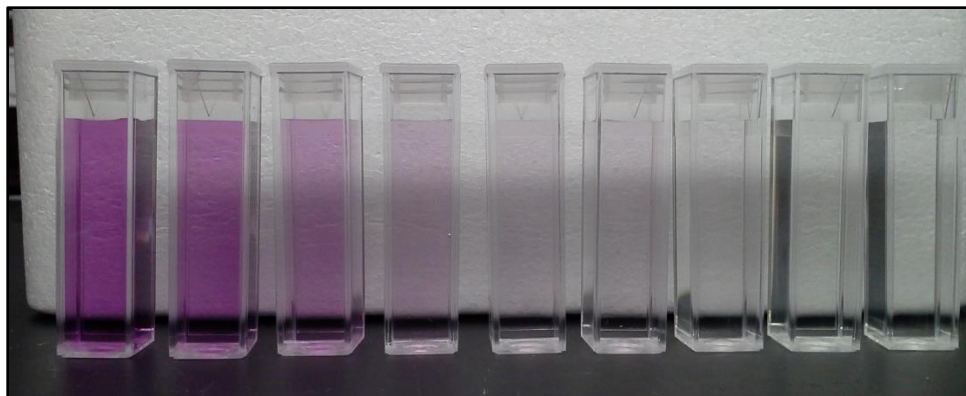


Figure 4-5. Ferrozine method calibration samples for Fe^{II} analysis. Fe^{II} concentrations decrease from left to right as indicated by the different shades of purple.

Specific ferrozine to sample ratios were used to determine Fe^{II} concentrations (Table 4-3). Each ferrozine-sample solution was made in a 4.5 mL cuvette, and the absorbance of each ferrozine-sample solution was analyzed using the Hach® DR2800 Spectrophotometer. Different calibration curves were created for each ferrozine to sample ratio by diluting ferrous ammonium sulfate hexahydrate ($\text{Fe}(\text{NH}_4)_2(\text{SO}_4)_2 \cdot 6\text{H}_2\text{O}$) (HACH, CO, USA) stock solutions of 100 mg/L Fe^{II} and 10 mg/L Fe^{II} . Once the calibration curves were created, Fe^{II} concentrations were calculated from absorbance values. A blank was prepared using ferrozine and a solution with the same pH (3 standard units) and ionic strength (0.1 M KCl) as the vessel solutions.

$\text{Fe}(\text{total})$ concentrations were analyzed using the same method as Fe^{II} analysis, except a solution of 0.5N hydroxylamine HCl (HX) (Acros Organics, NJ, USA) was added to each sample before adding ferrozine reagent (Table 4-3). HX is a reducing agent that converts all dissolved Fe to Fe^{II} . Ferrozine was added to each HX-sample solution and reacted with the Fe^{II} to form the purple colored complex, which was then analyzed spectrophotometrically for $\text{Fe}(\text{total})$. A separate calibration curve was completed for the $\text{Fe}(\text{total})$ analysis, and a separate blank was also prepared using ferrozine, HX, and a solution with the same pH and ionic strength as the vessel solutions. Fe^{III} concentrations were calculated by subtracting Fe^{II} concentrations from $\text{Fe}(\text{total})$ concentrations. The HACH DR 2800 method detection limit (MDL) for both Fe^{II} and $\text{Fe}(\text{total})$ is 0.02 mg/L.

4.4.2 Se sampling and analysis

Samples were collected in triplicate for Se^{IV} . Specific ratios of sample, DI water, and 6 M HCl were used (Table 4-4). Elemental Se concentrations were analyzed using a Perkin Elmer (CT, USA) Optima 2100 DV ICP-OES, which was operated in axial viewing mode at a wavelength of 196.03 nm (Table 4-5). A multimode sample introduction system (MSIS) was used in vapor generation mode (Figure 4-6).

In vapor generation mode, the nebulizer is used as the argon flow input to the chamber. The sample introduction line connected to the nebulizer is blocked off for this method. The Se^{IV} sample containing approximately 4.8 M HCl is introduced via the hydride sample input at the base of the chamber, which flows into the reaction cone. Sodium borohydride (NaBH_4) solution

Table 4-3. Ferrozine method sample to solution ratios for Fe^{II} and Fe(total) analysis

Type of Fe analysis	Sample to Ferrozine/HX ratios		
	Unfiltered Fe Sample (mL)	Ferozine (mL)	HX (mL)
Fe ^{II}	0.5	3	---
Fe(total)	0.5	1.5	1.5

Note: HX is hydroxylamine hydrochloride.

Table 4-4. Ratios of sample, DI water, and 6 M HCl prepared for
Se^{IV} HG-ICP-OES analysis

Se sample type	Sample component ratios		
	Sample (mL)	DI water (mL)	6 M HCl (mL)
Se ^{IV}	1	4	0.5

Note: DI is deionized water.

Table 4-5. HG-ICP-OES Se^{IV} analysis parameters

HG-ICP-OES method parameters	
Chamber type	MSIS
Nebulizer	Mira Mist
Plasma view	Axial
Wavelength (nm)	196.026
Reductant solution	0.5% (m/V) NaBH ₄ + 0.05% NaOH (m/V)
Reductant uptake rate (mL min ⁻¹)	1.2
Sample HCl acidity	4.8-7 M
Sample flow rate (mL min ⁻¹)	1.2
ICP RF Power (watts)	1300
Plasma Argon Flow (L min ⁻¹)	15
Nebulizer Argon (L min ⁻¹)	0.65
Auxiliary Argon (L min ⁻¹)	0.2
Delay time (s)	120
Integration time	Auto
Replicates	7
Calibration standards	0, 5, 10, 50, 100, 150, and 200 (µg/L Se ^{IV})

Note: MSIS is multimode sample introduction system.

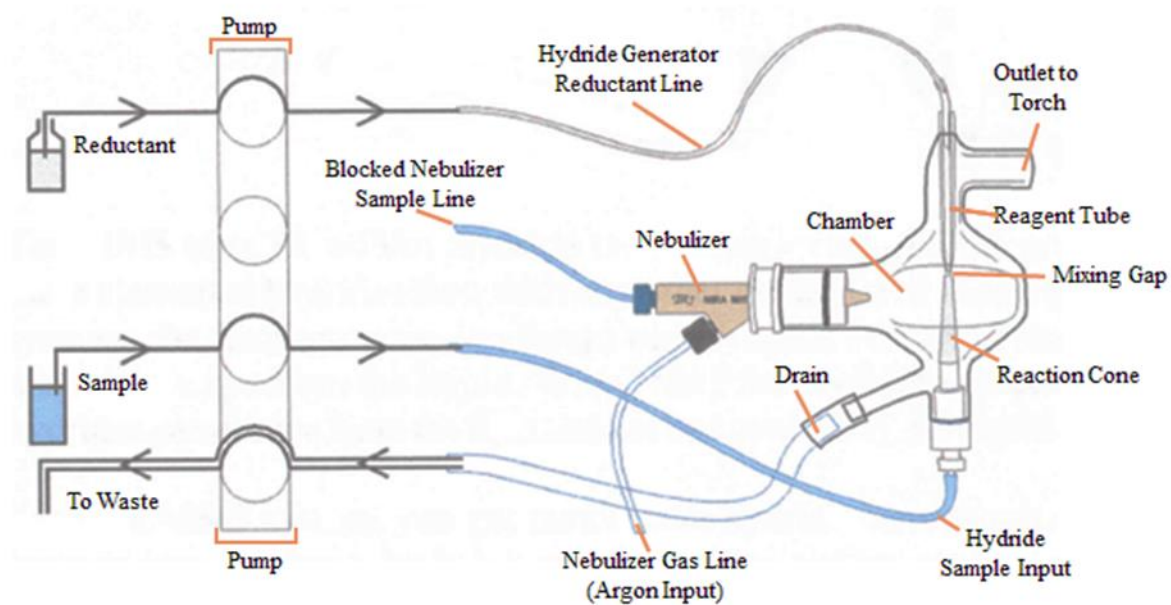
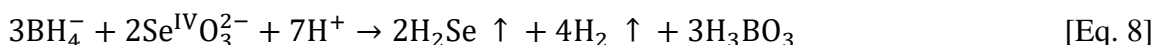


Figure 4-6. Multimode sample introduction system (MSIS) using vapor generation mode (modified from Marathon Scientific, 2007).

is introduced from the top of the chamber via the hydride generator reductant line and flows into the reagent tube. A thin-film of sample containing HCl and NaBH₄ meet in the mixing gap, a 1-3 mm gap between the tip of the reaction cone and the reagent tube (Figure 4-6). The reaction between the HCl and the NaBH₄ creates a volatile Se hydride, a process called hydride generation (HG), which is then introduced to the plasma for analysis via an alumina injector. The HG reaction between Se^{IV} (specifically the Se^{IV}O₃²⁻ species) and NaBH₄ is written as (Huang, 2010):



The liquid that does not volatilize inside the chamber exits the chamber through the drain into a waste container (Schroder and Zhang, 2009).

The reagents used to make Se standards included a 1000 mg/L Se⁴⁺ reference standard purchased from Spex CertiPrep (NJ, USA) and 12 M HCl (Fisher Scientific, NJ, USA). This is the same standard that was used to make the vessel solutions for sample collection. Therefore, Se is assumed to be in the Se^{IV} oxidation state for the HG-ICP-OES standards. Sodium borohydride (Acros, NJ, USA) was used to make a 0.5% (m/v) NaBH₄ solution. The resulting solution was stabilized with 0.05% (m/v) NaOH (Fisher Scientific, NJ, USA).

Six calibration standards of 5 µg/L, 10 µg/L, 50 µg/L, 100 µg/L, 150 µg/L, and 200 µg/L Se^{IV} were prepared with a reference stock Se^{IV} solution of 1000 µg/L in 10% (v/v) 6M HCl. The reference stock was prepared using the Spex CertiPrep 1000 mg/L Se⁴⁺ ICP-OES standard. This was also the same standard used to make the vessel solutions for sample collection. The blank was 10% (v/v) 6 M HCl and DI water. Instrument stability was evaluated before each sample run by taking three replicate readings of a blank and each Se standard. The ICP-OES was run using WinLab 32 ICP software, and results (analyzed as elemental Se) were printed at the end of each analysis. Results were accepted at relative standard deviation (RSD = standard deviation/mean x 100) values less than 3%.

The MDL was calculated by running a linear regression analysis on five different calibration curves in Microsoft Excel using the Data Analysis Toolpak. This method calculates the limit of detection (LOD), which is the same as the MDL for a single analyte (Se^{IV} is the only analyte in the HG-ICP-OES method). The values for the upper 95% confidence interval of the

regression analysis output were averaged for the five calibration curves to calculate the final LOD value. The LOD can also be calculated by following the method of Konieczka and Namiesnik (2009), in which the LOD for an individual calibration curve can be calculated as follows:

$$\text{LOD} = \frac{3 \times \text{SE(I)}}{S} \quad [\text{Eq. 9}]$$

Where SE(I) is the standard error of the intercept and S is the slope of the calibration curve. The LOD result for this equation is equivalent to the 95% confidence interval output value in Microsoft Excel. Therefore, the final MDL was calculated by averaging the LOD results for all five calibration curves. The average MDL was 5 µg/L Se^{IV}.

4.5 Data analysis

Graphs of each parameter (temperature, pH, Fe^{II} concentrations, Fe^{III} concentrations, Fe(total) concentrations, and Se^{IV} concentrations) versus time were created for each cycle with standard deviations for replicate samples. Replications of each experiment were performed to provide statistical validation. The Fe ratio was calculated and plotted for each cycle by dividing Fe^{II} concentrations by Fe(total) concentrations. Graphs of Se concentrations versus temperature were created to identify relationships between the two parameters. To test whether Se concentrations varied due to temperature-dependent sorption, 1/temperature (in Kelvin) was graphed versus the log of Se concentrations to determine the enthalpy of sorption for Se^{IV} onto 2-line ferrihydrite (Eq. 4 and Eq. 5).

Each cycle was also categorized into a group (Fe-only, Se-only, Fe-Se combined) to identify similarities and differences in the data.

4.6 Quality Control Assessment

Before and during the experiments, a few quality control tests were completed to determine the state of Fe (i.e. dissolved or colloidal) in the reaction vessels and to determine the

controlling processes of Se concentration changes and cycling. The possible states of Se in the reaction vessels are written in the mass balance equation below:

$$[\text{Se}]_{\text{Total}} = [\text{Se}^{\text{IV}}]_{\text{aqueous}} + [\text{Se}^{\text{IV}}]_{\text{sorbed to glass}} + [\text{Se}^{\text{IV}}]_{\text{sorbed to Fe}} + [\text{Se}^{\text{VI}}]_{\text{aqueous}} + [\text{Se}^{\text{VI}}]_{\text{sorbed to glass}} + [\text{Se}^{\text{VI}}]_{\text{sorbed to Fe}} \quad [\text{Eq. 10}]$$

Equation 10 shows that Se^{IV} may oxidize to Se^{VI} . However, Se^{IV} is expected to be the dominant Se species in solution, because Se^{IV} to Se^{VI} oxidation is kinetically slow (Torres et al., 2011). Both Se^{IV} and Se^{VI} are likely to sorb to solid 2-line ferrihydrite. It is also possible that Se^{IV} and Se^{VI} may sorb to the glass reaction vessels. Se^{IV} sorption to glassware is addressed in the quality control experiments (sections 4.6.3 and 4.6.4). Se^{IV} to Se^{VI} oxidation is discussed in section 6.2.5.

4.6.1 Filtering experiment for Fe analysis

An experiment was conducted to determine if ferrozine solution can react with both dissolved and colloidal/particulate Fe^{II} . Six vessels were prepared using the same solution as the Fe-only experiments; however, a different mass of 2-line ferrihydrite was added to each vessel (Table 4-6). The vessels equilibrated for 48 hours prior to sampling. Both filtered and unfiltered samples were collected from each vessel for Fe^{II} and Fe(total) analysis. Every sample was collected in replicates of six, and a dedicated 0.45- μm syringe filter was used for each vessel.

Two vessels (Vessel 1 and Vessel 6) were more turbid than the other four vessels (Figure 4-7). Vessels 1 and 6 were not water jacketed like the other four vessels. Therefore, better mixing of the solution occurred in these vessels due to a stronger response between the magnetic stirrer and stir plate.

For all vessels, the unfiltered Fe^{II} and Fe(total) concentrations were higher than the filtered Fe^{II} and Fe(total) concentrations (Table 4-6, Figure 4-8, Appendix B). Although the filtering process resulted in decreased Fe^{II} absorbance values, it is unlikely that all colloidal/particulate Fe^{II} was removed during the filtering process (i.e. some of the

Table 4-6. Filtering experiment for Fe analysis: A comparison of unfiltered and filtered samples

Vessel Number	FH added (mg)	Fe ^{II} Analysis				Fe(total) Analysis			
		Unfiltered (mg/L)	RSD (%)	Filtered (mg/L)	RSD (%)	Unfiltered (mg/L)	RSD (%)	Filtered (mg/L)	RSD (%)
1	100	0.252	4.5%	0.146	6.0%	0.759	1.6%	0.644	1.8%
2	200	0.204	8.0%	0.130	4.4%	0.525	3.1%	0.447	2.6%
3	300	0.232	2.4%	0.155	15%	0.597	0.0%	0.487	1.2%
4	400	0.268	3.9%	0.162	3.5%	0.640	0.0%	0.468	2.3%
5	500	0.232	2.4%	0.151	4.8%	0.398	6.5%	0.272	2.1%
6	600	0.507	<1%	0.160	<1%	0.602	1.2%	0.194	3.7%

Note: FH is 2-line ferrihydrite. Relative standard deviation (RSD) is the standard deviation divided by the mean reported as a percentage, where the corresponding mean value is listed as “Unfiltered” or “Filtered” data.



Figure 4-7. Photograph of the filtering experiment for Fe analysis. Vessels are numbered 1 through 6 from left to right. Vessels 1 and 6 are beakers, and vessels 2 through 5 are jacketed reaction vessels.

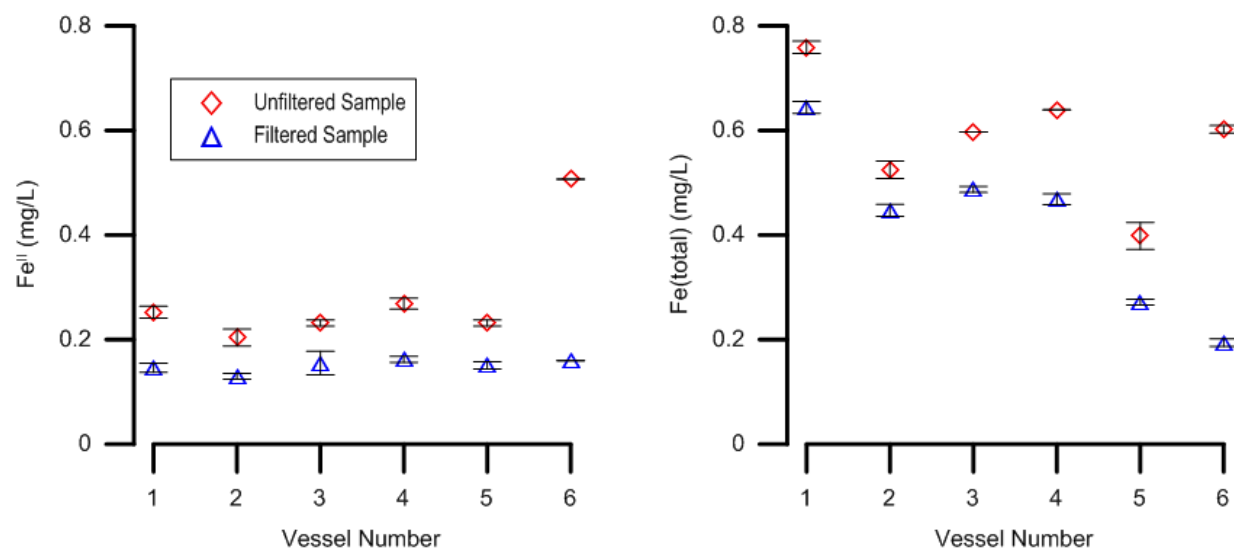


Figure 4-8. Results of the filtering experiment for Fe analysis showing the comparison between unfiltered and filtered samples analyzed for Fe^{II} and Fe(total). Standard deviations are represented by error bars for six replicate samples.

colloids/particles may have been small enough to pass through the 0.45 μm filter). Ferrozine solution reduces all dissolved Fe^{III} to Fe^{II} ; however, it is not known if the ferrozine solution breaks down solid Fe or Fe colloids. Therefore, it is likely that the change in Fe^{II} absorbance values from unfiltered to filtered samples was due to variations in light movement through the samples caused by the removal of particles during filtering. For Fe(total) samples, it is likely that the solid Fe/colloidal Fe was broken down by the hydroxylamine hydrochloride; however, this process was not confirmed during this experiment. All reported Fe^{II} and Fe(total) results for the light and temperature cycle experiments are for unfiltered samples which likely contained both dissolved and colloidal Fe.

Also, for Vessel 3 (which like the Fe-only and Fe-Se experiments contained 300 mg of 2-line ferrihydrite), an average of 0.597 mg/L Fe(total) was found in unfiltered samples. This small Fe(total) concentration indicated that minimal 2-line ferrihydrite dissolution was occurring in the vessel after the equilibration period. A difference of 0.11 mg/L was calculated between unfiltered and filtered Fe(total) samples signifying that Fe colloids may have been present; however, the relative mass of those potential Fe colloids was much less than that of solid 2-line ferrihydrite (the mass of Fe colloids was approximately 0.07% of the total Fe added to the vessel). Therefore, Se^{IV} sorption onto Fe colloids will likely be insignificant during light and temperature control experiments, because the mass of the Fe colloids will be much less than the mass of the solid 2-line ferrihydrite added to the vessels.

4.6.2 Evaporation experiment

Each reaction vessel remained uncovered throughout the duration of each Fe-only, Se-only, and Fe-Se cycle experiment. Therefore, an experiment was completed to determine if significant evaporation of the vessel solutions was occurring over the two day equilibration period before the Fe and Se cycle experiments began. This was important to determine, because it would explain increases in Fe and Se concentrations that might be observed over time.

For the evaporation experiment, four reaction vessels were prepared in the same manner as the Se-only experiments (section 4.2.2). Since the ionic strength was fixed with KCl (0.1 M KCl), K^+ concentrations were known for each vessel (3548 mg/L K^+) and could be analyzed.

Since K^+ acts as a conservative ion in the vessel solutions, an increase in K^+ concentrations over time can be attributed to evaporation.

Samples were collected from each vessel immediately after solution preparation (time = 0 days). The vessels stirred for 2.3 days, and samples were collected from each vessel after 2 days and 2.3 days (Table 4-7). The K^+ concentrations increased over the 2.3 day experiment for all vessels. Therefore, evaporation from the vessels was confirmed. The results (Table 4-7) illustrate that up to a 10% increase in Se concentrations may be linked to evaporation. However, this error should not affect the trends in the cycling behavior of Se with temperature.

4.6.3 Se^{IV} loss from sorption to glass

To determine if Se^{IV} sorption to the glass vessels was occurring, Se-only solutions were tested as part of a complementary sorption study (Vesper et al., 2015). The maximum Se^{IV} lost in those experiments was 15%. This introduces some error; however, it should not eliminate the cycling behavior of Se during the temperature control experiments.

4.6.4 Se^{IV} desorption from glass

An experiment was prepared to determine if Se^{IV} was desorbing from the glass vessels and then being released in solution during later experiments. Two reaction vessels were prepared with the Se-only solution (section 4.2.2). The solutions stirred and equilibrated for 48 hours. Then each vessel was cleaned thoroughly with two different detergents. One vessel was cleaned with Sparkleen detergent, and the other was cleaned with Citranox acid detergent. The magnetic stir bars were also cleaned. After cleaning, the vessels were filled with a background solution to match the temperature control experiments. Each vessel contained one liter of DI water, 0.1 M KCl, and was adjusted to a pH of 3 with HCl. The magnetic stir bars were placed back in the vessels and the solution equilibrated for 24 hours. Samples were collected at 4 hours, 6 hours, and 24 hours for Se^{IV} . All collected sample concentrations fell below the instrument MDL of 5 $\mu\text{g/L}$ Se^{IV} indicating that Se^{IV} sorption and subsequent desorption from the glass vessels could not be linked to increases in Se^{IV} concentrations.

Table 4-7. Evaporation experiment K⁺ results

Vessel No.	Elapsed time (days)	K (mg/L)	Change from background (%)
1	0	3579	0.87%
	2.03	3645	2.73%
	2.33	3753	5.78%
2	0	3577	0.82%
	2.03	3678	3.66%
	2.33	3856	8.68%
3	0	3679	3.69%
	2.03	3646	2.76%
	2.33	3766	6.14%
4	0	3561	0.37%
	2.03	3727	5.05%
	2.33	3883	9.44%

Since Se sorption and desorption from glassware was minimal, Equation 10 for the mass balance of Se in the reaction vessels can be reduced to:

$$[\text{Se}]_{\text{Total}} = [\text{Se}^{\text{IV}}]_{\text{aqueous}} + [\text{Se}^{\text{IV}}]_{\text{sorbed to Fe}} + [\text{Se}^{\text{VI}}]_{\text{aqueous}} + [\text{Se}^{\text{VI}}]_{\text{sorbed to Fe}} \quad [\text{Eq. 11}]$$

5 RESULTS

Seven experiments were conducted in which light, temperature, length of experiment, and Se^{IV} concentrations varied (Table 5-1). Raw data for each cycle can be found in Appendix C.

5.1 Cycle 1: 7/22-23/2014

A 22-hour Fe-only light cycle was conducted on July 22-23, 2014 (Table 5-1). The purpose of this experiment was to determine if Fe redox cycles could be generated by light only (no temperature control variations). One reaction vessel was set up for this experiment using a Fe-only solution (Table 4-1), which equilibrated for two hours before the experiment began. The light located above the reaction vessel was turned on and off two times during the experiment (Figure 5-1).

Results of this experiment (Figure 5-1 and Table 5-2) illustrated that Fe(total) concentrations continued to increase after the two hour equilibration period with the light on. Temperature was not intentionally cycled during this experiment; however, the solution temperature increased to 22.1°C when the light was turned on and decreased to 20.9°C when the light was turned off. Therefore, it was determined that the effects of temperature and light could not be separated (due to heating of the solution when the light was turned on). The average light intensity was 4119 Lux for periods when the light was turned on.

It was also determined that a longer equilibration time was needed before sample collection to obtain stable Fe(total) concentrations and values above the MDL of 0.02 mg/L. It took approximately 8 hours for the Fe(total) concentrations to rise above the MDL in this experiment. Fe(total) concentrations were low (≤ 0.228 mg/L), and Fe^{II} concentrations did not exceed the MDL, even during times when the light was turned on. Iron cycles were not observed during this experiment. The solution pH did not cycle with light or temperature changes.

Fe cycles did not occur during this light control experiment with changes in light or temperature. There are a few possible reasons why Fe^{III} photoreduction did not occur. First, the Fe(total) concentrations present in solution were low (Table 5-2). If Fe^{III} photoreduction was occurring, the Fe^{III} species concentrations in solution may not have been sufficient to

Table 5-1. Summary of light and temperature cycle experiments

Cycle No.	Purpose	Cycle date(s)	No. of Vessels	FH ^a (mg)	Se ^{IV} ^b (µg/L)	Light	Temp	Sampled for	Duration & sampling ^c
1	Generate Fe cycles using light only	7/22-23/14	1	500	---	cycle	stable ~25°C	Fe ^{II} Fe(total)	Equil.: 2 hr Cycle: 22 hr Samples: hourly
2	Generate Fe cycles using light only over a longer time period	10/17-18/14	4	500	---	cycle	stable ~25°C	Fe ^{II} Fe(total)	Equil.: 48 hr Cycle: 30 hr Samples: hourly
3	Generate Fe-Se cycles with temperature	10/25/14	4	500	3000	off	cycle	Fe ^{II} Fe(total) Se ^{IV}	Equil.: 48 hr Cycle: 10 hr Samples: hourly
4	Generate Fe-only and Fe-Se cycles with temperature	12/9/14	2	500	---	on	cycle	Fe ^{II} Fe(total) Se ^{IV}	Equil.: 48 hr Cycle: 10 hr Samples: hourly
			2	500	300				
5	Generate Se-only cycles with temperature over a shorter time period	1/29/15	4	---	300	on	cycle	Se ^{IV}	Equil.: 48 hr Cycle: 3.5 hr Samples: 15-30 mins
6	Generate Fe-only and Fe-Se combined cycles with temperature	2/28/15	2	500	---	off	cycle	Fe ^{II} Fe(total)	Equil.: 48 hr Cycle: 7 hr Samples: random
			2	500	300	off	cycle	Fe ^{II} Fe(total) Se ^{IV}	Equil.: 48 hr Cycle: 7 hr Samples: random
7	Generate Se-only cycles with temperature	4/26/15	4	---	300	on	cycle	Se ^{IV}	Equil.: 48 hr Cycle: 7 hr Samples: random

^a2-line ferrihydrite; ^bdiluted from 1000 mg/L Se^{IV} standard; ^c Equil. = equilibration time before experiment begins; Cycle = duration of test from end of equilibration; Samples = frequency of sample collection. All vessels contained 7.45 g KCl (0.1 M); adjusted to pH ~3 (adjusted with HCl); brought to a total of 1 L

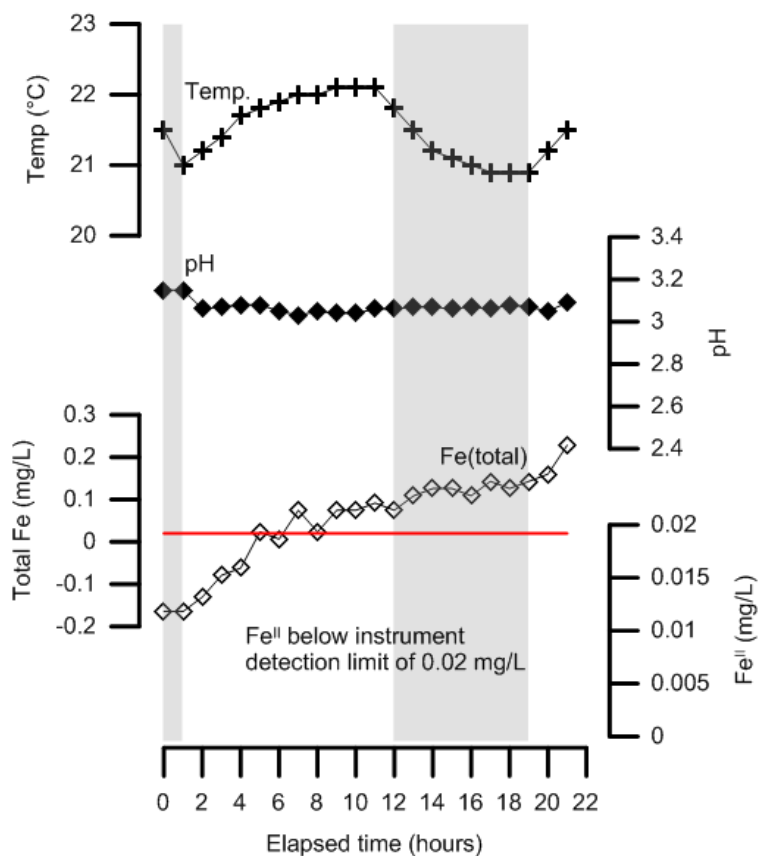


Figure 5-1. Cycle 1 (7/22-23/2014) results. A single vessel was set up for this experiment containing Fe-only solution. The straight, solid line indicates the MDL for Fe^{II} analysis (0.02 mg/L Fe^{II}) on the HACH DR2800 Spectrophotometer. The gray shaded areas indicate when the light was turned off (dark conditions).

Table 5-2. Cycle 1 (7/22-23/2014) parameter variability

Parameter	Units	Vessel No.	Min.	Max.	Range (Min. - Max.)	Average
Temperature	°C	1	20.9	22.1	1.2	21.5
pH	---	1	3.03	3.15	0.12	3.07
Fe(total)	mg/L	1	< 0.02	0.228	0.392	0.051

Note: Min. is the minimum parameter value, and Max. is the maximum parameter value.

produce Fe^{II} concentrations above the MDL. Second, the period in which the light was turned on may not have been long enough for Fe^{III} photoreduction to occur and yield Fe^{II} at detectable limits. Lastly, the light intensity may not have been strong enough to drive Fe^{III} photoreduction.

5.2 Cycle 2: 10/17-18/2014

A 30-hour Fe-only light cycle was conducted on October 17-18, 2014 (Table 5-1). The purpose of this experiment was to complete multiple Fe-only cycles with a longer equilibration time (48 hours) and a longer sampling period than the previous experiment. Similar to Cycle 1, the goal was to generate Fe cycles by light and/or temperature changes (temperature controlled by light only). The light was turned on and off twice during the experiment (Figures 5-2 and 5-3).

Four reaction vessels containing Fe-only solutions (Table 4-1) were prepared for this experiment. The temperature remained relatively stable in all vessels (Figures 5-2 and 5-3, Table 5-3). The average light intensity was 3759 Lux for periods when the light was turned on. The pH also remained relatively stable for all vessels, with the exception of Vessel 3. The Vessel 3 pH was adjusted to 3.14 during hour 13, because the pH of that vessel was low in comparison to the other three vessels (Figure 5-3, Table 5-3). The data clearly confirm that an adjustment in pH has an effect on Fe concentrations. As the pH increased in Vessel 3, Fe(total) concentrations decreased and Fe^{II} concentrations increased. Regardless of the change in pH for Vessel 3, each vessel displayed the same trends in Fe(total) and Fe^{II} concentrations over time (Figure 5-3). At approximately hour 22, Fe(total) concentrations appeared to increase with a slight lag behind an increase in temperature; however, the Fe(total) concentration changes did not correspond with changes in light intensity (light on versus light off conditions). In Vessel 2, Fe^{II} concentrations steadily increased in light on conditions and stabilized in light off conditions. In the other three vessels, Fe^{II} concentrations remained stable until hour 14 when the concentrations increased (Figure 5-3). This increase in concentration occurred one hour prior to when the light was turned off.

In comparison to Cycle 1, the Fe(total) concentrations were larger and more stable during this experiment. Fe^{II} concentrations were also above the MDL (Figure 5-2 and Table 5-3). The steady increase in Fe^{II} concentrations for Vessel 2 in light on conditions indicates that Fe^{III}

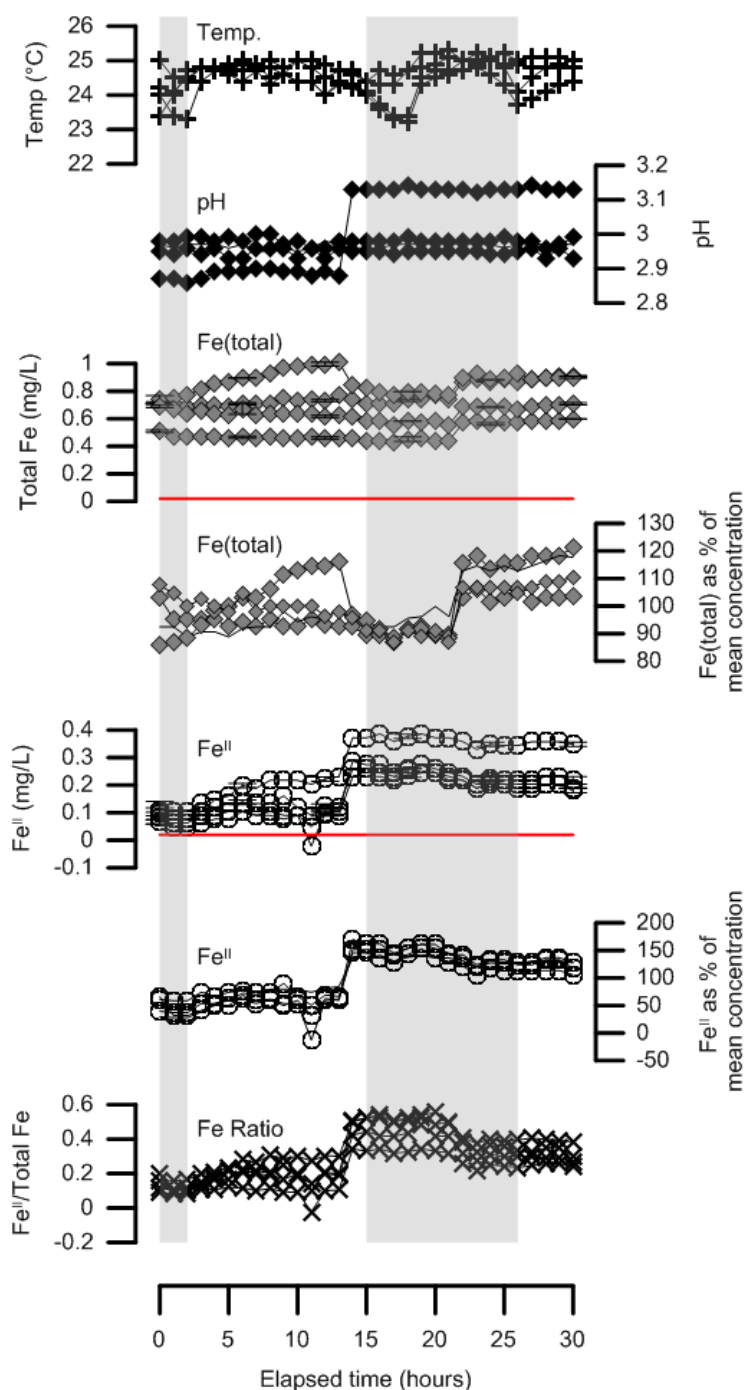


Figure 5-2. Cycle 2 (10/17-18/2014) results with all vessels (V1-V4) graphed together. All vessels contained Fe-only solutions. The solid red lines indicate the MDL for Fe^{II} analysis (0.02 mg/L Fe^{II}) on the HACH DR2800 Spectrophotometer. Fe(total) is equal to the sum of Fe^{II} and Fe^{III} species. Standard deviations are represented by error bars for triplicate samples. The gray shaded areas indicate when the light was turned off (dark conditions).

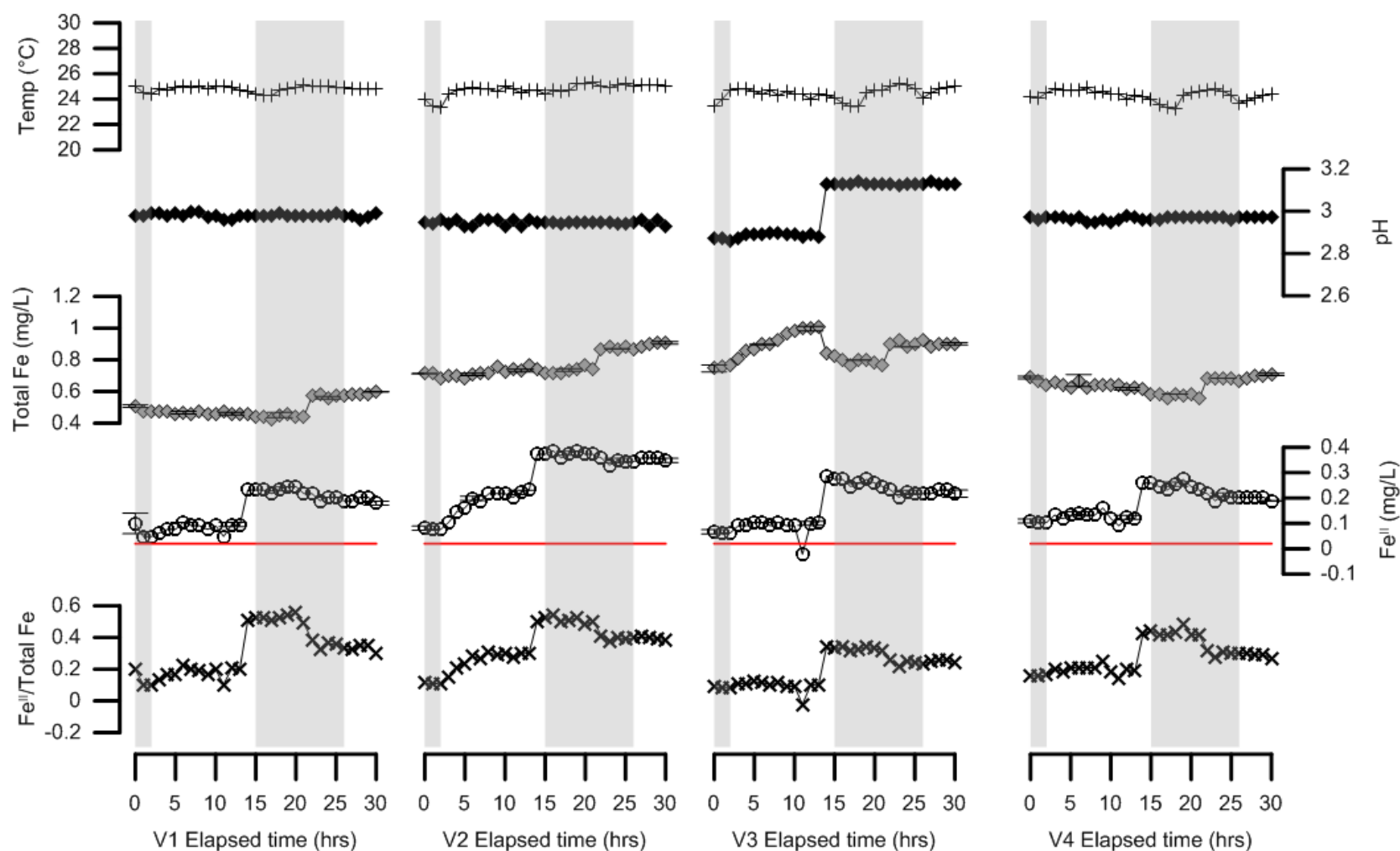


Figure 5-3. Cycle 2 (10/17-18/2014) results with all vessels (V1-V4) graphed separately. All vessels contained Fe-only solutions. The solid red lines indicate the MDL for Fe^{II} analysis (0.02 mg/L Fe^{II}) on the HACH DR2800 Spectrophotometer. Fe(total) is equal to the sum of Fe^{II} and Fe^{III} species. Standard deviations are represented by error bars for triplicate samples. The gray shaded areas indicate when the light was turned off (dark conditions). Note that the pH was adjusted in Vessel 3 during hour 13.

Table 5-3. Cycle 2 (10/17-18/2014) parameter variability

Parameter	Units	Vessel No.	Min.	Max.	Range (Min. - Max.)	Average
Temperature	°C	1	24.3	25.1	0.8	24.8
		2	23.3	25.3	2.0	24.7
		3	23.4	25.2	1.8	24.4
		4	23.2	24.9	1.7	24.3
pH	---	1	2.96	3.00	0.04	2.98
		2	2.93	2.96	0.03	2.95
		3	2.86	3.14	0.28	3.02
		4	2.95	2.98	0.03	2.97
Fe ^{II}	mg/L	1	0.048	0.245	0.197	0.153
		2	0.077	0.386	0.309	0.274
		3	< 0.02	0.288	0.310	0.169
		4	0.091	0.274	0.183	0.179
Fe(total)	mg/L	1	0.428	0.599	0.171	0.494
		2	0.684	0.911	0.227	0.770
		3	0.745	1.010	0.265	0.870
		4	0.556	0.708	0.152	0.640

Note: Min. is the minimum parameter value, and Max. is the maximum parameter value.

photoreduction may have occurred; however, the steady increase in Fe^{II} concentrations with the light on was not observed in Vessels 1, 3, and 4 (Figure 5-3). In these three vessels, the Fe^{II} concentrations abruptly increased around hour 14 (one hour before the light was turned off). This increase in Fe^{II} concentration did not correlate with changes in pH or temperature. This suggests that light on/off conditions were driving Fe^{II} concentration changes. For Vessel 3, the decrease in $\text{Fe}(\text{total})$ concentrations was likely due to HFO precipitation with increasing pH and decreasing temperature (Figure 5-3, V3). A combination of temperature and solution pH was the likely cause of $\text{Fe}(\text{total})$ concentration changes in this experiment.

5.3 Cycle 3: 10/25/2014

A 10-hour Fe-Se combined temperature cycle was conducted on October 25, 2014 (Table 5-1). The purpose of this experiment was to determine if Fe and Se concentration changes could be detected with increasing and decreasing temperature. In order to determine if temperature alone could drive Fe and Se cycles, this experiment was completed in the dark to eliminate the effects of Fe^{III} photoreduction.

Four reaction vessels containing Fe-Se solutions (Table 4-1) were prepared for this experiment. Each vessel contained 3000 $\mu\text{g/L}$ Se^{IV} . A full temperature cycle was not completed. Sampling was completed for one temperature increasing series and one temperature decreasing series (Figures 5-4 and 5-5). $\text{Fe}(\text{total})$ and Fe^{II} concentrations decreased slightly throughout the experiment, but were not directly linked to changes in temperature or pH. Se^{IV} concentrations cycled with temperature (Figures 5-4 and 5-5, Table 5-4).

A direct correlation between Fe concentrations and temperature was not observed. However, Se^{IV} cycled directly with temperature, and hysteresis was observed (Figure 5-6, Table 5-5). It is likely that Se^{IV} concentrations cycled due to temperature-dependent sorption of Se^{IV} onto 2-line ferrihydrite. The log of Se^{IV} concentrations (molar) was plotted versus $1/\text{temperature}$ (in Kelvin) to solve for enthalpy of sorption values in kJ/mol (Eq. 5, Figure 5-7, Table 5-6).

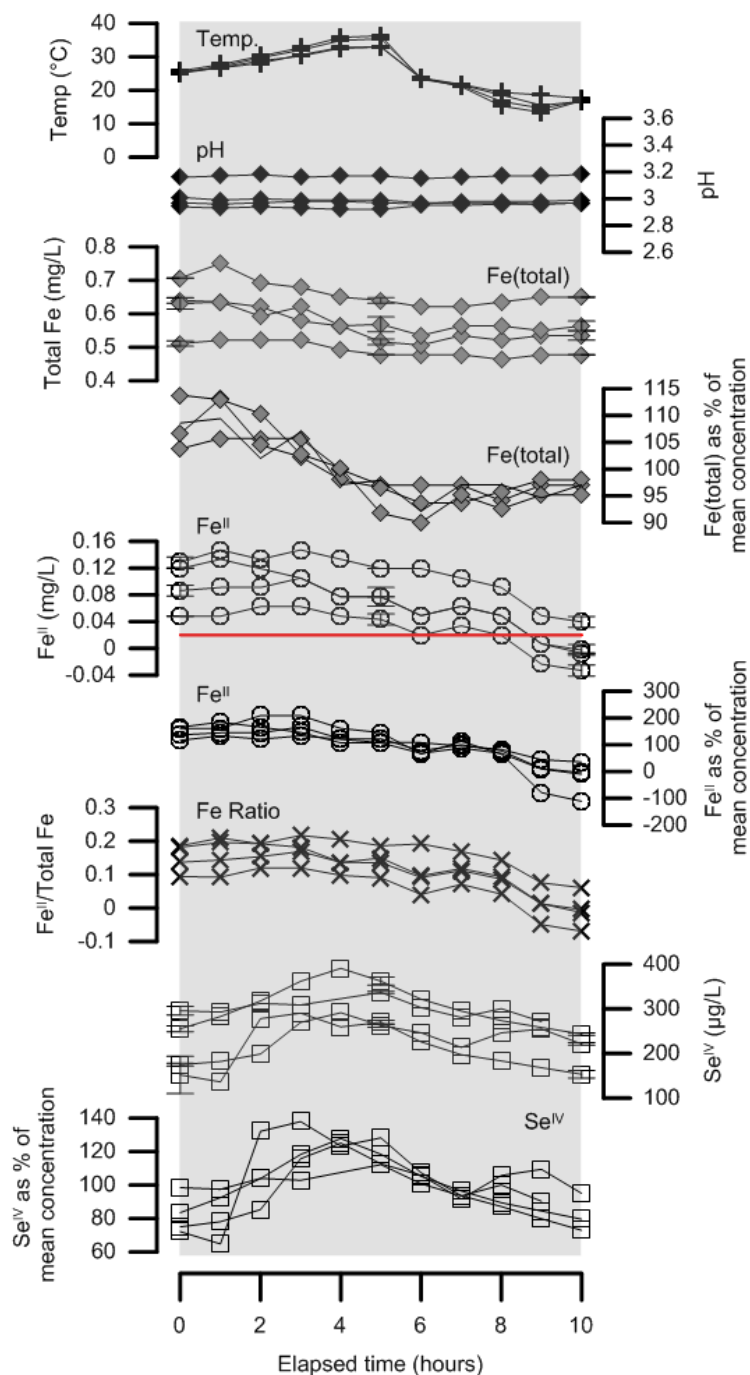


Figure 5-4. Cycle 3 (10/25/2014) results with all vessels (V1-V4) graphed together. All vessels contained Fe-Se solutions. The solid red line indicates the MDL for Fe^{II} analysis (0.02 mg/L Fe^{II}) on the HACH DR2800 Spectrophotometer. Fe(total) is equal to the sum of Fe^{II} and Fe^{III} species. Standard deviations are represented by error bars for triplicate samples. The gray shaded area indicates that the light was turned off for this experiment (dark conditions).

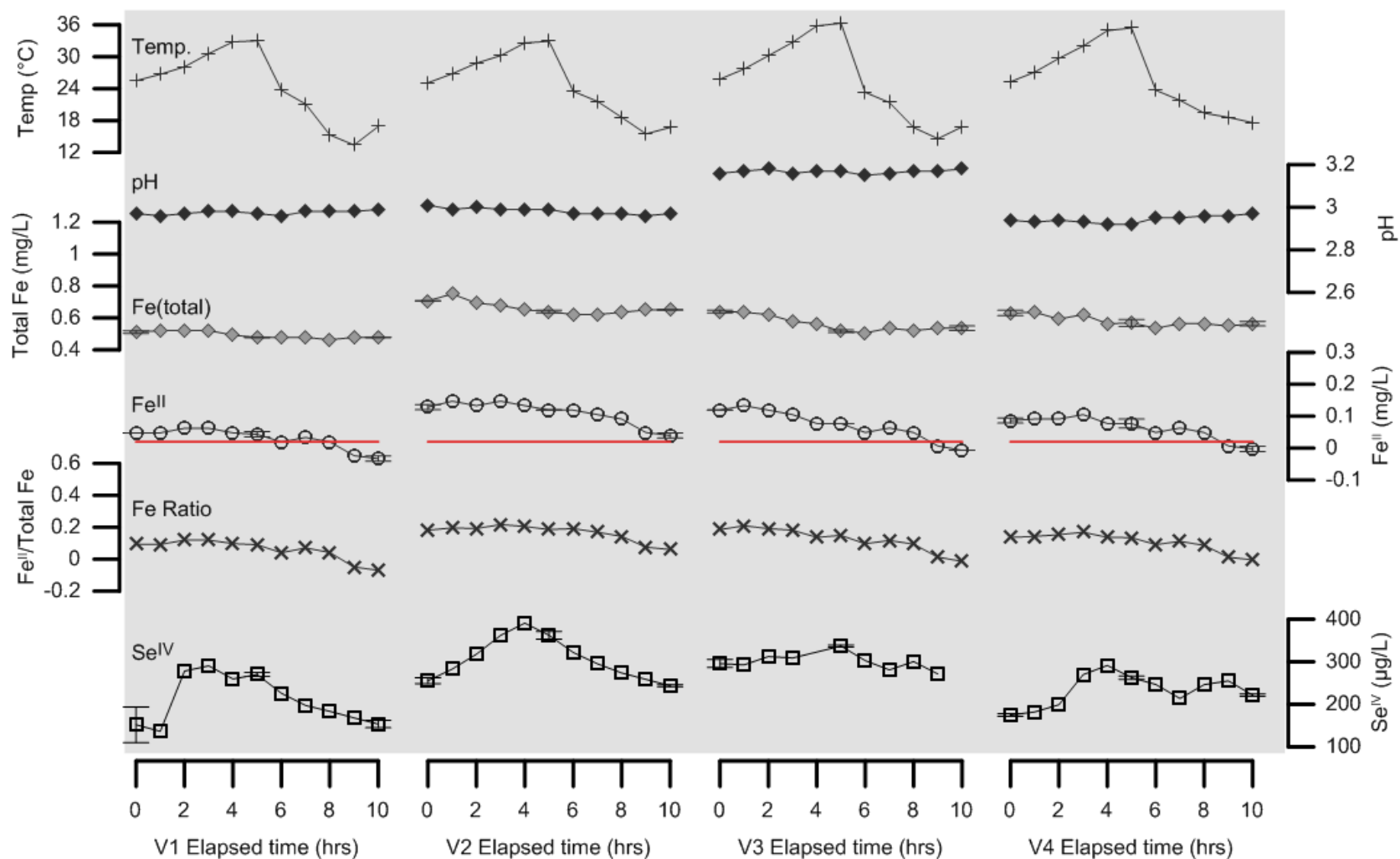


Figure 5-5. Cycle 3 (10/25/2014) results with all vessels (V1-V4) graphed separately. All vessels contained Fe-Se solutions. The solid red lines indicate the MDL for Fe^{II} analysis (0.02 mg/L Fe^{II}) on the HACH DR2800 Spectrophotometer. $\text{Fe}(\text{total})$ is equal to the sum of Fe^{II} and Fe^{III} species. Standard deviations are represented by error bars for triplicate samples. The gray shaded area indicates that the light was turned off for this experiment (dark conditions).

Table 5-4. Cycle 3 (10/25/2014) parameter variability

Parameter	Units	Vessel No.	Min.	Max.	Range (Min. - Max.)	Average
Temperature	°C	1	13.4	33.0	19.6	24.3
		2	15.5	32.9	17.4	24.8
		3	14.6	36.3	21.7	25.6
		4	17.6	35.4	17.8	26.0
pH	---	1	2.96	2.99	0.03	2.97
		2	2.96	3.01	0.05	2.98
		3	3.15	3.18	0.03	3.17
		4	2.92	2.97	0.05	2.94
Fe ^{II}	mg/L	1	< 0.02	0.062	0.095	0.030
		2	0.040	0.147	0.107	0.110
		3	< 0.02	0.133	0.140	0.072
		4	< 0.02	0.105	0.108	0.063
Fe(total)	mg/L	1	0.464	0.521	0.057	0.493
		2	0.621	0.750	0.129	0.663
		3	0.507	0.640	0.133	0.563
		4	0.535	0.636	0.101	0.581
Se ^{IV}	µg/L	1	136.4	290.4	154.0	210.4
		2	243.5	390.8	147.3	305.8
		3	271.4	337.0	65.6	300.2
		4	174.9	291.5	116.6	227.7

Note: Min. is the minimum parameter value, and Max. is the maximum parameter value.

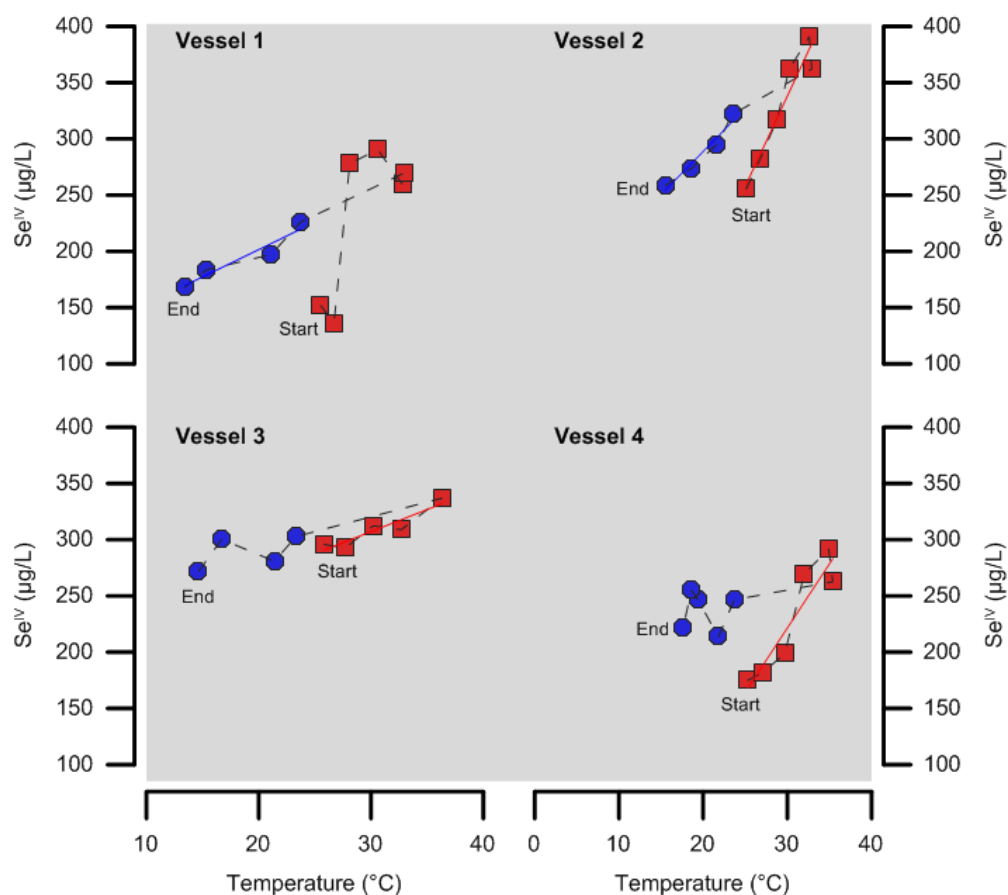


Figure 5-6. Cycle 3 (10/25/2014) relationship between Se^{IV} concentrations and temperature. The start and end of each cycle is labeled next to the corresponding data symbol (red square). Red squares represent the temperature increasing series, whereas the blue circles represent the temperature decreasing series. Solid red lines are linear regression lines for the temperature increasing series. Solid blue lines are linear regression lines for the temperature decreasing series. The black dashed lines indicate the order in which samples were collected over time. The gray shaded area indicates that the light was turned off for this experiment (dark conditions).

Table 5-5. Se^{IV} versus temperature linear regression results

Cycle No.	Vessel No.	Temperature (increase or decrease)	n	R ²	Slope	Intercept
3	1	increase	6	0.564	16.18	-245.5
	2	increase	6	0.921	16.07	-144.0
	3	increase	5	0.855	3.920	189.6
	4	increase	6	0.865	11.41	-120.8
	1	decrease	4	0.911	4.862	104.4
	2	decrease	4	0.951	7.647	135.9
	3	decrease	4	0.243	1.858	253.5
	4	decrease	5	1.40 x 10 ⁻⁵	0.027	236.0
4	3	increase 1	3	0.810	-0.323	20.91
	4	increase 1	4	0.859	2.417	-19.42
	3	decrease	6	0.219	-0.049	13.51
	4	decrease	6	0.916	1.974	25.28
	3	increase 2	6	0.602	-0.178	15.62
	4	increase 2	6	0.234	-0.081	37.74
6	3	increase 1	4	0.811	2.499	-19.01
	4	increase 1	4	0.647	-1.129	72.07
	3	decrease	6	0.819	0.684	35.83
	4	decrease	6	0.793	0.442	26.31
	3	increase 2	6	0.035	-0.001	0.479
	4	increase 2	6	0.315	0.490	32.20
7	1	increase 1	3	0.822	2.396	286.0
	2	increase 1	3	0.211	0.437	347.0
	3	increase 1	3	0.523	1.552	323.0
	4	increase 1	3	0.785	1.021	353.8
	1	decrease	6	0.861	0.769	342.1
	2	decrease	6	0.827	0.911	337.6
	3	decrease	6	0.811	1.149	346.1
	4	decrease	6	0.413	0.566	369.6
	1	increase 2	6	0.566	0.673	352.7
	2	increase 2	6	0.513	0.682	349.8
	3	increase 2	6	0.742	0.641	360.1
	4	increase 2	6	0.867	1.117	360.6

Note: n is the number of data points. R² is the coefficient of determination. Refer to Figures 5-6, 5-10, 5-16, and 5-20. Linear regression results were calculated using the Data Analysis ToolPak in Microsoft Excel. A separate linear regression was completed for each color coded series (increasing temperature 1, decreasing temperature, and increasing temperature 2) in the figures mentioned above. The linear results were graphed for R² values greater than 0.7.

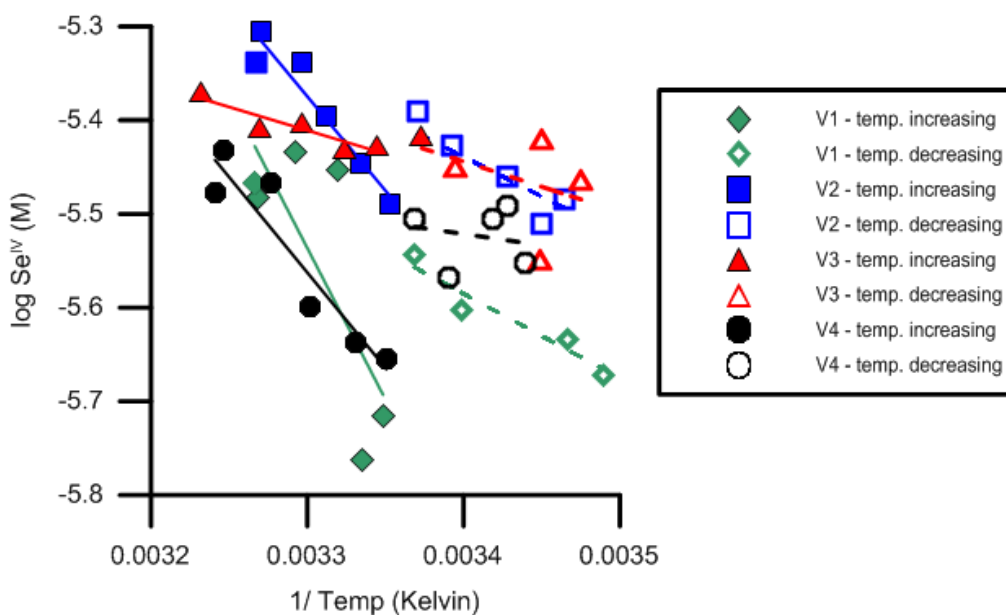


Figure 5-7. Enthalpy of sorption plot for Cycle 3 (10/25/2014). Increasing temperature series (solid symbols and lines) and decreasing temperature series (open symbols and dashed lines) data are plotted separately for each vessel. Vessel numbers are labelled V1 through V4.

Table 5-6. Conditional Enthalpies of Sorption for Cycle 3

Temperature (increase/decrease)	Vessel No.	R²	slope	n	Enthalpy (kJ/ mol)
Increase	1	0.585	-3232	6	-61.9
Increase	2	0.926	-2011	6	-38.5
Increase	3	0.854	-500.6	5	-9.58
Increase	4	0.883	-2036	6	-39.0
Decrease	1	0.973	-899.5	5	-17.2
Decrease	2	0.915	-849.2	5	-16.3
Decrease	3	0.183	-536.7	5	-10.3
Decrease	4	0.251	-242.1	5	-4.64

Note: R² is the coefficient of determination. n is the number of data points.

5.4 Cycle 4: 12/09/2014

Two experiments, a 10-hour Fe-only temperature cycle and a 10-hour Fe-Se combined temperature cycle, were conducted on December 9, 2014 (Table 5-1). The purpose of these experiments was to determine if Fe and Se concentration changes could be detected with increasing and decreasing temperature. Two vessels were prepared with Fe-only solution (Vessels 1 and 2) (Table 4-1). The other two vessels were prepared with Fe-Se solution (Vessels 3 and 4) (Table 4-1) to compare to the Cycle 3 (10/25/2014) results. The light remained on during these experiments to allow for Fe^{III} photoreduction. A full temperature cycle was completed for this experiment (temperature increase, temperature decrease, then a second temperature increase) (Figures 5-8 and 5-9).

The average light intensity was 3563 Lux. Fe^{II} cycled with temperature in both the Fe-only and Fe-Se combined experiments with a slight lag (Figures 5-8 and 5-9). Fe^{II} concentrations were larger in comparison with the previous dark (light off) cycle (Cycle 3). These larger Fe^{II} concentrations were likely the result of Fe^{III} photoreduction during light on conditions. $\text{Fe}(\text{total})$ concentrations remained relatively stable throughout the experiment (Figures 5-8 and 5-9, Table 5-7). Se^{IV} cycled with temperature in one of the two Fe-Se combined experiment vessels (Vessel 4) (Figures 5-8 and 5-9, Table 5-7).

Hysteresis was observed between temperature and Se^{IV} concentrations in Vessel 4 but was not observed in Vessel 3 (Figure 5-10, Table 5-5). The pH of Vessel 3 was likely too high for Se^{IV} cycling to occur (Table 5-7). In comparison, the pH of the other three vessels was less than 2.98. The log of Se^{IV} concentrations (molar) was plotted versus 1/temperature (in Kelvin) to solve for enthalpy of sorption values in kJ/mol (Eq. 5, Figure 5-11, Table 5-8).

5.5 Cycle 5: 1/29/2015

A 3.5 hour Se-only partial temperature cycle was completed on January 29, 2015 (Table 5-1). Sampling was completed for one temperature increasing series and one temperature decreasing series (Figures 5-12 and 5-13). The purpose of this experiment was to determine if Se

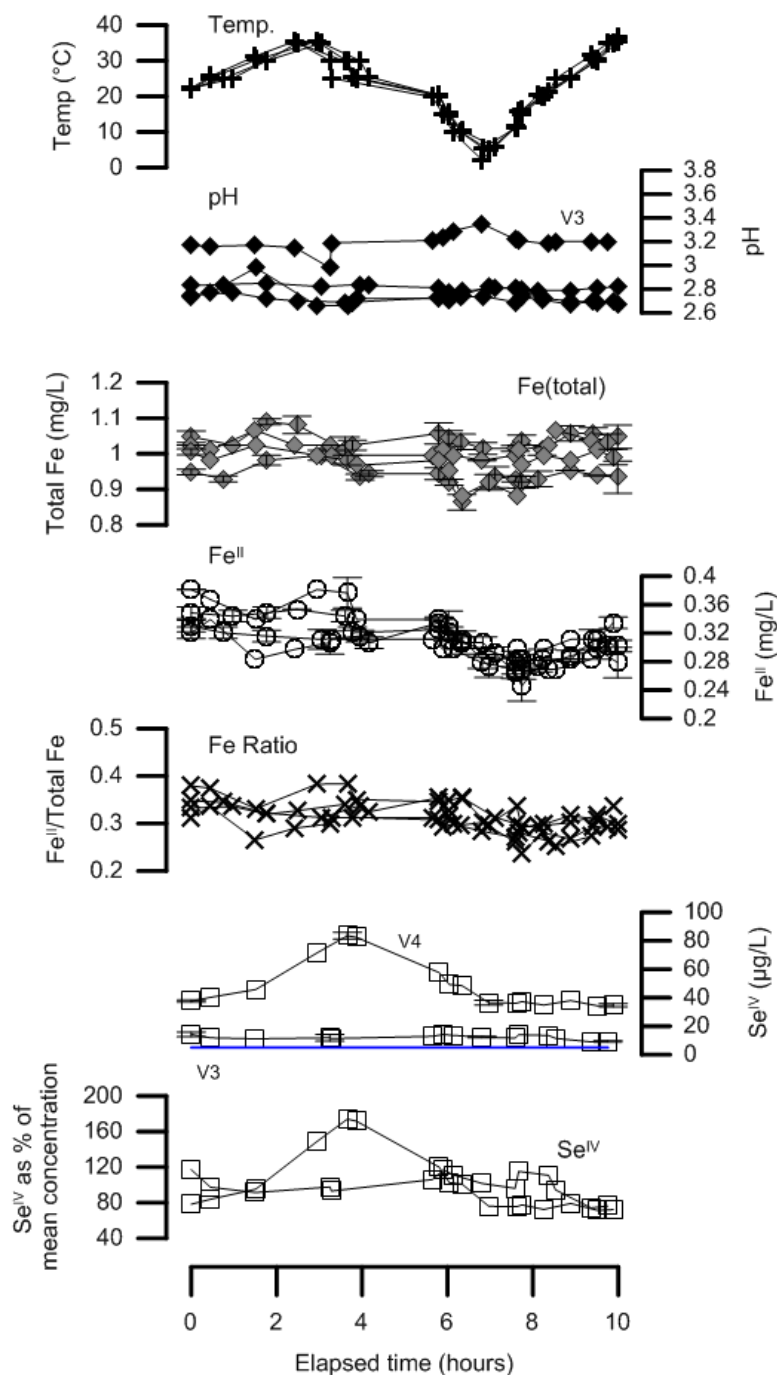


Figure 5-8. Cycle 4 (12/09/2014) results with all vessels (V1-V4) graphed together. Vessels 1 and 2 contained Fe-only solutions, whereas Vessels 3 and 4 contained Fe-Se solutions. The solid blue lines indicate the MDL for Se^{IV} analysis ($5 \mu\text{g/L Se}^{\text{IV}}$) on the Perkin Elmer Optima 2100 DV ICP-OES. Standard deviations are represented by error bars for triplicate samples.

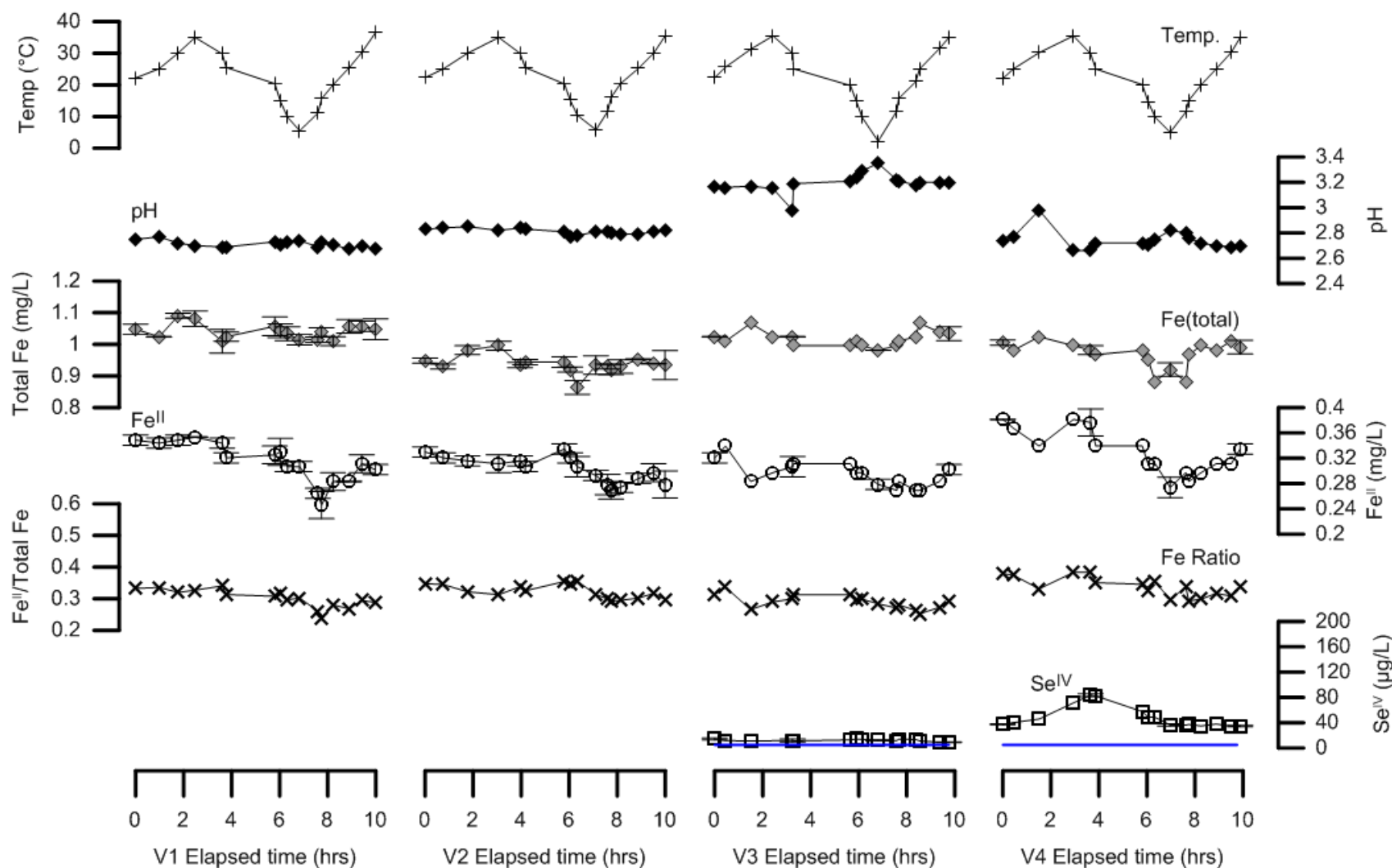


Figure 5-9. Cycle 4 (12/09/2014) results with all vessels (V1-V4) graphed separately. Vessels 1 and 2 contained Fe-only solutions, whereas Vessels 3 and 4 contained Fe-Se solutions. The solid blue lines indicate the MDL for Se^{IV} analysis (5 µg/L Se^{IV}) on the Perkin Elmer Optima 2100 DV ICP-OES. Standard deviations are represented by error bars for triplicate samples.

Table 5-7. Cycle 4 (12/9/2014) parameter variability

Parameter	Units	Vessel No.	Min.	Max.	Range (Min. - Max.)	Average
Temperature	°C	1	5.5	36.5	31.0	22.3
		2	5.8	35.4	29.6	22.4
		3	2.2	35.5	33.3	22.3
		4	5.0	35.5	30.5	22.1
pH	---	1	2.67	2.77	0.10	2.71
		2	2.77	2.85	0.08	2.81
		3	2.98	3.35	0.37	3.20
		4	2.66	2.98	0.32	2.74
Fe ^{II}	mg/L	1	0.246	0.353	0.107	0.314
		2	0.269	0.335	0.066	0.303
		3	0.269	0.339	0.070	0.295
		4	0.274	0.381	0.107	0.328
Fe(total)	mg/L	1	1.010	1.090	0.080	1.041
		2	0.864	0.996	0.132	0.938
		3	0.982	1.067	0.085	1.019
		4	0.882	1.024	0.142	0.970
Se ^{IV}	µg/L	3	9.0	14.2	5.2	12.1
		4	34.3	83.5	49.2	48.0

Note: Min. is the minimum parameter value, and Max. is the maximum parameter value.

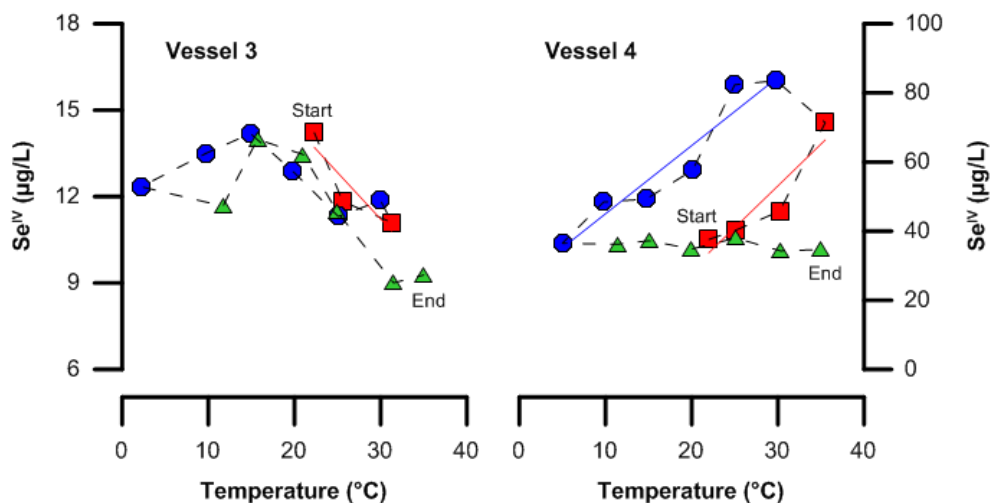


Figure 5-10. Cycle 4 (12/9/2014) relationship between Se^{IV} concentrations and temperature. The start and end of each cycle is labeled next to the corresponding data symbol (red square). Red squares represent the first temperature increasing series, blue circles represent the temperature decreasing series, and green triangles represent the second temperature increasing series. Solid red lines are linear regression lines for the first temperature increasing series. Solid blue lines are linear regression lines for the temperature decreasing series. The black dashed lines indicate the order in which samples were collected over time.

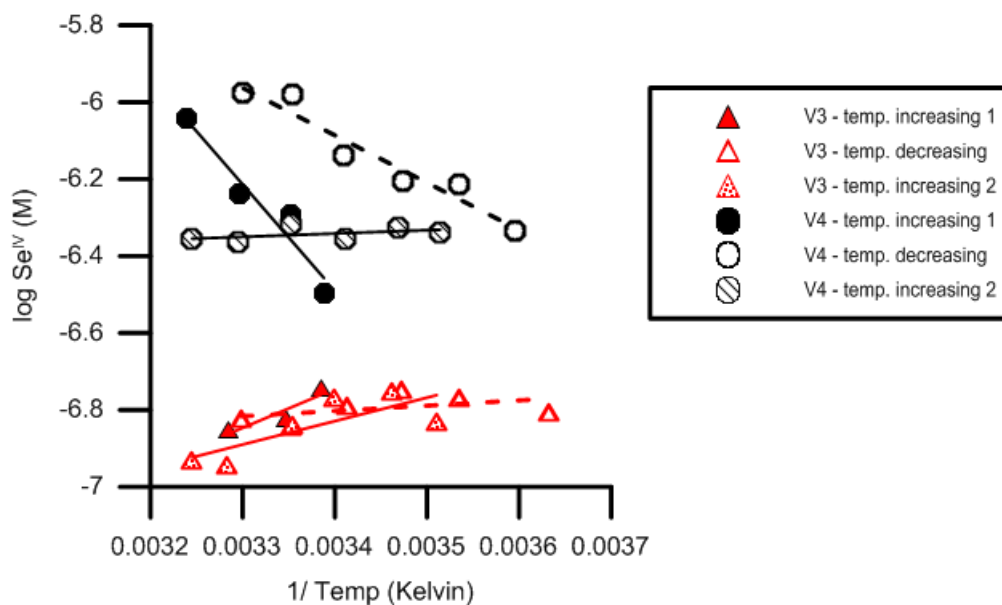


Figure 5-11. Enthalpy of sorption plot for Cycle 4 (12/9/2014). The increasing temperature series 1 (solid symbols and solid lines), decreasing temperature series (open symbols and dashed lines), and increasing temperature series 2 (patterned symbols and solid lines) data are plotted separately for each vessel. Vessel numbers are labelled V3 and V4.

Table 5-8. Conditional Enthalpies of Sorption for Cycle 4

Temperature (increase/decrease)	Vessel No.	R²	slope	n	Enthalpy (kJ/ mol)
Increase 1	3	0.835	-1011	3	19.4
Increase 1	4	0.932	-2758	4	-52.8
Decrease	3	0.212	137.4	6	2.63
Decrease	4	0.937	-1231	6	-23.6
Increase 2	3	0.615	609.6	6	11.7
Increase 2	4	0.237	-86.45	6	1.66

Note: R² is the coefficient of determination. n is the number of data points. An outlying data point was removed from the temperature increase 1 series calculation for Vessel 3.

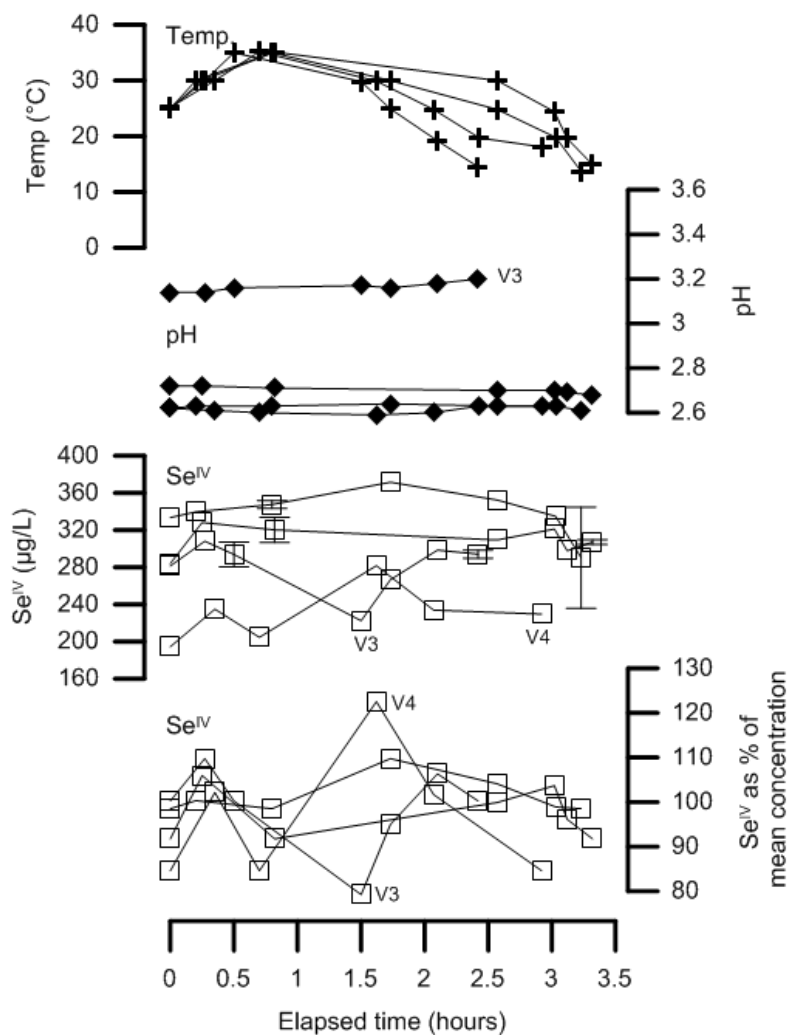


Figure 5-12. Cycle 5 (1/29/2015) results with all vessels (V1-V4) graphed together. All vessels contained Se-only solutions. Standard deviations are represented by error bars for triplicate samples.

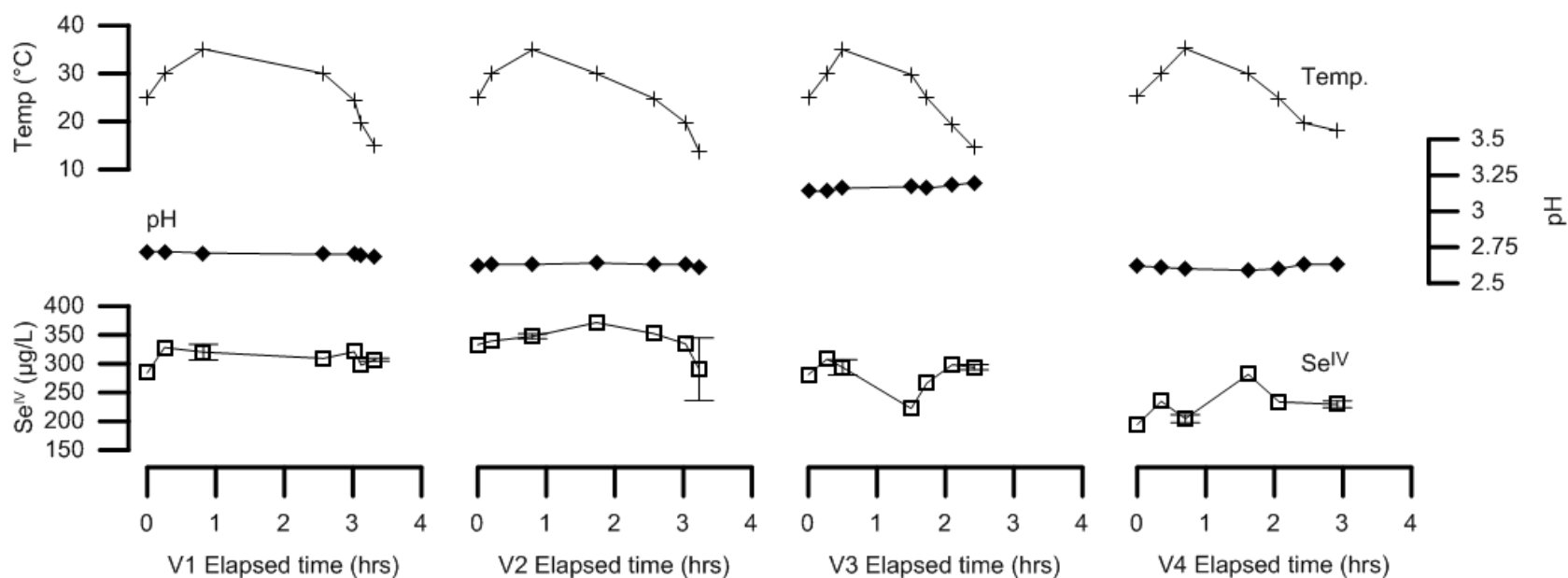


Figure 5-13. Cycle 5 (1/29/2015) results with all vessels (V1-V4) graphed separately. All vessels contained Se-only solutions. Standard deviations are represented by error bars for triplicate samples.

concentration changes could be detected with increasing or decreasing temperature over a short time period. The light remained on for this experiment with an average light intensity of 1346 Lux. Se photo-redox cycles were not probable during these experiments; therefore, the light intensity was lower compared to previous experiments, because the light was located at a greater distance from the reaction vessels for better ease of sampling.

The pH was adjusted to 3.00 for all vessels at the beginning of the 48 hour equilibration period; however, at the beginning of the experiment, the pH values differed in each vessel. The pH in Vessel 3, averaging 3.16 standard pH units, was higher than the other three vessels which averaged 2.70 (Vessel 1), 2.63 (Vessel 2), and 2.61 (Vessel 4) (Figures 5-12 and 5-13, Table 5-9). Se^{IV} concentrations did not cycle with temperature in this experiment. Se^{IV} concentrations also displayed different trends in each vessel (Figures 5-12 and 5-13). Se^{IV} cycles were likely not detected due to the short temperature cycle (< 3.5 hours).

5.6 Cycle 6: 2/28/2015

Two experiments, a 7-hour Fe-only temperature cycle and a 7-hour Fe-Se combined temperature cycle, were conducted on February 28, 2015 (Table 5-1). These experiments were conducted to determine if Fe and Se concentration changes could be detected with increasing and decreasing temperature. The light was turned off for these experiments to eliminate the possibility of Fe^{III} photoreduction.

Fe^{II} concentrations remained below the method detection limit in both the Fe-only and Fe-Se combined experiment vessels indicating that Fe^{III} photoreduction likely did not occur in light off conditions. Fe(total) concentrations did not display any cycling trends with temperature (Figures 5-14 and 5-15, Table 5-10). Se^{IV} cycled with temperature in one of the two Fe-Se combined experiment vessels (Vessel 3) (Figures 5-14 and 5-15).

Hysteresis was observed for Se^{IV} concentrations in Vessel 3 (Figure 5-16). The log of Se^{IV} concentrations (molar) was plotted versus $1/\text{temperature}$ (in Kelvin) to solve for enthalpy of sorption values in kJ/mol (Eq. 5, Figure 5-17, Table 5-11).

Table 5-9. Cycle 5 (1/29/2015) parameter variability

Parameter	Units	Vessel No.	Min.	Max.	Range (Min. - Max.)	Average
Temperature	°C	1	14.9	35.1	20.2	25.6
		2	13.7	35.0	21.3	25.5
		3	14.5	35.0	20.5	25.5
		4	18.1	35.2	17.1	26.1
pH	---	1	2.68	2.72	0.04	2.70
		2	2.61	2.64	0.03	2.63
		3	3.14	3.20	0.06	3.16
		4	2.59	2.63	0.04	2.61
Se ^{IV}	µg/L	1	284.1	328.2	44.1	309.7
		2	290.3	371.5	81.2	338.5
		3	222.4	308.1	85.7	280.7
		4	194.5	281.7	87.2	229.9

Note: Min. is the minimum parameter value, and Max. is the maximum parameter value.

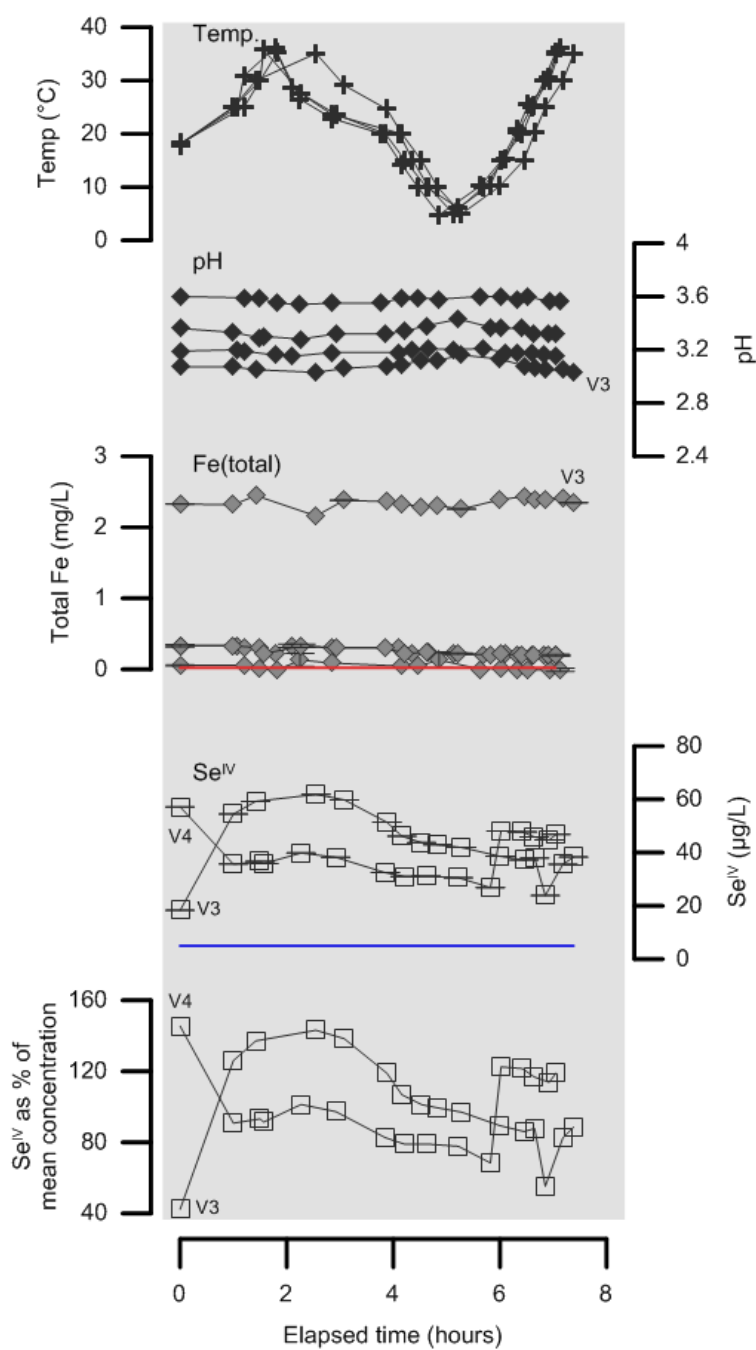


Figure 5-14. Cycle 6 (2/28/2015) results with all vessels (V1-V4) graphed together. Vessels 1 and 2 contained Fe-only solutions, whereas Vessels 3 and 4 contained Fe-Se solutions. The solid red line indicates the MDL for Fe^{II} analysis (0.02 mg/L Fe^{II}) on the HACH DR2800 Spectrophotometer. The solid blue line indicates the MDL for Se^{IV} analysis (5 $\mu\text{g/L}$ Se^{IV}) on the Perkin Elmer Optima 2100 DV ICP-OES. Standard deviations are represented by error bars for triplicate samples. The gray shaded area indicates that the light was turned off for this experiment (dark conditions).

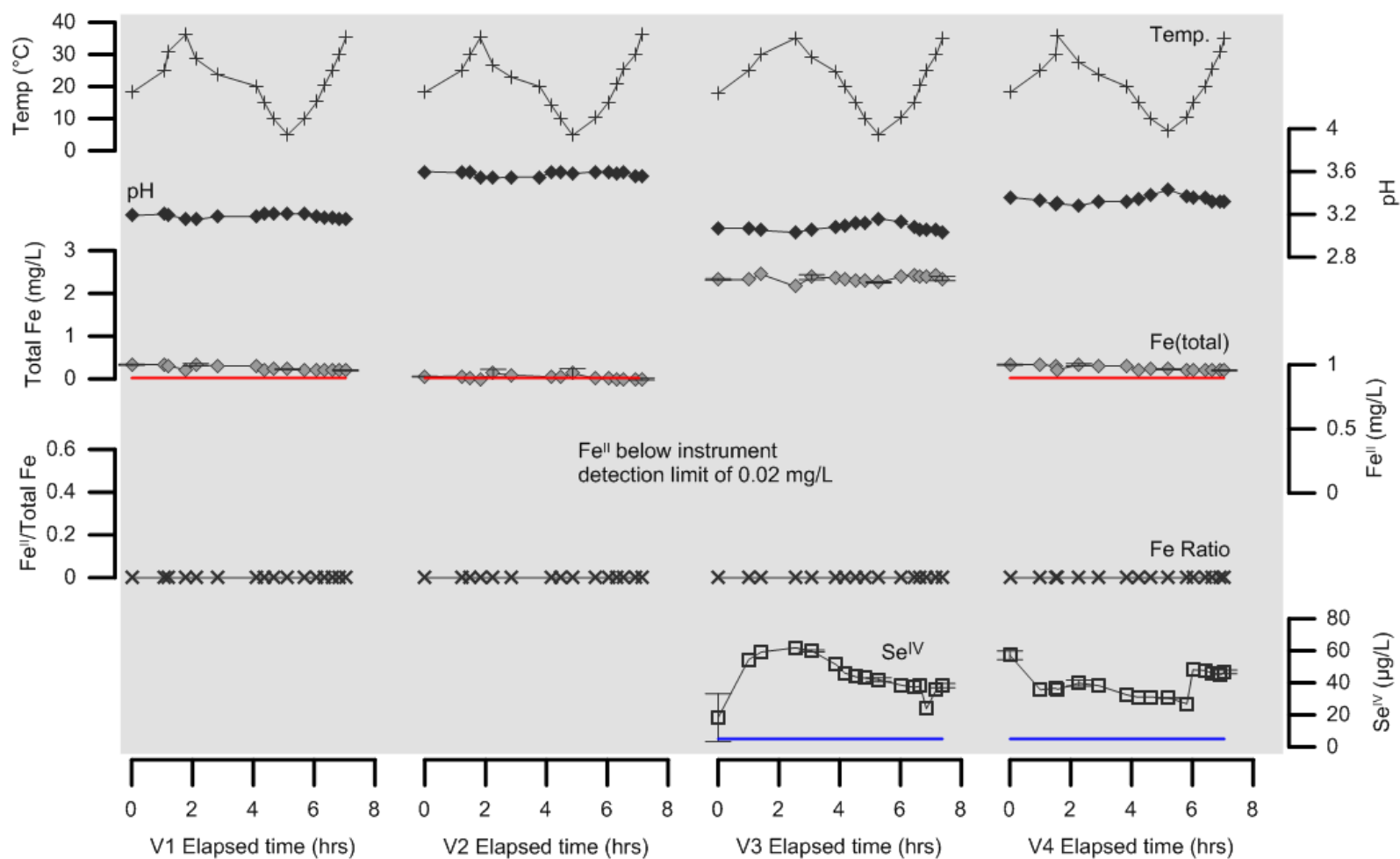


Figure 5-15. Cycle 6 (2/28/2015) results with all vessels (V1-V4) graphed separately. Vessels 1 and 2 contained Fe-only solutions, whereas Vessels 3 and 4 contained Fe-Se solutions. The solid red lines indicate the MDL for Fe^{II} analysis (0.02 mg/L Fe^{II}) on the HACH DR2800 Spectrophotometer. The solid blue lines indicate the MDL for Se^{IV} analysis (5 µg/L Se^{IV}) on the Perkin Elmer Optima 2100 DV ICP-OES. Standard deviations are represented by error bars for triplicate samples. The gray shaded area indicates that the light was turned off for this experiment (dark conditions).

Table 5-10. Cycle 6 (2/28/2015) parameter variability

Parameter	Units	Vessel No.	Min.	Max.	Range (Min. - Max.)	Average
Temperature	°C	1	5.0	36.2	31.2	21.8
		2	4.8	36.2	31.4	21.6
		3	5.0	35.1	30.1	21.7
		4	6.1	35.8	29.7	21.8
pH	---	1	3.19	3.25	0.06	3.22
		2	3.54	3.60	0.06	3.58
		3	3.03	3.16	0.13	3.08
		4	3.28	3.43	0.15	3.34
Fe(total)	mg/L	1	0.198	0.332	0.133	0.252
		2	< 0.02	0.132	0.143	0.036
		3	2.161	2.447	0.286	2.346
		4	0.198	0.332	0.133	0.252
Se ^{IV}	µg/L	3	18.3	61.8	43.6	43.2
		4	26.9	57.2	30.3	39.3

Note: Min. is the minimum parameter value, and Max. is the maximum parameter value. All Fe^{II} concentrations were below the MDL of 0.02 mg/L.

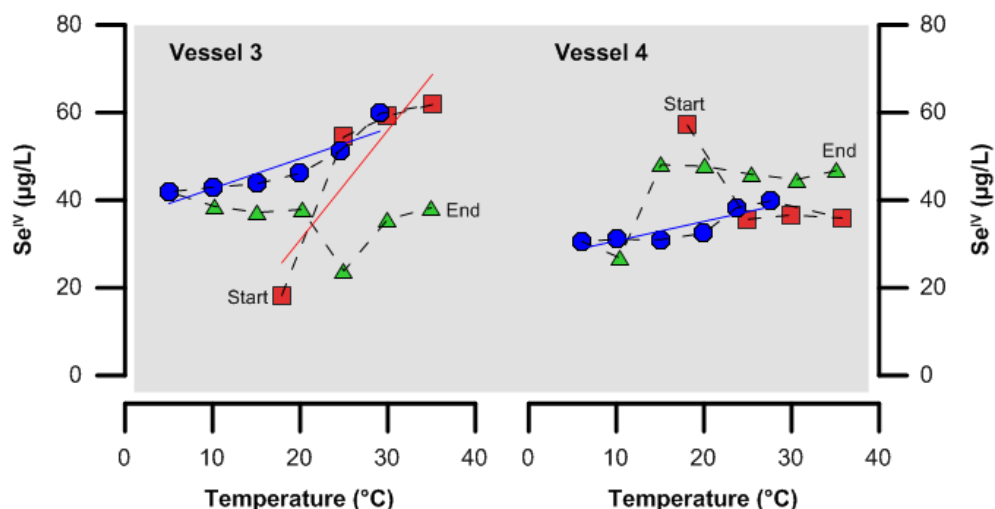


Figure 5-16. Cycle 6 (2/28/2015) relationship between Se^{IV} concentrations and temperature. The start and end of each cycle is labeled next to the corresponding data symbol (red square). Red squares represent the first temperature increasing series, blue circles represent the temperature decreasing series, and green triangles represent the second temperature increasing series. Solid red lines are linear regression lines for the first temperature increasing series. Solid blue lines are linear regression lines for the temperature decreasing series. The black dashed lines indicate the order in which samples were collected over time. The gray shaded area indicates that the light was turned off for this experiment (dark conditions).

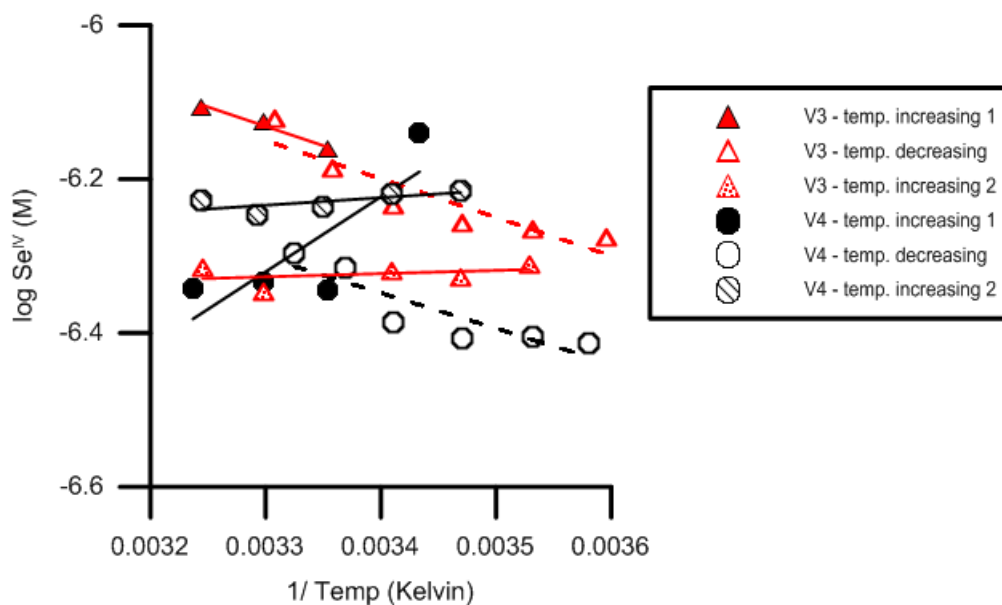


Figure 5-17. Enthalpy of sorption plot for Cycle 6 (2/28/2015). The increasing temperature series 1 (solid symbols and solid lines), decreasing temperature series (open symbols and dashed lines), and increasing temperature series 2 (patterned symbols and solid lines) data are plotted separately for each vessel. Vessel numbers are labelled V3 and V4.

Table 5-11. Conditional Enthalpies of Sorption for Cycle 6

Temperature (increase/decrease)	Vessel No.	R²	slope	n	Enthalpy (kJ/ mol)
Increase 1	3	0.967	-502.5	3	-9.62
Increase 1	4	0.660	973.0	4	18.6
Decrease	3	0.833	-500.4	6	-9.58
Decrease	4	0.789	-460.4	6	-8.82
Increase 2	3	0.126	41.68	5	0.798
Increase 2	4	0.466	98.35	5	1.88

Note: R² is the coefficient of determination. n is the number of data points. Outlying data points were removed from the temperature increase 1 series and from the temperature increase 2 series calculations for Vessel 3. An outlying data point was also removed from the temperature increase 2 series calculation for Vessel 4.

5.7 Cycle 7: 4/26/2015

A 7-hour Se-only temperature cycle was completed on April 26, 2015 (Table 5-1). The purpose of this experiment was to determine if Se concentration changes could be detected over a longer time period than Cycle 5. The light was turned on for this experiment, and the average light intensity was 110 Lux. Se photo-redox cycles were not probable during these experiments; therefore, the light intensity was lower compared to previous experiments, because the light was located at a greater distance from the reaction vessels for better ease of sampling.

Se^{IV} cycled with temperature in all four vessels (Figures 5-18 and 5-19, Table 5-12). Hysteresis was observed for all Se^{IV} concentrations versus temperature (Figure 5-20). The log of Se^{IV} concentrations (molar) was plotted versus 1/temperature (in Kelvin) to solve for enthalpy of sorption values in kJ/mol (Eq. 5, Figure 5-21, Table 5-13). This experiment revealed that Se concentrations can cycle with temperature, even without the presence of 2-line ferrihydrite or Fe species in solution.

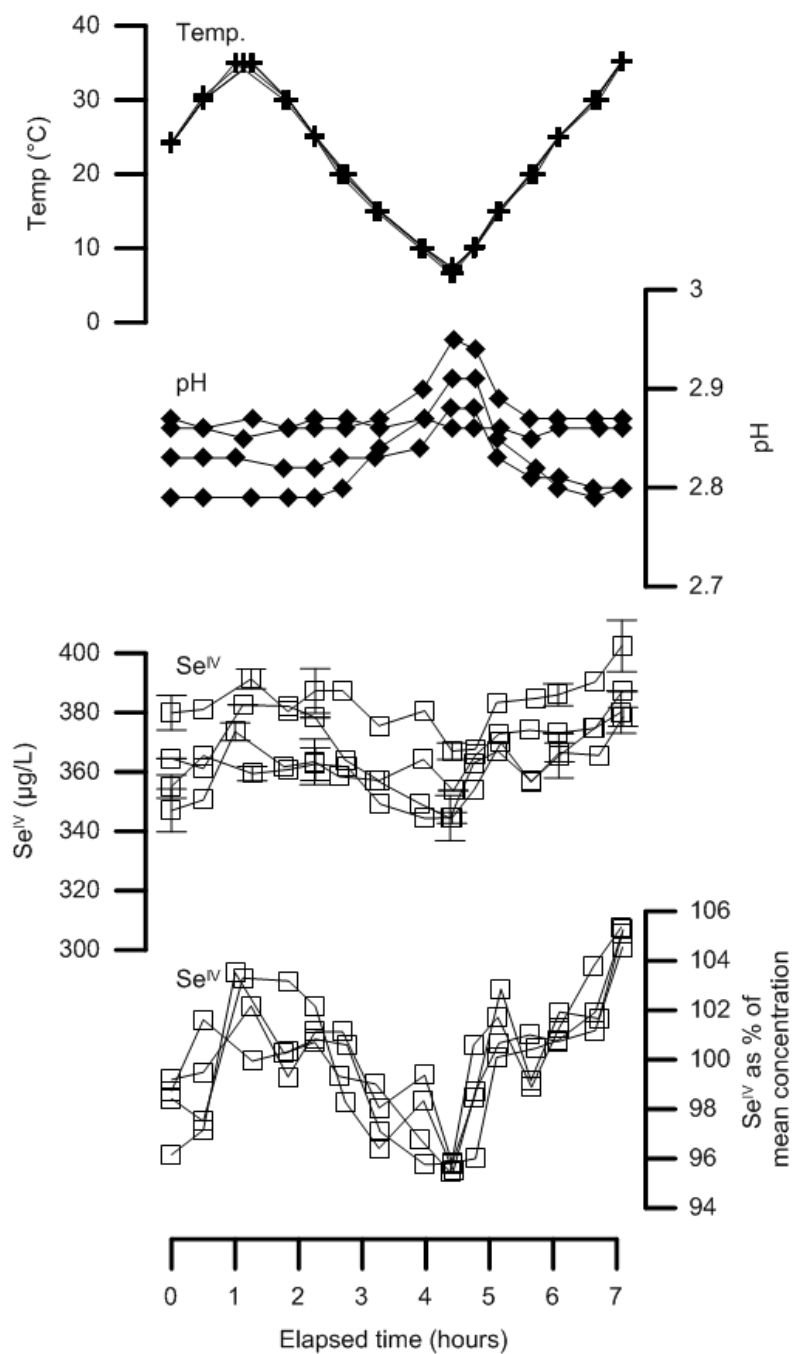


Figure 5-18. Cycle 7 (4/26/2015) results with all vessels (V1-V4) graphed together. All vessels contained Se-only solutions. Standard deviations are represented by error bars for triplicate samples.

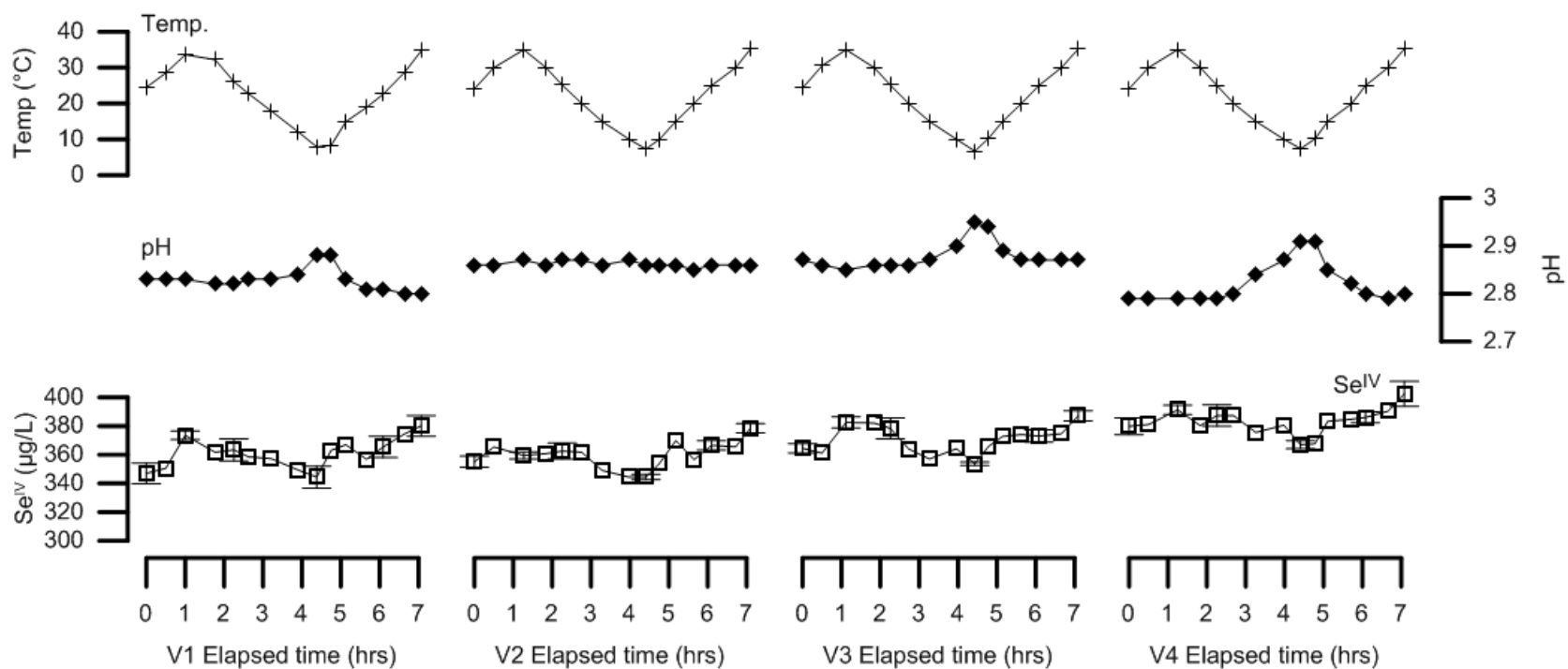


Figure 5-19. Cycle 7 (4/26/2015) results with all vessels (V1-V4) graphed separately. All vessels contained Se-only solutions. Standard deviations are represented by error bars for triplicate samples.

Table 5-12. Cycle 7 (4/26/2015) parameter variability

Parameter	Units	Vessel No.	Min.	Max.	Range (Min. - Max.)	Average
Temperature	°C	1	6.6	35.1	28.5	22.1
		2	7.3	35.2	27.9	22.1
		3	6.7	35.2	28.5	22.1
		4	7.4	35.2	27.8	22.1
pH	---	1	2.80	2.88	0.08	2.83
		2	2.85	2.87	0.02	2.86
		3	2.85	2.95	0.10	2.88
		4	2.79	2.91	0.12	2.82
Se ^{IV}	µg/L	1	344.4	380.2	35.8	360.8
		2	344.4	378.5	34.2	359.6
		3	353.7	387.2	33.5	370.4
		4	367.0	402.5	35.5	383.0

Note: Min. is the minimum parameter value, and Max. is the maximum parameter value.

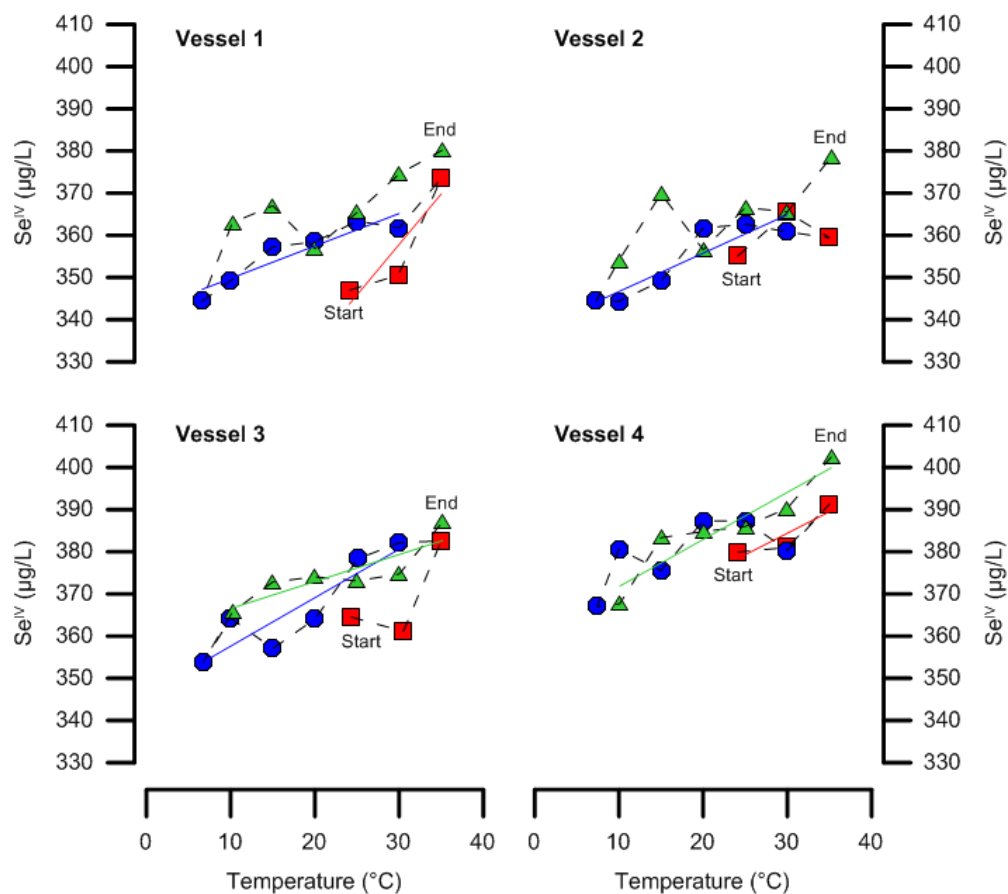


Figure 5-20. Cycle 7 (4/26/2015) relationship between Se^{IV} concentrations and temperature. The start and end of each cycle is labeled next to the corresponding data symbol (red square). Red squares represent the first temperature increasing series, blue circles represent the temperature decreasing series, and green triangles represent the second temperature increasing series. Solid red lines are linear regression lines for the first temperature increasing series. Solid blue lines are linear regression lines for the temperature decreasing series. Solid green lines are linear regression lines for the second temperature increasing series. The black dashed lines indicate the order in which samples were collected over time.

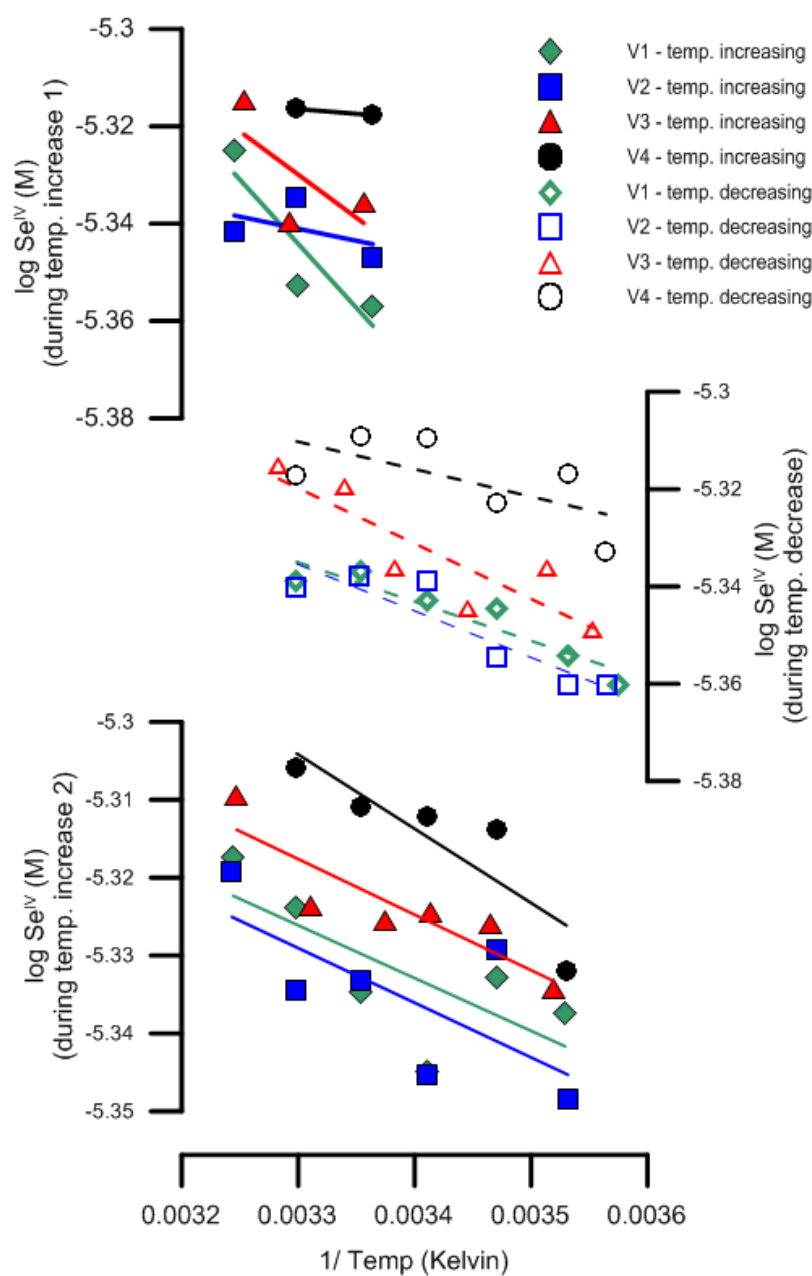


Figure 5-21. Enthalpy of sorption plot for Cycle 7 (4/26/2015). Increasing temperature (solid symbols and lines) and decreasing temperature (open symbols and dashed lines) data are plotted separately for each vessel. Vessel numbers are labelled V1 through V4.

Table 5-13. Conditional Enthalpies of Sorption for Cycle 7

Temperature (increase/decrease)	Vessel No.	R²	slope	n	Enthalpy (kJ/ mol)
Increase 1	1	0.817	-263.3	3	-5.0
Increase 1	2	0.223	-49.57	3	-0.9
Increase 1	3	0.468	-177.4	3	-3.4
Increase 1	4	1	-19.41	2	-0.4
Decrease	1	0.873	-80.60	6	-1.5
Decrease	2	0.838	-95.61	6	-1.8
Decrease	3	0.766	-113.8	6	-2.2
Decrease	4	0.429	-56.33	6	-1.1
Increase 2	1	0.543	-67.79	6	-1.3
Increase 2	2	0.507	-70.23	6	-1.3
Increase 2	3	0.786	-71.35	6	-1.4
Increase 2	4	0.773	-1825	5	-1.8

Note: R² is the coefficient of determination. n is the number of data points. An outlying data point was removed from the temperature increase 1 series calculation for Vessel 4.

6 DISCUSSION

6.1 Comparison of similar cycles

Since solution components and experiment conditions differed for each cycle, the cycles were separated into groups (Fe-only, Se-only, and Fe-Se combined experiments) (Table 6-1) for comparison. The purpose of this section is to identify similarities and differences within each group of cycles.

6.1.1 Fe-only cycles

The Fe-only experiments included cycles 1, 2, 4 and 6 (Table 6-1). For Cycles 1 and 2, the light was turned on and off in an attempt to drive Fe cycles with light via Fe^{III} photoreduction; however, it was found that the effects of temperature and light could not be separated due to the heating of solution when the light was turned on.

For Cycle 1, Fe^{II} concentrations were below the MDL. This was likely due to the short equilibration time and the short period of time the light was turned on. The Fe^{II} concentrations for Cycle 2 were above the MDL indicating that Fe^{III} photoreduction occurred during this light cycle experiment. In comparison to Cycle 1, Cycle 2 had a longer equilibration time which resulted in an increased Fe(total) concentration. Therefore, the likelihood of Fe^{III} photoreduction and Fe^{II} detection was higher, due to the larger Fe^{III} species concentration in solution when the light was turned on.

The temperature was manually controlled for Cycles 4 and 6. The light remained on for Cycle 4 and was turned off during Cycle 6 (Table 6-1). Fe^{II} concentrations were detected in Cycle 4, but were below the MDL in Cycle 6, indicating that Fe^{III} photoreduction was occurring only when the light was turned on. The Fe(total) concentration for Cycle 6 in Vessel 3 was much higher than the other vessels. This was due to the lower pH value of the Vessel 3 solution, ranging from 3.03 to 3.16. The pH values in Cycle 4 ranged from 2.66 to 3.35, and the Fe(total) concentrations were greater than those in Cycle 6. In both experiments, Fe(total) concentrations

Table 6-1. Summary of cycles by group (Fe-only, Se-only, and Fe-Se combined)

Cycle No.	Date	No. Vessels	2-line ferrihydrite (mg)	Se ^{IV} (µg/L)	Light	Approx. temperature range	Experiment time (hours)
Fe-only cycles							
1	7/22-23/14	1	500	---	Cycle	21-23 °C	22
2	10/17-18/14	4	500	---	Cycle	23-26 °C	30
4	12/9/14	2	500	---	On	0-35 °C	10
6	2/28/15	2	500	---	Off	0-35 °C	7
Se-only cycles							
5	1/29/15	4	---	300	On	10-35 °C	3.5
7	4/26/15	4	---	300	On	5-35 °C	7
Fe-Se cycles							
3	10/25/15	4	500	3000	Off	10-35 °C	10
4	12/9/14	2	500	300	On	0-35 °C	10
6	2/28/15	2	500	300	Off	0-35 °C	7

did not cycle with temperature. However, in Cycle 4, Fe^{II} concentrations appeared to cycle with a slight lag behind the change in temperature (Figure 5-9).

6.1.2 Se-only cycles

The Se-only experiments included cycles 5 and 7 (Table 6-1). The light was turned on for both experiments, because Fe was not present in solution. Se oxidation state and Se sorption to glassware are also not known to change in light off versus light on conditions. Cycle 5 was a partial temperature cycle (temperature increase then temperature decrease), whereas Cycle 7 was a full temperature cycle (temperature increase, temperature decrease, then a second temperature increase). Se^{IV} concentrations did not cycle in phase with temperature in Cycle 5. This was likely due to the short run time of the experiment (3.5 hours). Cycle 7 did display Se^{IV} concentration cycles with temperature. For all vessels, the initial Se^{IV} concentration was 300 $\mu\text{g/L}$; however, due to solution preparation and potential evaporation loss, a -20 to +50 $\mu\text{g/L}$ uncertainty was estimated. Although the initial and reported Se^{IV} concentrations throughout the experiment may be biased high, the overall trends in concentration with temperature are consistent for each vessel. The cycling of Se^{IV} with changes in temperature suggests that Se^{IV} was likely sorbing to the glass reaction vessels during the experiments. The magnitude of these concentration changes are small in comparison to Fe-Se combined cycles (Table 6-2), likely due to the additional sorption surfaces provided by the solid 2-line ferrihydrite in Fe-Se experiments.

6.1.3 Fe-Se combined cycles

The Fe-Se experiments included cycles 3, 4, and 6 (Table 6-1). Cycle 3 and Cycle 6 were completed in the dark, whereas Cycle 4 was completed in the light. The solutions for Cycles 4 and 6 consisted of 300 $\mu\text{g/L}$ Se^{IV} , whereas the Cycle 3 solution consisted of 3000 $\mu\text{g/L}$ Se^{IV} . Se^{IV} concentration cycles were observed in both light and dark conditions. Cycle 6 and Cycle 4 each had one vessel in which Se^{IV} concentrations did not cycle with temperature. These two vessels had the highest pH values of all Fe-Se experiments (Figures 5-9 and 5-15).

Table 6-2. Comparison of Se-only and Fe-Se cycles

Cycle No.	Vessel	Light (on/off)	Se cycle (yes/no)	Initial Se ^{IV} (µg/L)	Mean Se ^{IV} (µg/L)	% Se ^{IV} lost ^a	Max. pH	Min. pH	Mean pH	Se ^{IV} % Range ^b
Se-only cycles										
5	V1	on	no	300	310	x	2.72	2.68	2.70	15
5	V2	on	no	300	339	x	2.64	2.61	2.63	27
5	V3	on	no	300	281	6.3	3.20	3.14	3.16	29
5	V4	on	no	300	230	23	2.63	2.59	2.61	38
7	V1	on	yes	300	361	x	2.88	2.80	2.83	9.9
7	V2	on	yes	300	360	x	2.87	2.85	2.86	9.6
7	V3	on	yes	300	370	x	2.95	2.85	2.88	9.9
7	V4	on	yes	300	383	x	2.91	2.79	2.82	9.5
Fe-Se cycles										
3	V1	off	yes	3000	233	92	2.99	2.96	2.97	73
3	V2	off	yes	3000	306	90	3.00	2.96	2.98	48
3	V3	off	yes	3000	293	90	3.18	3.16	3.17	39
3	V4	off	yes	3000	233	92	2.97	2.92	2.94	50
4	V3	on	no	300	12.1	96	3.35	2.98	3.20	43
4	V4	on	yes	300	48.0	84	2.98	2.66	2.74	103
6	V3	off	yes	300	43.2	86	3.16	3.03	3.08	88
6	V4	off	no	300	39.4	87	3.43	3.30	3.34	77

^a The difference between the initial and mean concentrations, divided by the initial concentration; ^b The difference in the maximum and minimum values for the percent of mean concentration. This parameter is provided to compare the magnitudes of Se^{IV} cycles; x is effectively zero within the error of the measurement.

The magnitude of Se^{IV} concentration cycles was much larger for Fe-Se experiments than Se-only experiments. This was likely due to the greater affinity for Se^{IV} species sorption to solid 2-line ferrihydrite rather than the glass reaction vessels. For each individual Fe-Se and Se-only cycle, the “ Se^{IV} % Range” was calculated by taking the difference between the maximum and minimum Se^{IV} values, divided by the mean Se^{IV} concentration, and reported as a percentage. This value was used to determine the difference in Se^{IV} concentration cycle magnitudes between experiments. For Se-only experiments, the Se^{IV} % range was less than 10% (Cycle 7 only; no Se^{IV} cycles reported for Cycle 5). The Se^{IV} % range values ranged from 39% to 88% in Fe-Se combined experiments indicating that the magnitude of Se^{IV} concentration changes were greater for these experiments.

For Cycles 3, 4, 6 and 7, the observed Se^{IV} cycles displayed increasing Se^{IV} concentrations with increasing temperature and decreasing Se^{IV} concentrations with decreasing temperature. Graphs of Se^{IV} concentration versus temperature resulted in a hysteresis relationship between sorption (decreasing Se^{IV} concentrations) and desorption (increasing Se^{IV} concentrations) processes. Conditional enthalpy of sorption values were calculated for Cycles 3, 4, 6, and 7 and ranged from -61.9 to 19.4 kJ/mol for the first increasing temperature series, from -23.6 to 2.6 kJ/mol for the temperature decreasing series, and from -17.2 to 11.7 kJ/mol for the second temperature increasing series. Anions, such as the aqueous Se^{IV} species present in the experiment solutions, are known to cycle out of phase with cations (Nimick et al., 2003). Nimick et al. (2003) calculated negative conditional enthalpies of sorption for As, which like Se, forms anionic species in solution. Therefore, the negative conditional enthalpy of sorption values reported above for Se^{IV} are consistent with the Nimick et al. (2003) findings for As. The large range of values reported for Se^{IV} in these experiments are likely due to the differing vessel conditions. It is also important to note that not all Se^{IV} loss may have been due to sorption onto 2-line ferrihydrite and that oxidation-reduction reactions are not considered in the conditional enthalpy of sorption calculation.

6.2 Evaluation of mechanisms

6.2.1 Light

It was predicted that Fe^{III} photoreduction would occur during light on conditions, resulting in increased Fe^{II} concentrations. During light control experiments (turning the light on and off while holding temperature constant), this process was predicted to result in Fe redox cycling. However, Fe^{III} photoreduction and Fe redox cycling did not occur during Fe-only light control experiments (Cycles 1 and 2). Therefore, Se^{IV} concentration changes could not be evaluated relative to Fe redox or precipitation cycles in these experiments.

There are a few possible reasons why Fe^{III} photoreduction was not observed. The light bulbs used in these experiments were within the optimum wavelength (360 to 450 nm) for Fe^{III} photoreduction, and the pH was also within the correct range (3 to 4) (Gammons et al., 2008; King et al., 1993; McKnight et al., 2001); however, the light intensity emitted from the bulbs may not have been strong enough for Fe^{III} photoreduction to occur. Second, if Fe^{III} photoreduction was occurring, the time period in which the light was turned on may not have been long enough to observe any changes in Fe^{II} concentrations. Lastly, the dissolution of 2-line ferrihydrite was minimal, and the solid remained at the base of the reaction vessels during the experiments. The concentrations of $\text{Fe}(\text{OH})^{2+}$, the aqueous Fe species needed for Fe^{III} photoreduction, may not have been high enough for Fe^{III} photoreduction to occur (Kimball et al., 1992) (Eq. 6). Kimball et al. (1992) also described how Fe^{III} can be released from Fe oxide minerals into solution by direct photoreduction at the mineral surface (Eq. 7a and 7b); however, in the light and temperature cycle experiments, the light intensity was likely not strong enough to reach the mineral surface at the bottom of the reaction vessels.

During temperature control experiments with the light off (Cycles 3 and 6), Fe^{II} concentrations remained relatively low, ranging from below the MDL to 0.147 mg/L. The Fe^{II} concentrations during the temperature control experiment with the light on (Cycle 4) ranged from 0.246 mg/L to 0.381 mg/L. These higher Fe^{II} concentration values suggest that Fe^{III} photoreduction did occur during light on conditions. However, the Fe^{II} concentrations did not continue to increase throughout the light on temperature control experiment (Cycle 4), meaning that Fe^{III} photoreduction may have reached its maximum during the 48 hour equilibration period

prior to the experiment. Overall, the lights and Fe species concentration changes had no effect on Se^{IV} concentrations.

6.2.2 Temperature

Fe(total) concentration variations did not directly correlate with changes in temperature, and the concentrations remained relatively stable throughout the light and temperature cycle experiments, ranging from <0.02 mg/L to 2.45 mg/L ($<0.01\%$ to 1.56% of the total mass of Fe added to each vessel). Parker et al. (2007) found that the solubility of HFO decreases with increasing temperature. This is also observed in the ferrihydrite solubility diagram (Figure 2.6) which was created with the same parameters (ionic strength and Fe concentration) as the reaction vessel Fe-only solution. At a pH of 3 in Figure 2.6, the Fe(total) concentrations were 19.3 mg/L at 10°C , 3.42 mg/L at 25°C , and 1.22 mg/L at 30°C . The maximum Fe(total) concentration in the temperature cycle experiments was 2.45 mg/L which lies between the 25°C and 30°C Fe(total) concentration values in Figure 2.6. Since Fe(total) concentrations did not decrease with increasing temperature during the temperature control experiments, it is likely that the temperature changes occurred too quickly to detect changes in Fe(total) concentrations associated with HFO dissolution and precipitation.

Fe redox cycling was also not observed with changes in temperature. In Cycle 4, the Fe^{II} concentrations cycled with a slight lag behind temperature changes in all four vessels. Fe^{II} concentration changes with temperature were not observed in any other cycles. Fe^{II} concentration increases with temperature increases have been observed in natural waters (Parker et al., 2007; Gammons et al., 2005a); however, it was determined that Fe^{III} photoreduction was a stronger influence on Fe^{II} cycles in those studies. Gammons et al. (2005a) found that Fe^{II} concentrations had larger magnitude diel cycles than Fe^{III} concentrations. Temperature is known to create a kinetic effect for Fe cycles by increasing Fe oxidation rates in warmer water (Wakao and Shiota, 1982). Therefore, the increase in temperature during daytime hours in the Gammons et al. (2005a) study should have favored Fe^{II} oxidation. The larger magnitude of Fe^{II} diel cycles in comparison with Fe^{III} diel cycles indicates that Fe^{III} photoreduction was the dominant process in their study.

Temperature was the main driver of all observed Se^{IV} cycles. Se^{IV} concentrations were positively correlated with temperature in both Se-only and Fe-Se combined vessels. This resulted in negative ΔH_{ads} values, indicating that Se^{IV} sorption was increasing with decreasing temperature and vice versa. These results are consistent with the Nimick et al. (2003) findings for As concentration changes with temperature. The time period in which temperature changes occur is also important. If the temperature changes too quickly, then Se^{IV} concentration changes may not be detected (e.g. Cycle 5).

6.2.3 Se sorption onto 2-line ferrihydrite

The changes in Se^{IV} concentrations during Se-only and Fe-Se experiments were likely due to temperature-dependent sorption onto 2-line ferrihydrite. In comparison to Se-only cycles, larger magnitude Se^{IV} cycles were observed in Fe-Se combined cycles. This was attributed to the presence of 2-line ferrihydrite in the Fe-Se vessels providing additional sorption sites for Se^{IV} . For all Se-only and Fe-Se experiments, Se^{IV} was always present in solution, meaning that not all Se^{IV} sorbed to the glassware and 2-line ferrihydrite.

Majority of the calculated ΔH_{ads} values were negative, which is consistent with anion sorption (Nimick et al., 2003) (Tables 5-6, 5-8, 5-11, and 5-13). Machesky's (1990) chemical modeling approach for ΔH_{ads} of Se^{IV} onto ferrihydrite resulted in exothermic ΔH_{ads} values of -82 kJ/mol to -22 kJ/mol. For Fe-Se temperature control experiments, 5 out of 20 ΔH_{ads} values fell within this range. ΔH_{ads} values for Se^{IV} onto HFO have not been reported in natural waters. For Fe-Se temperature cycle experiments, ΔH_{ads} values for Se^{IV} onto 2-line ferrihydrite ranged from -61.9 kJ/mol to 19.4 kJ/mol (20 values total) for both temperature increasing and temperature decreasing series. Out of those 20 ΔH_{ads} values, 13 were negative. For the Se-only temperature cycle experiments, ΔH_{ads} values for Se^{IV} onto the glassware ranged from -5.0 kJ/mol to -0.4 kJ/mol, and all 12 values were negative.

The reported studies of Se diel cycles in nature (Carling et al., 2011; Dicataldo et al., 2011) concluded that Se cycled due to sorption interactions with metal oxides caused by changes in pH and redox conditions. The changes in pH were attributed to photosynthesis, and a direct correlation between Se^{IV} concentration changes and temperature was not observed. It is important to note that the pH range in these studies (7.5 to 9.7) was significantly different from

the pH range used in the laboratory experiments, therefore, resulting in different Se species concentrations and sorption behavior. Also, photosynthesis did not occur in the laboratory experiments. Laboratory sorption studies have shown that Se^{IV} sorption onto ferrihydrite increases with decreasing temperature and pH (Balistrieri and Chao, 1990; Parida et al., 1997). Se^{IV} concentrations during the Se-only and Fe-Se temperature cycle experiments followed this same trend. As the vessel solution temperatures decreased, Se^{IV} concentrations also decreased (Se^{IV} sorbed onto the glassware and 2-line ferrihydrite).

There are several other factors that may affect Se^{IV} sorption onto ferrihydrite, including ionic strength, surface loading, timing, pH, and the Se species present (Sparks, 2003). KCl was used to fix the ionic strength of solution; however, the ionic strength of solution was found to increase throughout the temperature cycle experiments due to evaporation. KCl was chosen, because K^+ and Cl^- both act as conservative ions and did not interfere with Fe or Se species in solution. It is also unlikely that full surface loading of Se species was occurring in these experiments, because the mass of 2-line ferrihydrite added to the vessels was much greater than the mass of Se^{IV} added. Timing is also important. For example, Se^{IV} cycles were not observed in Cycle 5, which was likely due to the temperature cycling too quickly. The pH of vessel solutions did not cycle in the temperature cycle experiments, but different pH values were observed in each vessel. Slight changes in pH may affect Se species concentrations in solution, and each Se species may have a different affinity for sorption onto 2-line ferrihydrite.

6.2.4 pH

For all experiments, the solution pH was adjusted to 3 prior to the 48 hour equilibration period. After the equilibration period, pH values ranged from 2.59 to 3.60 during the light and temperature cycle experiments. The change in pH values after equilibration could be due to 2-line ferrihydrite dissolution and/or Fe species conversions. The solution pH values did not cycle with temperature or light and remained relatively constant in each vessel.

At low pH values, Se^{IV} and Se^{VI} species will protonate to form acids (Eq. 1, 2, and 3). Each Se species may have a different affinity for sorption onto 2-line ferrihydrite. Also, Se^{IV} sorption is more likely to occur with decreasing pH (Parida et al., 1997). Se^{IV} cycles were not observed in vessel solutions with a pH value greater than 3. Therefore, the pH of the vessel

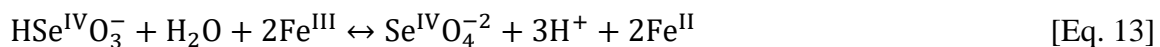
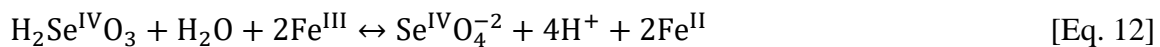
solutions was critical for Se^{IV} sorption and cycling. As pH increases, the protonation of HFO surfaces decreases, which results in an increased negative surface charge (Nimick et al., 2003). This may explain why clear Se^{IV} cycles were not observed in vessel solutions with pH values greater than 3. Parida et al. (1997) found that Se^{IV} will adsorb onto ferrihydrite at pH values greater than the pH_{PZC} (ferrihydrite $\text{pH}_{\text{PZC}} = 7.89 \pm 0.1$). This occurs when Se^{IV} and ferrihydrite interactions are able to exceed electrostatic forces. Since pH values in the light and temperature cycle experiments were less than the pH_{PZC} for ferrihydrite, this process did not have an effect on Se^{IV} cycles; however, other types of specific interactions (non-electrostatic) may have occurred between the Se^{IV} species and 2-line ferrihydrite surface.

The importance of pH in As diel cycles was described by Nimick et al. (1998). Like Se, As forms oxyanions in water and should display similar behavior in response to pH changes. Nimick et al. (1998) found that As diel cycles were only present in the Madison and Missouri Rivers within certain pH ranges. If the pH was too high, As concentrations did not cycle. Although Nimick et al.'s (1998) study was completed in natural waters with higher pH values (ranging from 7.2 to 9.0) than the light and temperature cycle experiments of this study, it highlights the significance of pH on oxyanion cycling.

The pH of solution is also important for 2-line ferrihydrite dissolution and precipitation. Specific Fe species may only be present in certain pH ranges (Figure 2-6). Other HFOs may also precipitate or dissolve at specific pH values, therefore, impacting Fe species and Se^{IV} concentrations in solution. Gammons et al. (2005a) reported that Fe(total) concentrations decreased with increasing pH values downstream at their study site (Fishing Creek, Montana). The decrease in Fe(total) concentrations was due to HFO precipitation with increasing pH. Nimick et al. (2003) concluded that the dissolution of HFO is associated with acidic waters and could be linked with increases in Fe^{II} and Fe(total) concentrations.

6.2.5 Oxidation-reduction reactions

It is unlikely that Se^{IV} oxidation occurred during the Se-only and Fe-Se experiments. However, it is possible that Se^{IV} oxidation can be coupled with Fe^{III} reduction (Eq.12 and Eq. 13).



These reactions are dependent on the solution pH, because it affects the protonation and deprotonation of Fe and Se species. Equation 12 may occur at pH values between 1.66 and 2.62, and Equation 13 may occur between pH values of 2.62 and 8.32 (Figure 6-1). The Gibbs Free Energy of Reaction (ΔG_R) can also be used to determine whether Equations 12 and 13 were likely to occur during temperature controlled experiments. The ΔG_R for Equation 12 is greater than zero, indicating that the thermodynamics are not favorable for the reaction to occur. However, the ΔG_R for Equation 13 is negative at pH values above 3.5, indicating that Se^{IV} oxidation to Se^{VI} may occur when Fe^{III} exists in solution at pH values greater than 3.5. Since all vessel solution pH values were less than 3.5, the oxidation of Se^{IV} to Se^{VI} likely did not occur during these experiments. Based on solution pH, all Se^{IV} cycles were observed due to sorption onto 2-line ferrihydrite. Therefore, the final mass balance equation for Se in the reaction vessels is written as:

$$[\text{Se}]_{\text{Total}} = [\text{Se}^{\text{IV}}]_{\text{aqueous}} + [\text{Se}^{\text{IV}}]_{\text{sorbed to Fe}} \quad [\text{Eq. 14}]$$

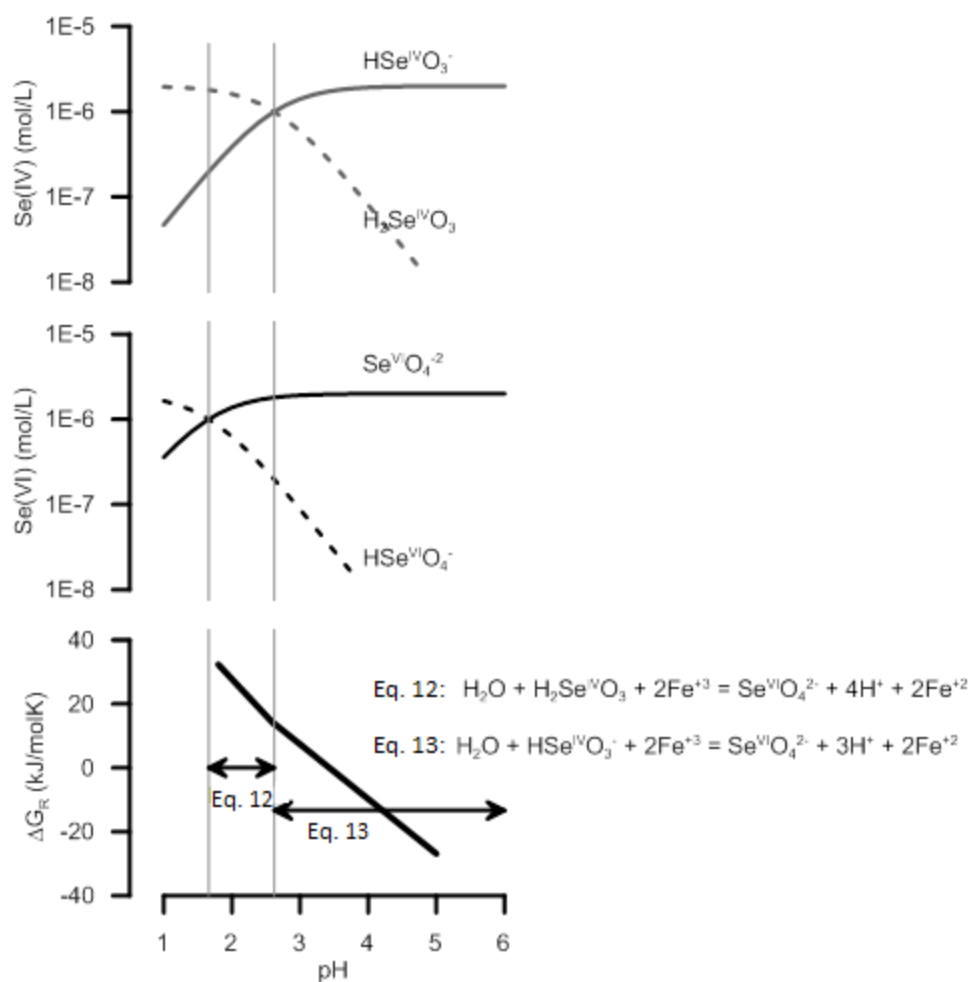


Figure 6-1. Gibbs Free Energy (ΔG_R) calculated using thermodynamic data from Stumm and Morgan (1996) for $[\text{Se}^{\text{IV}}] = [\text{Se}^{\text{VI}}] = 3.8 \times 10^{-6} \text{ M}$ and $[\text{Fe}^{\text{III}}] = [\text{Fe}^{\text{II}}] = 9 \times 10^{-6} \text{ M}$. Activity-concentration corrections not included. Modified from the final OSMRE report (Vesper et al., 2015).

7 CONCLUSIONS

This research demonstrates that Se concentration cycles can be controlled by temperature change in acidic solutions ($\text{pH} < 3$). The hypothesis that Se^{IV} (including the protonated and deprotonated species) will cycle in phase with Fe due to Se^{IV} species sorption onto 2-line ferrihydrite (i.e. as Fe moves from the solid to the dissolved phase it will release the existing sorbed Se^{IV} species) could not be verified from this research due to the existence of Se^{IV} cycles in Se-only experiments and the lack of Fe cycles. Although clear Fe cycles were not observed, the magnitude of Se^{IV} cycles was more pronounced in Fe-Se vessels than in Se-only vessels indicating that Se^{IV} was being sorbed onto and released from the 2-line ferrihydrite. The results of these experiments provide insight to the possible causes and limitations of Se^{IV} diel cycles in natural waters. The time period over which temperature changed, the solution pH, and the presence of an adsorbent (2-line ferrihydrite) were all important for defining the magnitude of Se^{IV} cycles observed.

8 FUTURE WORK

Further study is needed to determine if Se cycles can be linked to Fe redox cycles. If Fe redox cycles are created, then Se^{IV} concentration changes could be observed. It would be necessary to obtain a light source that emits a greater light intensity than the standard UV bulbs used in these experiments to generate Fe^{III} photoreduction. This would increase the chances of Fe^{III} photoreduction for light control experiments. The effects of temperature and light must also be separated by manually controlling temperature (keeping it constant) during light control experiments. Other Fe^{III} minerals with equivalent or greater solubility than 2-line ferrihydrite could be used to introduce Fe into solution. Similar studies can also be completed to determine the effect of trace metal redox cycles on Se^{IV} concentrations with light and temperature (e.g. Are Se^{IV} cycles linked to manganese (Mn) redox cycles?).

REFERENCES

- Allison, J.D., Brown, D.S. and Novo-Gradac, K., 1991. MINTEQA2/PRODEFA2, A Geochemical Assessment Model for Environmental Systems.
- Balistrieri, L.S. and Chao, T.T., 1987. Selenium Adsorption by Goethite. *Soil Science Society of America Journal*, 51(5): 1145-1151.
- Benjamin, M.M., 2002. Water Chemistry. Waveland Press, Inc., Long Grove, Illinois, 368 pp.
- Carling, G.T., Fernandez, D.P., Rudd, A., Pazmino, E. and Johnson, W.P., 2011. Trace Element Diel Variations and Particulate Pulses in Perimeter Freshwater Wetlands of the Great Salt Lake, Utah. *Chemical Geology*, 283: 87-98.
- Coleman, L., Bragg, L.J. and Finkelman, R.B., 1993. Distribution and Mode of Occurrence of Selenium in US Coals. *Environmental Geochemistry and Health*, 15: 215-227.
- Das, S., Hendry, M.J. and Essilfie-Dughan, J., 2013. Adsorption of Selenate onto Ferrihydrite, Goethite, and Lepidocrocite Under Neutral pH Conditions. *Applied Geochemistry*, 28: 185-193.
- Dicataldo G., Johnson W.P., Naftz, D.L., Hayes, D.F., Moellmer, W.O. and Miller, T., 2011. Diel Variation of Selenium and Arsenic in a Wetland of the Great Salt Lake, Utah. *Applied Geochemistry*, 26: 28-36.
- Duc, M., Lefèvre, G. and Fédoroff, M., 2006. Sorption of Selenite Ions on Hematite. *Journal of Colloid and Interface Science*, 298(2): 556–563.
- Drever, J.I., 1997. The Geochemistry of Natural Waters: Surface and Groundwater Environments. Prentice Hall, Upper Saddle River, New Jersey, 142 pp.
- Emmenegger, L., Schonenberger, R., Sigg, L. and Sulzberger, B., 2011. Light-induced Redox Cycling of Iron in Lakes. *Limnol. Oceanogr.*, 46(1): 49-61.
- Fuller, C.C. and Davis, J.A., 1989. Influence of Coupling of Sorption and Photosynthetic Processes on Trace Element Cycles in Natural Waters. *Nature*, 340: 52-54.
- Gammons, C. H., Nimick D. A., Parker S.R., Cleasby T. E. and McCleskey R. B., 2005a. Diel Behavior of Iron and Other Heavy Metals in a Mountain Stream with Acidic to Neutral pH: Fisher Creek, Montana, USA. *Geochimica Et Cosmochimica Acta*, 69(10): 2505-2516.
- Gammons, C.H., Nimick, D.A., Parker, S.R., Snyder, D.M., McCleskey, R.B., Amils, R. and Poulson, S.R., 2008. Photoreduction Fuels Biogeochemical Cycling of Iron in Spain's Acid Rivers. *Chemical Geology*, 252: 202 -213.
- Gammons, C.H., Wood, S.A. and Nimick, D.A., 2005b. Diel Behavior of Rare Earth Elements in a Mountain Stream with Acidic to Neutral pH. *Geochimica Et Cosmochimica Acta*, 69: 3747-3758.
- Huang, D. & West Virginia University, 2010. Heterogeneous Reduction of Selenite by Zero Valent Iron-steel Wool. Morgantown, W. Va: West Virginia University Libraries.
- Kimball, B.A., McKnight, D.M., Wetherbee, G.A. and Harnish, R.A., 1992. Mechanisms of Iron Photoreduction in a Metal-rich, Acidic Stream (St. Kevin Gulch, Colorado, U.S.A.). *The Geochemistry of Acid Groundwater Systems*, 1(2): 227-239.
- King, D.W., Aldrich, R.A. and Charnecki, S.E., 1993. Photochemical Redox Cycling of Iron in NaCl Solutions. *Marine Chemistry*, 44(2-4): 105-120.
- Konieczka, P., Namiesnik, J., 2009. Quality Assurance and Quality Control in the Analytical Chemical Laboratory. CRC Press, Boca Raton, FL, 146-147 pp.

- Lee, W.C., Kim, S., Ranville, J., Yun, S. and Choi, S.H., 2014. Sequestration of Arsenate from Aqueous Solution Using 2-line Ferrihydrite: Equilibria, Kinetics, and X-ray Absorption Spectroscopic Analysis. *Environmental Earth Science*, 71: 3307–3318.
- Lenz, M. and Lens, P.N.L., 2009. The Essential Toxin: the Changing Perception of Selenium in Environmental Sciences. *Science of the Total Environment*, 407: 3620–3633.
- Lide, D.R. (Editor), 2003. CRC Handbook of Chemistry and Physics, 84th Edition. CRC Press, Boca Raton, Florida, Appendix F.
- Machesky M., 1990. Influence of Temperature on Ion Adsorption by Hydrous Metal Oxides. *Chemical Modeling of Aqueous Systems II*, 416: 282–292.
- Manceau A. and Charlet, L., 1994. The Mechanism of Selenate Adsorption on Goethite and Hydrous Ferric Oxide. *Journal of Colloid and Interface Science*, 168(1): 87–93.
- Marathon Scientific, 2007. Multimode Sample Introduction System (MSIS) User's Guide US Patent # 6,891,605. Marathon Scientific, Canada, 3–4 pp.
- McKnight, D.M., Kimball, B.A. and Bencala, K.E., 1988. Iron Photoreduction and Oxidation in an Acidic Mountain Stream. *Science*, 240: 637–639.
- McKnight D. M., Kimball B. A. and Runkel R. L., 2001. pH Dependence of Iron Photoreduction in a Rocky Mountain Stream Affected by Acid Mine Drainage. *Hydrological Processes*, 15(10): 1979–1992.
- Nimick, D.A., 2003. Diurnal Variation in Trace-Metal Concentrations in Streams: U.S. Geological Survey Fact Sheet FS-086-03, 4 pp.
- Nimick, D.A., Cleasby, T.E. and McCleskey, R.B., 2005. Seasonality of Diel Cycles of Dissolved Trace-Metal Concentrations in a Rocky Mountain Stream. *Environmental Geology*, 47: 603–614.
- Nimick, D.A., Gammons, C.H., Cleasby, T.E., Madison, J.P., Skaar, D. and Brick, C.M., 2003. Diel Cycles in Dissolved Metal Concentrations in Streams: Occurrence and Possible Causes. *Water Resources Research*, 39: 1247–1264.
- Nimick, D.A., Gammons, C.H. and Parker, S.R., 2011. Diel Biogeochemical Processes and Their Effect on the Aqueous Chemistry of Streams: A Review. *Chemical Geology*, 283: 3–17.
- Nimick, D.A., Moore, J.N., Dalby, C.E. and Savka, M.W., 1998. The Fate of Geothermal Arsenic in the Madison and Missouri Rivers, Montana and Wyoming. *Water Resources Research*, 34(11): 3051–3067.
- Parida, K.M., Gorai, B., Das, N.N. and Rao, S.B., 1997. Studies on Ferric Oxide Hydroxides: III. Adsorption of Selenite (SeO_3^{2-}) on Different Forms of Iron Oxyhydroxides. *Journal of Colloid and Interface Science*, 185(2): 355–362.
- Parker, S.R., Gammons, C.H., Jones, C.A. and Nimick, D.A., 2007. Role of Hydrous Iron Oxide Formation in Attenuation and Diel Cycling of Dissolved Trace Metals in a Stream Affected by Acid Rock Drainage. *Water, Air, & Soil Pollution*, 181: 247–263.
- Reddy, K.R. and DeLaune, R.D., 2008. Biogeochemistry of Wetlands: Science and Applications. CRC Press, Boca Raton, Florida, 495 pp.
- Rovira, M., Gimenez, J., Martinez, M., Martinez-Llado, X., Pablo, J.d., Marti, V. and Duro, L., 2008. Sorption of Selenium(IV) and Selenium(VI) onto Natural Iron Oxides: Goethite and Hematite. *Journal of Hazardous Materials*, 150: 279–284.
- Schroder, J.L. and Zhang, H., 2009. Using the Multimode Sample Introduction System (MSIS) for Low Level Analysis of Arsenic and Selenium in Water. *Soil Science Society of America Journal*, 73: 1804–1807.
- Schwertmann, U., 1991. Solubility and Dissolution of Iron Oxides. *Plant and Soil*, 130: 1–25.

- Schwertmann, U. and Cornell, R.M., 2007. Iron Oxides in the Laboratory: Preparation and Characterization. Wiley-VCH Verlag GmbH, D-69469 Weinheim, 90-94 pp.
- Sparks, D.L., 2003. Environmental Soil Chemistry, Second Edition. Elsevier Science, USA, 144 pp.
- Stookey, L.L., 1970. Ferrozine – A New Spectrophotometric Reagent for Iron. *Analytical Chemistry*, 42(7): 779-781.
- Stumm, W. and Morgan, J.J., 1996. Aquatic Chemistry, Chemical Equilibria and Rates in Natural Waters, 3rd ed. John Wiley & Sons, Inc., New York.
- Torres, J., Pintos, V., Gonzatto, L., Dominguez, S., Kremer, C. and Kremer, E., 2011. Selenium Chemical Speciation in Natural Waters: Protonation and Complexation Behavior of Selenite and Selenate in the Presence of Environmentally Relevant Cations. *Chemical Geology*, 288: 32-38.
- United States Environmental Protection Agency, 2013. Aquatic Life Criteria Table. Updated 12/3/2014, Accessed 3/20/2015. <http://water.epa.gov/scitech/swguidance/standards/criteria/current/index.cfm>
- Vesper, D., Waltemyer, K., McDonald, L. 2015. Selenium Diel Cycling and Sorption Kinetics. OSMRE-WV ADTI Cooperative Agreement S14AC20009, 32-34 pp.
- Wakao, N. and Shiota, H., 1982. Effect of Temperature on the Bacterial Iron Oxidation Rate in a River Contaminated with Acid Mine Water. *Journal of General and Applied Microbiology*, 28: 465-467.
- Younger, P.L., Banwart, S.A. and Hedin, R.S., 2002. Mine Water: Hydrology, Pollution, Remediation. Kluwer Academic Publishers, Norwell, Massachusetts, 65-73 pp.
- Zhao, J., Huggins, F.E., Feng, Z. and Huffman, G.P., 1994. Ferrihydrite: Surface Structure and its Effects on Phase Transformation. *Clays and Clay Minerals*, 42(6): 737-746.

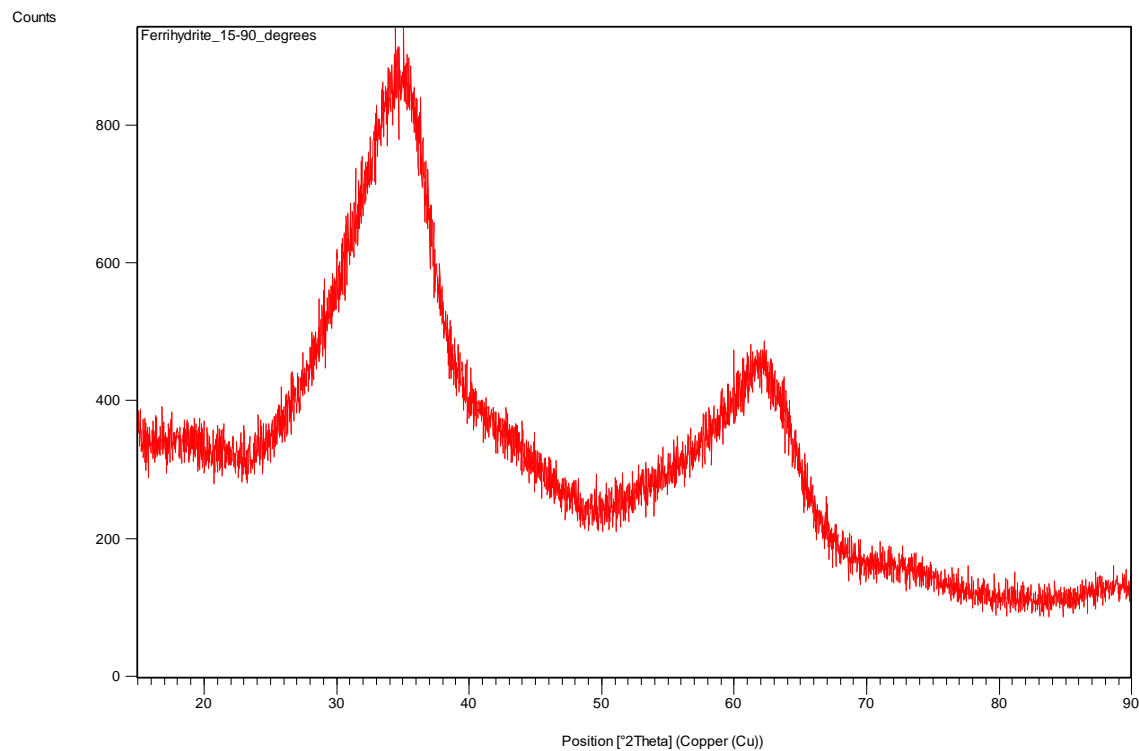
APPENDICES

Appendix A. X-ray diffraction (XRD) results

Measurement Conditions:

Dataset Name	Ferrihydrite_15-90_degrees
File name	C:\X'Pert Data\EKH\Ferrihydrite_15-90_degrees.xrdml
Comment	Configuration=Bracket Flat Sample Stage, Owner=User-1,
Creation date=11/26/2002 10:15:54 AM	Goniometer=PW3050/60 (Theta/Theta); Minimum step size
2Theta:0.001; Minimum step size Omega:0.001	Sample stage=PW3071/xx Bracket
	Diffraction system=XPRT-PRO
	Measurement program=EKH_Ferrihydrite, Owner=User-1,
Creation date=8/28/2014 1:50:38 PM	
Measurement Date / Time	8/28/2014 1:53:24 PM
Operator	xrd
Raw Data Origin	XRD measurement (*.XRDML)
Scan Axis	Gonio
Start Position [°2Th.]	15.0000
End Position [°2Th.]	90.0000
Step Size [°2Th.]	0.0200
Scan Step Time [s]	30.0000
Scan Type	Pre-set time
Offset [°2Th.]	0.0000
Divergence Slit Type	Fixed
Divergence Slit Size [°]	0.9570
Specimen Length [mm]	10.00
Receiving Slit Size [mm]	3.0300
Measurement Temperature [°C]	25.00
Anode Material	Cu
K-Alpha1 [Å]	1.54060
K-Alpha2 [Å]	1.54443
K-Beta [Å]	1.39225
K-A2 / K-A1 Ratio	0.50000
Generator Settings	40 mA, 45 kV
Diffraction Type	0000000013030095
Diffraction Number	0
Goniometer Radius [mm]	240.00
Dist. Focus-Diverg. Slit [mm]	91.00
Incident Beam Monochromator	No
Spinning	No

Main Graphics, Analyze View:



Comments from the XRD technician:

Both samples showed patterns that would generally be considered amorphous. We did a wider range run on one of them - I've attached the report - and it matches pretty well to one of two high areas (they're not really peaks) of 2-line ferrihydrite. The second area is offset in the sample. The scan was a 24-hour scan so it's unlikely that peaks were there but not showing up as can sometimes happen. I can run a wider range scan on the sample labeled B1 if you would like and see if it matches the 2-line ferrihydrite spectrum better. Right now the scan I have for that is just up to 50 or 60 deg and it shows that same first high amorphous area.

Appendix B. Filtering Experiment for Fe Analysis
Data

Vessel No.	Unfiltered Fe^{II} (mg/L)	Filtered Fe^{II} (mg/L)	Unfiltered Fe(total) (mg/L)	Filtered Fe(total) (mg/L)
Vessel 1	0.27	0.15	0.77	0.63
	0.26	0.15	0.75	0.65
	0.26	0.13	0.78	0.65
	0.24	0.15	0.75	0.65
	0.24	0.15	0.75	0.64
	0.24	0.16	0.75	0.64
Vessel 2	0.23	0.13	0.51	0.46
	0.19	0.13	0.51	0.44
	0.22	0.13	0.53	0.43
	0.19	0.13	0.51	0.44
	0.20	0.13	0.56	0.46
	0.20	0.12	0.53	0.46
Vessel 3	0.23	0.20	0.60	0.48
	0.23	0.15	0.60	0.48
	0.23	0.15	0.60	0.48
	0.24	0.15	0.60	0.48
	0.23	0.15	0.60	0.48
	0.23	0.15	0.60	0.50
Vessel 4	0.28	0.17	0.64	0.46
	0.27	0.16	0.64	0.46
	0.26	0.16	0.64	0.47
	0.26	0.16	0.64	0.47
	0.27	0.16	0.64	0.47
	0.27	0.16	0.64	0.48
Vessel 5	0.23	0.15	0.37	0.27
	0.24	0.15	0.43	0.27
	0.23	0.15	0.39	0.26
	0.23	0.16	0.40	0.27
	0.23	0.16	0.43	0.27
	0.23	0.15	0.37	0.27
Vessel 6	0.51	0.16	0.60	0.19
	0.51	0.16	0.60	0.20
	0.51	0.16	0.60	0.19
	0.51	0.16	0.61	0.19
	0.51	0.16	0.61	0.20
	0.51	0.16	0.60	0.19

Appendix C. Diel Cycle Data

Appendix C-1. Cycle 1 (7/22/2014) Data

	Sample No.	Sample Name	Elapsed time (hr)	Temp. ⁺ (°C)	pH ⁺	Light (on/off)	Light intensity ⁺⁺ (Lux)	Fe ^{II} * (mg/L)	Fe(total)* (mg/L)
Vessel 1	1	V1 - 1	0	21.5	3.15	off	0	< 0.02 ^x	< 0.02 ^x
	2	V1 - 2	1	21.0	3.15	off	0	< 0.02 ^x	< 0.02 ^x
	3	V1 - 3	2	21.2	3.06	on	3961.1	< 0.02 ^x	< 0.02 ^x
	4	V1 - 4	3	21.4	3.07	on	4133.4	< 0.02 ^x	< 0.02 ^x
	5	V1 - 5	4	21.7	3.08	on	4477.8	< 0.02 ^x	< 0.02 ^x
	6	V1 - 6	5	21.8	3.08	on	4305.6	< 0.02 ^x	0.023
	7	V1 - 7	6	21.9	3.05	on	3961.1	< 0.02 ^x	< 0.02 ^x
	8	V1 - 8	7	22.0	3.03	on	4650.0	< 0.02 ^x	0.075
	9	V1 - 9	8	22.0	3.05	on	4133.4	< 0.02 ^x	0.023
	10	V1 - 10	9	22.1	3.04	on	4305.6	< 0.02 ^x	0.075
	11	V1 - 11	10	22.1	3.04	on	4477.8	< 0.02 ^x	0.075
	12	V1 - 12	11	22.1	3.06	on	3961.1	< 0.02 ^x	0.092
	13	V1 - 13	12	21.8	3.06	off	0	< 0.02 ^x	0.075
	14	V1 - 14	13	21.5	3.07	off	0	< 0.02 ^x	0.11
	15	V1 - 15	14	21.2	3.07	off	0	< 0.02 ^x	0.13
	16	V1 - 16	15	21.1	3.06	off	0	< 0.02 ^x	0.13
	17	V1 - 17	16	21.0	3.07	off	0	< 0.02 ^x	0.11
	18	V1 - 18	17	20.9	3.06	off	0	< 0.02 ^x	0.14
	19	V1 - 19	18	20.9	3.08	off	0	< 0.02 ^x	0.13
	20	V1 - 20	19	20.9	3.07	off	0	< 0.02 ^x	0.14
	21	V1 - 21	20	21.2	3.05	on	4133.4	< 0.02 ^x	0.16
	22	V1 - 22	21	21.5	3.09	on	4133.4	< 0.02 ^x	0.23

⁺ Measured using DrDAQ PicoLog Recorder

⁺⁺ Measured using HOBO Pendant Light/Temperature Loggers

* Samples analyzed using HACH DR2800 Spectrophotometer

^x Sample below ferrozine MDL of 0.02 mg/L for Fe^{II} and Fe(total)

Appendix C-2. Cycle 2 (10/17-18/2014) Data

	Sample No.	Sample Name	Elapsed time (hr)	Temp. ⁺ (°C)	pH ⁺	Light (on/off)	Light intensity ⁺⁺ (Lux)	Fe ^{II} * (mg/L)	Fe(total)* (mg/L)
Vessel 1	1	V1 - 1a	0	25.0	2.98	off	0	0.077	0.51
	2	V1 - 1b	0	25.0	2.98	off	0	0.15	0.50
	3	V1 - 1c	0	25.0	2.98	off	0	0.077	0.51
	4	V1 - 2	1	24.5	2.98	off	0	0.048	0.47
	5	V1 - 3	2	24.4	2.99	off	0	0.048	0.47
	6	V1 - 4	3	24.8	2.99	on	3702.8	0.063	0.47
	7	V1 - 5	4	24.7	2.98	on	3961.1	0.077	0.47
	8	V1 - 6	5	24.9	2.99	on	3961.1	0.077	0.46
	9	V1 - 7a	6	25.0	2.98	on	3616.7	0.11	0.47
	10	V1 - 7b	6	25.0	2.98	on	3616.7	0.11	0.46
	11	V1 - 7c	6	25.0	2.98	on	3616.7	0.11	0.47
	12	V1 - 8	7	24.9	3.00	on	3788.9	0.091	0.46
	13	V1 - 9	8	25.0	3.00	on	3961.1	0.091	0.47
	14	V1 - 10	9	24.8	2.97	on	3702.8	0.077	0.46
	15	V1 - 11	10	25.0	2.98	on	3875.0	0.091	0.46
	16	V1 - 12	11	25.0	2.96	on	3875.0	0.048	0.47
	17	V1 - 13a	12	24.9	2.96	on	3875.0	0.091	0.46
	18	V1 - 13b	12	24.9	2.96	on	3875.0	0.091	0.47
	19	V1 - 13c	12	24.9	2.96	on	3875.0	0.11	0.46
	20	V1 - 14	13	24.7	2.98	on	3961.1	0.091	0.46
	21	V1 - 15	14	24.6	2.98	on	3616.7	0.23	0.46
	22	V1 - 16	15	24.4	2.98	off	0	0.23	0.44
	23	V1 - 17	16	24.3	2.98	off	0	0.23	0.44
	24	V1 - 18	17	24.3	2.98	off	0	0.22	0.43
	25	V1 - 19a	18	24.7	2.99	off	0	0.23	0.47
	26	V1 - 19b	18	24.7	2.99	off	0	0.25	0.44
	27	V1 - 19c	18	24.7	2.99	off	0	0.23	0.44
	28	V1 - 20	19	24.8	2.98	off	0	0.25	0.46
	29	V1 - 21	20	24.9	2.98	off	0	0.25	0.44
	30	V1 - 22	21	25.1	2.98	off	0	0.22	0.44
	31	V1 - 23	22	25.0	2.98	off	0	0.22	0.57
	32	V1 - 24	23	25.0	2.98	off	0	0.19	0.58

Appendix C-2. Cycle 2 (10/17-18/2014) Data Continued

	Sample No.	Sample Name	Elapsed time (hr)	Temp. ⁺ (°C)	pH ⁺	Light (on/off)	Light intensity ⁺⁺ (Lux)	Fe ^{II*} (mg/L)	Fe(total) [*] (mg/L)
Vessel 1	33	V1 - 25a	24	25.0	2.98	off	0	0.20	0.56
	34	V1 - 25b	24	25.0	2.98	off	0	0.20	0.57
	35	V1 - 25c	24	25.0	2.98	off	0	0.20	0.56
	36	V1 - 26	25	24.9	2.99	off	0	0.20	0.57
	37	V1 - 27	26	24.9	2.98	off	0	0.19	0.57
	38	V1 - 28	27	24.8	2.98	on	3616.7	0.19	0.58
	39	V1 - 29	28	24.8	2.96	on	3401.5	0.20	0.58
	40	V1 - 30	29	24.8	2.97	on	3530.6	0.20	0.58
	41	V1 - 31a	30	24.8	2.99	on	3702.8	0.18	0.60
	42	V1 - 31b	30	24.8	2.99	on	3702.8	0.18	0.60
	43	V1 - 31c	30	24.8	2.99	on	3702.8	0.19	0.60
Vessel 2	44	V2 - 1a	0	24.0	2.95	off	0	0.077	0.71
	45	V2 - 1b	0	24.0	2.95	off	0	0.077	0.71
	46	V2 - 1c	0	24.0	2.95	off	0	0.091	0.71
	47	V2 - 2	1	23.4	2.94	off	0	0.077	0.71
	48	V2 - 3	2	23.3	2.96	off	0	0.077	0.68
	49	V2 - 4	3	24.4	2.94	on	3702.8	0.11	0.70
	50	V2 - 5	4	24.7	2.96	on	3961.1	0.15	0.70
	51	V2 - 6	5	24.8	2.93	on	3961.1	0.16	0.68
	52	V2 - 7a	6	24.9	2.93	on	3616.7	0.20	0.70
	53	V2 - 7b	6	24.9	2.93	on	3616.7	0.19	0.71
	54	V2 - 7c	6	24.9	2.93	on	3616.7	0.20	0.71
	55	V2 - 8	7	24.8	2.96	on	3788.9	0.19	0.71
	56	V2 - 9	8	24.8	2.96	on	3961.1	0.22	0.71
	57	V2 - 10	9	24.6	2.96	on	3702.8	0.22	0.76
	58	V2 - 11	10	25.0	2.93	on	3875.0	0.22	0.73
	59	V2 - 12	11	24.8	2.96	on	3875.0	0.20	0.74
	60	V2 - 13a	12	24.5	2.93	on	3875.0	0.22	0.73
	61	V2 - 13b	12	24.5	2.93	on	3875.0	0.22	0.73
	62	V2 - 13c	12	24.5	2.93	on	3875.0	0.23	0.74
	63	V2 - 14	13	24.7	2.96	on	3961.1	0.23	0.77
	64	V2 - 15	14	24.7	2.95	on	3616.7	0.37	0.74

Appendix C-2. Cycle 2 (10/17-18/2014) Data Continued

	Sample No.	Sample Name	Elapsed time (hr)	Temp. ⁺ (°C)	pH ⁺	Light (on/off)	Light intensity ⁺⁺ (Lux)	Fe ^{II*} (mg/L)	Fe(total) [*] (mg/L)
Vessel 2	65	V2 - 16	15	24.4	2.95	off	0	0.37	0.71
	66	V2 - 17	16	24.7	2.95	off	0	0.39	0.71
	67	V2 - 18	17	24.6	2.94	off	0	0.36	0.71
	68	V2 - 19a	18	24.7	2.95	off	0	0.37	0.74
	69	V2 - 19b	18	24.7	2.95	off	0	0.39	0.74
	70	V2 - 19c	18	24.7	2.95	off	0	0.37	0.73
	71	V2 - 20	19	25.2	2.95	off	0	0.39	0.74
	72	V2 - 21	20	25.2	2.95	off	0	0.37	0.77
	73	V2 - 22	21	25.3	2.95	off	0	0.37	0.74
	74	V2 - 23	22	25.0	2.95	off	0	0.36	0.87
	75	V2 - 24	23	24.9	2.95	off	0	0.33	0.88
	76	V2 - 25a	24	25.1	2.94	off	0	0.34	0.87
	77	V2 - 25b	24	25.1	2.94	off	0	0.34	0.87
	78	V2 - 25c	24	25.1	2.94	off	0	0.36	0.87
	79	V2 - 26	25	25.2	2.94	off	0	0.34	0.88
	80	V2 - 27	26	25.0	2.95	off	0	0.34	0.87
	81	V2 - 28	27	25.1	2.96	on	3616.7	0.36	0.88
	82	V2 - 29	28	25.1	2.93	on	3401.5	0.36	0.90
	83	V2 - 30	29	25.1	2.96	on	3530.6	0.36	0.91
	84	V2 - 31a	30	25.0	2.93	on	3702.8	0.34	0.91
	85	V2 - 31b	30	25.0	2.93	on	3702.8	0.34	0.91
	86	V2 - 31c	30	25.0	2.93	on	3702.8	0.36	0.90
Vessel 3	87	V3 - 1a	0	23.4	2.87	off	0	0.063	0.77
	88	V3 - 1b	0	23.4	2.87	off	0	0.077	0.73
	89	V3 - 1c	0	23.4	2.87	off	0	0.063	0.74
	90	V3 - 2	1	24.0	2.87	off	0	0.063	0.76
	91	V3 - 3	2	24.7	2.86	off	0	0.063	0.77
	92	V3 - 4	3	24.8	2.87	on	3702.8	0.091	0.81
	93	V3 - 5	4	24.8	2.89	on	3961.1	0.091	0.85
	94	V3 - 6	5	24.6	2.89	on	3961.1	0.11	0.87
	95	V3 - 7a	6	24.4	2.89	on	3616.7	0.11	0.90
	96	V3 - 7b	6	24.4	2.89	on	3616.7	0.11	0.90

Appendix C-2. Cycle 2 (10/17-18/2014) Data Continued

	Sample No.	Sample Name	Elapsed time (hr)	Temp. ⁺ (°C)	pH ⁺	Light (on/off)	Light intensity ⁺⁺ (Lux)	Fe ^{II*} (mg/L)	Fe(total) [*] (mg/L)
Vessel 3	97	V3 - 7c	6	24.4	2.89	on	3616.7	0.11	0.90
	98	V3 - 8	7	24.7	2.90	on	3788.9	0.091	0.90
	99	V3 - 9	8	24.3	2.90	on	3961.1	0.11	0.93
	100	V3 - 10	9	24.6	2.89	on	3702.8	0.091	0.97
	101	V3 - 11	10	24.4	2.89	on	3875.0	0.091	0.98
	102	V3 - 12	11	24.4	2.88	on	3875.0	< 0.02 ^x	1.0
	103	V3 - 13a	12	24.0	2.89	on	3875.0	0.091	1.0
	104	V3 - 13b	12	24.0	2.89	on	3875.0	0.11	1.0
	105	V3 - 13c	12	24.0	2.89	on	3875.0	0.11	0.98
	106	V3 - 14	13	24.4	2.88	on	3961.1	0.11	1.0
	107	V3 - 15	14	24.3	3.13	on	3616.7	0.29	0.84
	108	V3 - 16	15	24.1	3.13	off	0	0.27	0.83
	109	V3 - 17	16	23.7	3.13	off	0	0.27	0.80
	110	V3 - 18	17	23.4	3.13	off	0	0.25	0.77
	111	V3 - 19a	18	23.4	3.14	off	0	0.26	0.80
	112	V3 - 19b	18	23.4	3.14	off	0	0.26	0.80
	113	V3 - 19c	18	23.4	3.14	off	0	0.26	0.80
	114	V3 - 20	19	24.5	3.13	off	0	0.27	0.80
	115	V3 - 21	20	24.7	3.13	off	0	0.26	0.78
	116	V3 - 22	21	24.7	3.13	off	0	0.25	0.77
	117	V3 - 23	22	25.0	3.13	off	0	0.23	0.90
	118	V3 - 24	23	25.2	3.12	off	0	0.20	0.93
	119	V3 - 25a	24	25.1	3.13	off	0	0.23	0.88
	120	V3 - 25b	24	25.1	3.13	off	0	0.22	0.88
	121	V3 - 25c	24	25.1	3.13	off	0	0.22	0.88
	122	V3 - 26	25	24.8	3.13	off	0	0.22	0.90
	123	V3 - 27	26	24.1	3.13	off	0	0.22	0.93
	124	V3 - 28	27	24.5	3.14	on	3616.7	0.22	0.88
	125	V3 - 29	28	24.8	3.13	on	3401.5	0.23	0.90
	126	V3 - 30	29	24.9	3.13	on	3530.6	0.23	0.90
	127	V3 - 31a	30	25.0	3.13	on	3702.8	0.22	0.90
	128	V3 - 31b	30	25.0	3.13	on	3702.8	0.23	0.90

Appendix C-2. Cycle 2 (10/17-18/2014) Data Continued

	Sample No.	Sample Name	Elapsed time (hr)	Temp. ⁺ (°C)	pH ⁺	Light (on/off)	Light intensity ⁺⁺ (Lux)	Fe ^{II*} (mg/L)	Fe(total) [*] (mg/L)
V3	129	V3 - 31c	30	25.0	3.13	on	3702.8	0.20	0.91
Vessel 4	130	V4 - 1a	0	24.2	2.97	off	0	0.12	0.70
	131	V4 - 1b	0	24.2	2.97	off	0	0.11	0.68
	132	V4 - 1c	0	24.2	2.97	off	0	0.11	0.68
	133	V4 - 2	1	24.1	2.96	off	0	0.11	0.67
	134	V4 - 3	2	24.5	2.97	off	0	0.11	0.64
	135	V4 - 4	3	24.8	2.97	on	3702.8	0.13	0.66
	136	V4 - 5	4	24.7	2.97	on	3961.1	0.12	0.64
	137	V4 - 6	5	24.7	2.96	on	3961.1	0.13	0.63
	138	V4 - 7a	6	24.7	2.97	on	3616.7	0.13	0.64
	139	V4 - 7b	6	24.7	2.97	on	3616.7	0.13	0.66
	140	V4 - 7c	6	24.7	2.97	on	3616.7	0.15	0.71
	141	V4 - 8	7	24.9	2.95	on	3788.9	0.13	0.63
	142	V4 - 9	8	24.5	2.95	on	3961.1	0.13	0.64
	143	V4 - 10	9	24.6	2.96	on	3702.8	0.16	0.64
	144	V4 - 11	10	24.4	2.95	on	3875.0	0.12	0.64
	145	V4 - 12	11	24.4	2.96	on	3875.0	0.091	0.64
	146	V4 - 13a	12	24.0	2.98	on	3875.0	0.13	0.61
	147	V4 - 13b	12	24.0	2.98	on	3875.0	0.12	0.61
	148	V4 - 13c	12	24.0	2.98	on	3875.0	0.12	0.63
	149	V4 - 14	13	24.3	2.97	on	3961.1	0.12	0.63
	150	V4 - 15	14	24.2	2.96	on	3616.7	0.26	0.61
	151	V4 - 16	15	24.0	2.96	off	0	0.26	0.58
	152	V4 - 17	16	23.6	2.96	off	0	0.25	0.58
	153	V4 - 18	17	23.3	2.97	off	0	0.23	0.56
	154	V4 - 19a	18	23.2	2.97	off	0	0.26	0.58
	155	V4 - 19b	18	23.2	2.97	off	0	0.26	0.58
	156	V4 - 19c	18	23.2	2.97	off	0	0.25	0.58
	157	V4 - 20	19	24.3	2.97	off	0	0.27	0.57
	158	V4 - 21	20	24.5	2.97	off	0	0.25	0.58
	159	V4 - 22	21	24.6	2.97	off	0	0.23	0.56
	160	V4 - 23	22	24.7	2.97	off	0	0.22	0.68

Appendix C-2. Cycle 2 (10/17-18/2014) Data Continued

	Sample No.	Sample Name	Elapsed time (hr)	Temp. ⁺ (°C)	pH ⁺	Light (on/off)	Light intensity ⁺⁺ (Lux)	Fe ^{II} * (mg/L)	Fe(total) [*] (mg/L)
Vessel 4	161	V4 - 24	23	24.8	2.97	off	0	0.19	0.68
	162	V4 - 25a	24	24.6	2.97	off	0	0.22	0.68
	163	V4 - 25b	24	24.6	2.97	off	0	0.20	0.68
	164	V4 - 25c	24	24.6	2.97	off	0	0.22	0.68
	165	V4 - 26	25	24.3	2.96	off	0	0.20	0.68
	166	V4 - 27	26	23.7	2.97	off	0	0.20	0.67
	167	V4 - 28	27	23.9	2.97	on	3616.7	0.20	0.68
	168	V4 - 29	28	24.1	2.97	on	3401.5	0.20	0.70
	169	V4 - 30	29	24.3	2.97	on	3530.6	0.20	0.70
	170	V4 - 31a	30	24.4	2.97	on	3702.8	0.19	0.70
	171	V4 - 31b	30	24.4	2.97	on	3702.8	0.19	0.71
	172	V4 - 31c	30	24.4	2.97	on	3702.8	0.19	0.71

⁺ Measured using DrDAQ PicoLog Recorder

⁺⁺ Measured using HOBO Pendant Light/Temperature Loggers

* Samples analyzed using HACH DR2800 Spectrophotometer

^x Sample below ferrozine MDL of 0.02 mg/L for Fe^{II} and Fe(total)

Sample names including a,b,c are triplicate samples

Appendix C-3. Cycle 3 (10/25/2014) Data

	Sample No.	Sample Name	Elapsed time (hr)	Temp. ⁺ (°C)	pH ⁺	Light (on/off)	Fe ^{II} * (mg/L)	Fe(total)* (mg/L)	Se ^{IV} ** (µg/L)
Vessel 1	1	V1 - 1a	0	25.5	2.97	off	0.048	0.51	126.0
	2	V1 - 1b	0	25.5	2.97	off	0.048	0.51	129.6
	3	V1 - 1c	0	25.5	2.97	off	0.048	0.52	200.1
	4	V1 - 2	1	26.7	2.96	off	0.048	0.52	136.4
	5	V1 - 3	2	28.1	2.97	off	0.062	0.52	278.1
	6	V1 - 4	3	30.6	2.98	off	0.062	0.52	290.4
	7	V1 - 5	4	32.8	2.98	off	0.048	0.49	259.6
	8	V1 - 6a	5	33.0	2.97	off	0.034	0.48	264.5
	9	V1 - 6b	5	33.0	2.97	off	0.048	0.48	271.7
	10	V1 - 6c	5	33.0	2.97	off	0.048	0.48	273.5
	11	V1 - 7	6	23.7	2.96	off	< 0.02 ^x	0.48	226.0
	12	V1 - 8	7	21.1	2.98	off	0.034	0.48	197.2
	13	V1 - 9	8	15.3	2.98	off	< 0.02 ^x	0.46	183.5
	14	V1 - 10	9	13.4	2.98	off	< 0.02 ^x	0.48	168.1
	15	V1 - 11a	10	16.9	2.99	off	< 0.02 ^x	0.48	144.7
	16	V1 - 11b	10	16.9	2.99	off	< 0.02 ^x	0.48	161.8
	17	V1 - 11c	10	16.9	2.99	off	< 0.02 ^x	0.48	154.0
Vessel 2	18	V2 - 1a	0	25.1	3.01	off	0.13	0.71	249.9
	19	V2 - 1b	0	25.1	3.01	off	0.13	0.71	262.9
	20	V2 - 1c	0	25.1	3.01	off	0.12	0.71	253.5
	21	V2 - 2	1	26.8	2.99	off	0.15	0.75	282.8
	22	V2 - 3	2	28.8	3.00	off	0.13	0.69	317.8
	23	V2 - 4	3	30.2	2.99	off	0.15	0.68	361.9
	24	V2 - 5	4	32.6	2.99	off	0.13	0.65	390.8
	25	V2 - 6a	5	32.9	2.99	off	0.12	0.64	353.3
	26	V2 - 6b	5	32.9	2.99	off	0.12	0.65	361.9
	27	V2 - 6c	5	32.9	2.99	off	0.12	0.64	371.3
	28	V2 - 7	6	23.5	2.97	off	0.12	0.62	321.8
	29	V2 - 8	7	21.6	2.97	off	0.11	0.62	295.1
	30	V2 - 9	8	18.6	2.97	off	0.091	0.64	273.7
	31	V2 - 10	9	15.5	2.96	off	0.049	0.65	258.5
	32	V2 - 11a	10	16.7	2.97	off	0.049	0.65	243.7

Appendix C-3. Cycle 3 (10/25/2014) Data Continued

	Sample No.	Sample Name	Elapsed time (hr)	Temp. ⁺ (°C)	pH ⁺	Light (on/off)	Fe ^{II} * (mg/L)	Fe(total)* (mg/L)	Se ^{IV} ** (µg/L)
V2	33	V2 - 11b	10	16.7	2.97	off	0.035	0.65	240.9
	34	V2 - 11c	10	16.7	2.97	off	0.035	0.65	245.9
Vessel 3	35	V3 - 1a	0	25.8	3.16	off	0.12	0.64	293.0
	36	V3 - 1b	0	25.8	3.16	off	0.12	0.65	306.4
	37	V3 - 1c	0	25.8	3.16	off	0.12	0.64	288.0
	38	V3 - 2	1	27.7	3.17	off	0.13	0.64	292.8
	39	V3 - 3	2	30.2	3.18	off	0.12	0.62	312.3
	40	V3 - 4	3	32.7	3.16	off	0.12	0.58	308.9
	41	V3 - 5	4	35.8	3.17	off	0.077	0.56	520.4
	42	V3 - 6a	5	36.3	3.17	off	0.077	0.52	335.4
	43	V3 - 6b	5	36.3	3.17	off	0.077	0.52	339.6
	44	V3 - 6c	5	36.3	3.17	off	0.077	0.51	335.9
	45	V3 - 7	6	23.3	3.15	off	0.049	0.51	302.7
	46	V3 - 8	7	21.4	3.16	off	0.063	0.54	280.8
	47	V3 - 9	8	16.7	3.17	off	0.049	0.52	300.4
	48	V3 - 10	9	14.6	3.17	off	< 0.02 ^x	0.54	271.4
	49	V3 - 11a	10	16.8	3.18	off	< 0.02 ^x	0.54	224.0
Vessel 4	50	V3 - 11b	10	16.8	3.18	off	< 0.02 ^x	0.55	223.1
	51	V3 - 11c	10	16.8	3.18	off	< 0.02 ^x	0.52	141.9
	52	V4 - 1a	0	25.3	2.94	off	0.091	0.62	175.8
	53	V4 - 1b	0	25.3	2.94	off	0.077	0.65	171.5
	54	V4 - 1c	0	25.3	2.94	off	0.091	0.62	177.4
	55	V4 - 2	1	27.1	2.93	off	0.091	0.64	182.0
	56	V4 - 3	2	29.7	2.94	off	0.091	0.59	198.9
	57	V4 - 4	3	32.0	2.93	off	0.11	0.62	269.7
	58	V4 - 5	4	34.9	2.92	off	0.077	0.56	291.5
	59	V4 - 6a	5	35.4	2.92	off	0.077	0.55	259.1
	60	V4 - 6b	5	35.4	2.92	off	0.091	0.59	262.0
	61	V4 - 6c	5	35.4	2.92	off	0.063	0.56	266.7
	62	V4 - 7	6	23.7	2.95	off	0.049	0.54	246.6
	63	V4 - 8	7	21.8	2.95	off	0.063	0.56	213.7
	64	V4 - 9	8	19.4	2.96	off	0.049	0.56	246.3

Appendix C-3. Cycle 3 (10/25/2014) Data Continued

	Sample No.	Sample Name	Elapsed time (hr)	Temp. ⁺ (°C)	pH ⁺	Light (on/off)	Fe ^{II} * (mg/L)	Fe(total)* (mg/L)	Se ^{IV} ** (µg/L)
Vessel 4	65	V4 - 10	9	18.6	2.96	off	< 0.02 ^x	0.55	255.0
	66	V4 - 11a	10	17.6	2.97	off	< 0.02 ^x	0.58	221.4
	67	V4 - 11b	10	16.6	2.97	off	< 0.02 ^x	0.55	218.7
	68	V4 - 11c	10	15.6	2.97	off	< 0.02 ^x	0.56	224.1

⁺ Measured using DrDAQ PicoLog Recorder

^{*} Samples analyzed using HACH DR2800 Spectrophotometer

^{**} Samples analyzed using HG-ICP-OES (MDL 5 µg/L Se^{IV})

^x Sample below ferrozine MDL of 0.02 mg/L for Fe^{II} and Fe(total)

--- Sample not analyzed

Sample names including a,b,c are triplicate samples

Appendix C-4. Cycle 4 (12/9/2014) Data

	Sample No.	Sample Name	Elapsed time (hr)	Temp. ⁺ (°C)	pH ⁺	Light (on/off)	Light Intensity (Lux)	Fe ^{II*} (mg/L)	Fe(total) [*] (mg/L)	Se ^{IV**} (µg/L)
Vessel 1	1	V1 - 1a	0	22.2	2.75	on	3616.7	0.34	1.0	---
	2	V1 - 1b	0	22.2	2.75	on	3616.7	0.35	1.1	---
	3	V1 - 1c	0	22.2	2.75	on	3616.7	0.35	1.0	---
	4	V1 - 2a	0.98	25.1	2.77	on	3788.9	0.34	1.0	---
	5	V1 - 2b	0.98	25.1	2.77	on	3788.9	0.35	1.0	---
	6	V1 - 2c	0.98	25.1	2.77	on	3788.9	0.34	1.0	---
	7	V1 - 3a	1.77	30.1	2.72	on	3444.5	0.35	1.1	---
	8	V1 - 3b	1.77	30.1	2.72	on	3444.5	0.35	1.1	---
	9	V1 - 3c	1.77	30.1	2.72	on	3444.5	0.34	1.1	---
	10	V1 - 4a	2.48	35.0	2.70	on	3616.7	0.35	1.1	---
	11	V1 - 4b	2.48	35.0	2.70	on	3616.7	0.35	1.1	---
	12	V1 - 4c	2.48	35.0	2.70	on	3616.7	0.35	1.1	---
	13	V1 - 5a	3.61	29.8	2.69	on	3702.8	0.34	1.0	---
	14	V1 - 5b	3.61	29.8	2.69	on	3702.8	0.35	0.97	---
	15	V1 - 5c	3.61	29.8	2.69	on	3702.8	0.34	1.0	---
	16	V1 - 6a	3.77	25.5	2.69	on	3358.4	0.33	1.0	---
	17	V1 - 6b	3.77	25.5	2.69	on	3358.4	0.31	1.0	---
	18	V1 - 6c	3.77	25.5	2.69	on	3358.4	0.33	1.0	---
	19	V1 - 7a	5.80	20.4	2.73	on	3702.8	0.33	1.1	---
	20	V1 - 7b	5.80	20.4	2.73	on	3702.8	0.34	1.0	---
	21	V1 - 7c	5.80	20.4	2.73	on	3702.8	0.31	1.1	---
	22	V1 - 8a	6.02	14.9	2.71	on	3702.8	0.31	1.1	---
	23	V1 - 8b	6.02	14.9	2.71	on	3702.8	0.35	1.0	---
	24	V1 - 8c	6.02	14.9	2.71	on	3702.8	0.33	1.0	---
	25	V1 - 9a	6.33	9.8	2.73	on	3530.6	0.30	1.0	---
	26	V1 - 9b	6.33	9.8	2.73	on	3530.6	0.31	1.0	---
	27	V1 - 9c	6.33	9.8	2.73	on	3530.6	0.31	1.1	---
	28	V1 - 10a	6.83	5.5	2.74	on	3616.7	0.31	1.0	---
	29	V1 - 10b	6.83	5.5	2.74	on	3616.7	0.31	1.0	---
	30	V1 - 10c	6.83	5.5	2.74	on	3616.7	0.30	1.0	---
	31	V1 - 11a	7.59	11.1	2.69	on	3702.8	0.27	1.0	---
	32	V1 - 11b	7.59	11.1	2.69	on	3702.8	0.26	1.0	---

Appendix C-4. Cycle 4 (12/9/2014) Data Continued

	Sample No.	Sample Name	Elapsed time (hr)	Temp. ⁺ (°C)	pH ⁺	Light (on/off)	Light Intensity ⁺⁺ (Lux)	Fe ^{II*} (mg/L)	Fe(total) [*] (mg/L)	Se ^{IV**} (µg/L)
Vessel 1	33	V1 - 11c	7.59	11.1	2.69	on	3702.8	0.27	1.0	---
	34	V1 - 12a	7.74	15.6	2.73	on	3530.6	0.27	1.0	---
	35	V1 - 12b	7.74	15.6	2.73	on	3530.6	0.23	1.0	---
	36	V1 - 12c	7.74	15.6	2.73	on	3530.6	0.24	1.1	---
	37	V1 - 13a	8.22	20.0	2.71	on	3444.5	0.28	1.0	---
	38	V1 - 13b	8.22	20.0	2.71	on	3444.5	0.27	1.0	---
	39	V1 - 13c	8.22	20.0	2.71	on	3444.5	0.30	1.0	---
	40	V1 - 14a	8.88	25.4	2.67	on	3444.5	0.28	1.1	---
	41	V1 - 14b	8.88	25.4	2.67	on	3444.5	0.28	1.1	---
	42	V1 - 14c	8.88	25.4	2.67	on	3444.5	0.28	1.0	---
	43	V1 - 15a	9.41	30.2	2.70	on	3444.5	0.33	1.1	---
	44	V1 - 15b	9.41	30.2	2.70	on	3444.5	0.30	1.0	---
	45	V1 - 15c	9.41	30.2	2.70	on	3444.5	0.31	1.1	---
	46	V1 - 16a	9.99	36.5	2.67	on	3358.4	0.30	1.0	---
	47	V1 - 16b	9.99	36.5	2.67	on	3358.4	0.30	1.1	---
	48	V1 - 16c	9.99	36.5	2.67	on	3358.4	0.31	1.1	---
Vessel 2	49	V2 - 1a	0	22.3	2.83	on	3616.7	0.33	0.94	---
	50	V2 - 1a	0	22.3	2.83	on	3616.7	0.33	0.95	---
	51	V2 - 1a	0	22.3	2.83	on	3616.7	0.34	0.95	---
	52	V2 - 2a	0.75	25.0	2.84	on	3788.9	0.31	0.94	---
	53	V2 - 2b	0.75	25.0	2.84	on	3788.9	0.33	0.93	---
	54	V2 - 2c	0.75	25.0	2.84	on	3788.9	0.33	0.93	---
	55	V2 - 3a	1.76	30.0	2.85	on	3444.5	0.31	0.97	---
	56	V2 - 3b	1.76	30.0	2.85	on	3444.5	0.31	1.0	---
	57	V2 - 3c	1.76	30.0	2.85	on	3444.5	0.33	0.98	---
	58	V2 - 4a	3.06	35.0	2.82	on	3616.7	0.30	1.0	---
	59	V2 - 4b	3.06	35.0	2.82	on	3616.7	0.31	1.0	---
	60	V2 - 4c	3.06	35.0	2.82	on	3616.7	0.33	0.98	---
	61	V2 - 5a	3.95	30.0	2.84	on	3702.8	0.31	0.94	---
	62	V2 - 5b	3.95	30.0	2.84	on	3702.8	0.31	0.94	---
	63	V2 - 5c	3.95	30.0	2.84	on	3702.8	0.33	0.93	---
	64	V2 - 6a	4.17	25.5	2.83	on	3358.4	0.31	0.94	---

Appendix C-4. Cycle 4 (12/9/2014) Data Continued

	Sample No.	Sample Name	Elapsed time (hr)	Temp. ⁺ (°C)	pH ⁺	Light (on/off)	Light Intensity ⁺⁺ (Lux)	Fe ^{II*} (mg/L)	Fe(total) [*] (mg/L)	Se ^{IV**} (µg/L)
Vessel 2	65	V2 - 6b	4.17	25.5	2.83	on	3358.4	0.31	0.95	---
	66	V2 - 6c	4.17	25.5	2.83	on	3358.4	0.30	0.94	---
	67	V2 - 7a	5.80	20.3	2.81	on	3702.8	0.34	0.95	---
	68	V2 - 7b	5.80	20.3	2.81	on	3702.8	0.33	0.95	---
	69	V2 - 7c	5.80	20.3	2.81	on	3702.8	0.34	0.93	---
	70	V2 - 8a	6.04	15.2	2.77	on	3702.8	0.33	0.91	---
	71	V2 - 8b	6.04	15.2	2.77	on	3702.8	0.31	0.93	---
	72	V2 - 8c	6.04	15.2	2.77	on	3702.8	0.33	0.93	---
	73	V2 - 9a	6.34	10.4	2.78	on	3530.6	0.33	0.88	---
	74	V2 - 9b	6.34	10.4	2.78	on	3530.6	0.30	0.84	---
	75	V2 - 9c	6.34	10.4	2.78	on	3530.6	0.30	0.87	---
	76	V2 - 10a	7.11	5.8	2.81	on	3616.7	0.30	0.93	---
	77	V2 - 10b	7.11	5.8	2.81	on	3616.7	0.28	0.91	---
	78	V2 - 10c	7.11	5.8	2.81	on	3616.7	0.30	0.97	---
	79	V2 - 11a	7.60	11.6	2.81	on	3702.8	0.30	0.94	---
	80	V2 - 11b	7.60	11.6	2.81	on	3702.8	0.27	0.93	---
	81	V2 - 11c	7.60	11.6	2.81	on	3702.8	0.27	0.93	---
	82	V2 - 12a	7.74	16.0	2.80	on	3530.6	0.26	0.94	---
	83	V2 - 12b	7.74	16.0	2.80	on	3530.6	0.27	0.91	---
	84	V2 - 12c	7.74	16.0	2.80	on	3530.6	0.28	0.91	---
	85	V2 - 13a	8.13	20.4	2.79	on	3444.5	0.28	0.95	---
	86	V2 - 13b	8.13	20.4	2.79	on	3444.5	0.27	0.93	---
	87	V2 - 13c	8.13	20.4	2.79	on	3444.5	0.27	0.91	---
	88	V2 - 14a	8.88	25.2	2.79	on	3444.5	0.30	0.95	---
	89	V2 - 14b	8.88	25.2	2.79	on	3444.5	0.28	0.95	---
	90	V2 - 14c	8.88	25.2	2.79	on	3444.5	0.28	0.95	---
	91	V2 - 15a	9.51	30.0	2.81	on	3444.5	0.30	0.94	---
	92	V2 - 15b	9.51	30.0	2.81	on	3444.5	0.28	0.94	---
	93	V2 - 15c	9.51	30.0	2.81	on	3444.5	0.31	0.94	---
	94	V2 - 16a	9.99	35.4	2.82	on	3358.4	0.28	0.97	---
	95	V2 - 16b	9.99	35.4	2.82	on	3358.4	0.26	0.95	---
	96	V2 - 16c	9.99	35.4	2.82	on	3358.4	0.30	0.88	---

Appendix C-4. Cycle 4 (12/9/2014) Data Continued

	Sample No.	Sample Name	Elapsed time (hr)	Temp. ⁺ (°C)	pH ⁺	Light (on/off)	Light Intensity ⁺⁺ (Lux)	Fe ^{II*} (mg/L)	Fe(total) [*] (mg/L)	Se ^{IV**} (µg/L)
Vessel 3	97	V3 - 1a	0	22.3	3.17	on	3616.7	0.31	1.0	15.60
	98	V3 - 1b	0	22.3	3.17	on	3616.7	0.33	1.0	14.69
	99	V3 - 1c	0	22.3	3.17	on	3616.7	0.33	1.0	12.38
	100	V3 - 2	0.45	25.6	3.16	on	3788.9	0.34	1.0	11.83
	101	V3 - 3	1.50	31.3	3.17	on	3444.5	0.28	1.1	11.10
	102	V3 - 4	2.43	35.5	3.15	on	3616.7	0.30	1.0	81.47
	103	V3 - 5a	3.25	30.0	2.98	on	3702.8	0.33	1.0	10.33
	104	V3 - 5b	3.25	30.0	2.98	on	3702.8	0.30	1.0	10.60
	105	V3 - 5c	3.25	30.0	2.98	on	3702.8	0.30	1.0	14.66
	106	V3 - 6	3.28	25.1	3.19	on	3358.4	0.31	1.0	11.31
	107	V3 - 7	5.65	19.8	3.21	on	3702.8	0.31	1.0	12.88
	108	V3 - 8	5.90	14.9	3.24	on	3702.8	0.30	1.0	14.19
	109	V3 - 9	6.14	9.8	3.29	on	3530.6	0.30	1.0	13.51
	110	V3 - 10a	6.81	2.2	3.35	on	3616.7	0.28	0.98	11.81
	111	V3 - 10b	6.81	2.2	3.35	on	3616.7	0.28	0.98	12.81
	112	V3 - 10c	6.81	2.2	3.35	on	3616.7	0.27	0.98	12.41
	113	V3 - 11	7.58	11.7	3.22	on	3702.8	0.27	1.0	11.67
	114	V3 - 12	7.67	15.7	3.21	on	3530.6	0.28	1.0	13.99
	115	V3 - 13	8.37	21.0	3.18	on	3444.5	0.27	1.0	13.46
	116	V3 - 14	8.54	25.0	3.20	on	3444.5	0.27	1.1	11.46
Vessel 4	117	V3 - 15	9.36	31.5	3.20	on	3444.5	0.28	1.0	9.000
	118	V3 - 16a	9.76	35.0	3.20	on	3358.4	0.31	1.0	9.630
	119	V3 - 16b	9.76	35.0	3.20	on	3358.4	0.30	1.1	8.920
	120	V3 - 16c	9.76	35.0	3.20	on	3358.4	0.30	1.0	< 5 ^{xx}
	121	V4 - 1a	0	22.0	2.74	on	3616.7	0.38	1.0	< 5 ^{xx}
	122	V4 - 1b	0	22.0	2.74	on	3616.7	0.38	1.0	38.18
	123	V4 - 1c	0	22.0	2.74	on	3616.7	0.38	1.0	37.03
	124	V4 - 2	0.45	25.1	2.77	on	3788.9	0.37	0.98	40.25
	125	V4 - 3	1.51	30.2	2.98	on	3444.5	0.34	1.0	45.78
	126	V4 - 4	2.94	35.5	2.66	on	3616.7	0.38	1.0	71.37
	127	V4 - 5a	3.66	29.8	2.66	on	3702.8	0.40	0.98	84.74
	128	V4 - 5b	3.66	29.8	2.66	on	3702.8	0.38	0.97	80.81

Appendix C-4. Cycle 4 (12/9/2014) Data Continued

	Sample No.	Sample Name	Elapsed time (hr)	Temp. [†] (°C)	pH [†]	Light (on/off)	Light Intensity ⁺⁺ (Lux)	Fe ^{II} * (mg/L)	Fe(total)* (mg/L)	Se ^{IV} ** (µg/L)
Vessel 4	129	V4 - 5c	3.66	29.8	2.66	on	3702.8	0.35	1.0	85.07
	130	V4 - 6	3.87	25.0	2.72	on	3358.4	0.34	0.97	82.37
	131	V4 - 7	5.80	20.1	2.72	on	3702.8	0.34	0.98	57.63
	132	V4 - 8	6.04	14.7	2.71	on	3702.8	0.31	0.95	49.26
	133	V4 - 9	6.34	9.8	2.75	on	3530.6	0.31	0.88	48.44
	134	V4 - 10a	6.97	5.0	2.82	on	3616.7	0.28	0.93	34.87
	135	V4 - 10b	6.97	5.0	2.82	on	3616.7	0.28	0.94	36.33
	136	V4 - 10c	6.97	5.0	2.82	on	3616.7	0.26	0.90	38.29
	137	V4 - 11	7.62	11.4	2.80	on	3702.8	0.30	0.88	36.23
	138	V4 - 12	7.74	15.1	2.76	on	3530.6	0.28	1.0	37.25
	139	V4 - 13	8.25	20.0	2.72	on	3444.5	0.30	1.0	34.82
	140	V4 - 14	8.89	25.1	2.70	on	3444.5	0.31	0.98	38.00
	141	V4 - 15	9.51	30.3	2.69	on	3444.5	0.31	1.0	34.30
	142	V4 - 16a	9.88	35.0	2.70	on	3358.4	0.34	1.0	33.46
	143	V4 - 16b	9.88	35.0	2.70	on	3358.4	0.34	0.97	35.66
	144	V4 - 16c	9.88	35.0	2.70	on	3358.4	0.33	1.0	34.92

[†] Measured using DrDAQ PicoLog Recorder

⁺⁺ Measured using HOBO Pendant Light/Temperature Loggers

* Samples analyzed using HACH DR2800 Spectrophotometer (MDL 0.02 mg/L for Fe^{II} and Fe(total))

** Samples analyzed using HG-ICP-OES

^{xx} Sample below HG-ICP-OES MDL of 5 µg/L for Se^{IV}

--- Sample not analyzed

Sample names including a,b,c are triplicate samples

Appendix C-5. Cycle 5 (1/29/2015) Data

	Sample No.	Sample Name	Elapsed time (hr)	Temp. ⁺ (°C)	pH ⁺	Light (on/off)	Light Intensity ⁺⁺ (Lux)	Se ^{IV**} (µg/L)
Vessel 1	1	V1 - 1	0	25.0	2.72	on	1431.6	284.1
	2	V1 - 2	0.25	30.0	2.72	on	1437.0	328.2
	3	V1 - 3a	0.82	35.1	2.71	on	1334.8	333.3
	4	V1 - 3b	0.82	35.1	2.71	on	1334.8	306.0
	5	V1 - 3c	0.82	35.1	2.71	on	1334.8	321.4
	6	V1 - 4	2.57	30.0	2.70	on	1237.9	309.4
	7	V1 - 5	3.02	24.4	2.70	on	1243.3	321.1
	8	V1 - 6	3.12	19.6	2.69	on	1173.3	297.7
	9	V1 - 7a	3.32	14.9	2.68	on	1211.0	309.0
	10	V1 - 7b	3.32	14.9	2.68	on	1211.0	305.3
Vessel 2	11	V2 - 1	0	25.0	2.62	on	1431.6	333.5
	12	V2 - 2	0.20	30.0	2.63	on	1437.0	339.6
	13	V2 - 3a	0.80	35.0	2.63	on	1334.8	343.3
	14	V2 - 3b	0.80	35.0	2.63	on	1334.8	347.6
	15	V2 - 3c	0.80	35.0	2.63	on	1334.8	351.8
	16	V2 - 4	1.73	30.0	2.64	on	1237.9	371.5
	17	V2 - 5	2.57	24.8	2.63	on	1243.3	352.4
	18	V2 - 6	3.03	19.8	2.63	on	1173.3	334.8
	19	V2 - 7a	3.23	13.7	2.61	on	1211.0	328.8
	20	V2 - 7b	3.23	13.7	2.61	on	1211.0	251.8
Vessel 3	21	V3 - 1	0	25.0	3.14	on	1431.6	281.4
	22	V3 - 2	0.27	30.0	3.14	on	1437.0	308.1
	23	V3 - 3a	0.50	35.0	3.16	on	1334.8	309.1
	24	V3 - 3b	0.50	35.0	3.16	on	1334.8	284.5
	25	V3 - 3c	0.50	35.0	3.16	on	1334.8	287.9
	26	V3 - 4	1.50	29.8	3.17	on	1237.9	222.4
	27	V3 - 5	1.73	24.9	3.16	on	1243.3	266.6
	28	V3 - 6	2.10	19.2	3.18	on	1173.3	298.5
	29	V3 - 7a	2.42	14.5	3.20	on	1211.0	291.0
	30	V3 - 7b	2.42	14.5	3.20	on	1211.0	297.2
V4	31	V4 - 1	0	25.2	2.62	on	1431.6	194.5
	32	V4 - 2	0.35	30.0	2.61	on	1437.0	234.9

Appendix C-5. Cycle 5 (1/29/2015) Data Continued

	Sample No.	Sample Name	Elapsed time (hr)	Temp. ⁺ (°C)	pH ⁺	Light (on/off)	Light Intensity ⁺⁺ (Lux)	Se ^{IV**} (µg/L)
Vessel 4	33	V4 - 3a	0.70	35.2	2.60	on	1334.8	202.4
	34	V4 - 3b	0.70	35.2	2.60	on	1334.8	199.2
	35	V4 - 3c	0.70	35.2	2.60	on	1334.8	212.2
	36	V4 - 4	1.62	29.9	2.59	on	1237.9	281.7
	37	V4 - 5	2.07	24.8	2.60	on	1243.3	233.8
	38	V4 - 6	2.43	19.7	2.63	on	1173.3	---
	39	V4 - 7a	2.92	18.1	2.63	on	1211.0	225.3
	40	V4 - 7b	2.92	18.1	2.63	on	1211.0	233.9

⁺ Measured using DrDAQ PicoLog Recorder

⁺⁺ Measured using HOBO Pendant Light/Temperature Loggers

^{**} Samples analyzed using HG-ICP-OES

^{xx} Sample below HG-ICP-OES MDL of 5 µg/L for Se^{IV}

--- Sample not analyzed

Sample names including a,b,c are double or triplicate samples

Appendix C-6. Cycle 6 (2/28/2015) Data

	Sample No.	Sample Name	Elapsed time (hr)	Temp. ⁺ (°C)	pH ⁺	Light (on/off)	Fe ^{II} * (mg/L)	Fe(total)* (mg/L)	Se ^{IV**} (µg/L)
Vessel 1	1	V1 - 1a	0	18.1	3.19	off	< 0.02 ^x	0.35	---
	2	V1 - 1b	0	18.1	3.19	off	< 0.02 ^x	0.32	---
	3	V1 - 1c	0	18.1	3.19	off	< 0.02 ^x	0.33	---
	4	V1 - 2	1.08	25.0	3.20	off	< 0.02 ^x	0.33	---
	5	V1 - 3	1.20	30.9	3.19	off	< 0.02 ^x	0.30	---
	6	V1 - 4	1.78	36.2	3.16	off	< 0.02 ^x	0.22	---
	7	V1 - 5a	2.11	28.6	3.15	off	< 0.02 ^x	0.32	---
	8	V1 - 5b	2.11	28.6	3.15	off	< 0.02 ^x	0.32	---
	9	V1 - 5c	2.11	28.6	3.15	off	< 0.02 ^x	0.36	---
	10	V1 - 6	2.84	23.7	3.18	off	< 0.02 ^x	0.30	---
	11	V1 - 7	4.11	20.1	3.18	off	< 0.02 ^x	0.30	---
	12	V1 - 8	4.36	15.1	3.20	off	< 0.02 ^x	0.22	---
	13	V1 - 9	4.66	10.0	3.21	off	< 0.02 ^x	0.25	---
	14	V1 - 10a	5.13	5.0	3.20	off	< 0.02 ^x	0.22	---
	15	V1 - 10b	5.13	5.0	3.20	off	< 0.02 ^x	0.22	---
	16	V1 - 10c	5.13	5.0	3.20	off	< 0.02 ^x	0.23	---
	17	V1 - 11	5.68	10.0	3.21	off	< 0.02 ^x	0.20	---
	18	V1 - 12	6.10	15.3	3.18	off	< 0.02 ^x	0.22	---
	19	V1 - 13	6.33	20.2	3.17	off	< 0.02 ^x	0.20	---
	20	V1 - 14	6.60	25.1	3.17	off	< 0.02 ^x	0.20	---
	21	V1 - 15	6.83	30.1	3.16	off	< 0.02 ^x	0.20	---
	22	V1 - 16a	7.04	35.2	3.15	off	< 0.02 ^x	0.19	---
	23	V1 - 16b	7.04	35.2	3.15	off	< 0.02 ^x	0.20	---
	24	V1 - 16c	7.04	35.2	3.15	off	< 0.02 ^x	0.20	---
Vessel 2	25	V2 - 1a	0	18.2	3.60	off	< 0.02 ^x	0.046	---
	26	V2 - 1b	0	18.2	3.60	off	< 0.02 ^x	0.060	---
	27	V2 - 1c	0	18.2	3.60	off	< 0.02 ^x	0.060	---
	28	V2 - 2	1.20	25.0	3.59	off	< 0.02 ^x	0.060	---
	29	V2 - 3	1.50	30.0	3.59	off	< 0.02 ^x	< 0.02 ^x	---
	30	V2 - 4	1.82	35.2	3.55	off	< 0.02 ^x	< 0.02 ^x	---
	31	V2 - 5a	2.25	26.5	3.54	off	< 0.02 ^x	< 0.02 ^x	---
	32	V2 - 5b	2.25	26.5	3.54	off	< 0.02 ^x	0.12	---

Appendix C-6. Cycle 6 (2/28/2015) Data Continued

	Sample No.	Sample Name	Elapsed time (hr)	Temp. ⁺ (°C)	pH ⁺	Light (on/off)	Fe ^{II*} (mg/L)	Fe(total) [*] (mg/L)	Se ^{IV**} (µg/L)
Vessel 2	33	V2 - 5c	2.25	26.5	3.54	off	< 0.02 ^x	0.15	---
	34	V2 - 6	2.85	22.9	3.55	off	< 0.02 ^x	0.089	---
	35	V2 - 7	3.78	20.0	3.55	off	< 0.02 ^x	1.3	---
	36	V2 - 8	4.16	14.2	3.59	off	< 0.02 ^x	0.046	---
	37	V2 - 9	4.46	10.0	3.59	off	< 0.02 ^x	0.046	---
	38	V2 - 10a	4.86	4.8	3.58	off	< 0.02 ^x	0.060	---
	39	V2 - 10b	4.86	4.8	3.58	off	< 0.02 ^x	0.26	---
	40	V2 - 10c	4.86	4.8	3.58	off	< 0.02 ^x	0.074	---
	41	V2 - 11	5.63	10.2	3.60	off	< 0.02 ^x	< 0.02 ^x	---
	42	V2 - 12	6.03	15.0	3.60	off	< 0.02 ^x	< 0.02 ^x	---
	43	V2 - 13	6.33	20.8	3.58	off	< 0.02 ^x	< 0.02 ^x	---
	44	V2 - 14	6.53	25.5	3.60	off	< 0.02 ^x	< 0.02 ^x	---
	45	V2 - 15	6.93	30.0	3.56	off	< 0.02 ^x	< 0.02 ^x	---
	46	V2 - 16a	7.13	36.2	3.56	off	< 0.02 ^x	< 0.02 ^x	---
	47	V2 - 16b	7.13	36.2	3.56	off	< 0.02 ^x	< 0.02 ^x	---
	48	V2 - 16c	7.13	36.2	3.56	off	< 0.02 ^x	< 0.02 ^x	---
Vessel 3	49	V3 - 1a	0	17.9	3.07	off	< 0.02 ^x	2.3	10.15
	50	V3 - 1b	0	17.9	3.07	off	< 0.02 ^x	2.3	9.160
	51	V3 - 1c	0	17.9	3.07	off	< 0.02 ^x	2.3	35.53
	52	V3 - 2	1.00	25.0	3.07	off	< 0.02 ^x	2.3	54.45
	53	V3 - 3	1.42	30.0	3.05	off	< 0.02 ^x	2.5	59.24
	54	V3 - 4	2.55	35.1	3.03	off	< 0.02 ^x	2.2	61.83
	55	V3 - 5a	3.08	29.1	3.06	off	< 0.02 ^x	2.3	60.29
	56	V3 - 5b	3.08	29.1	3.06	off	< 0.02 ^x	2.4	60.03
	57	V3 - 5c	3.08	29.1	3.06	off	< 0.02 ^x	2.4	59.08
	58	V3 - 6	3.88	24.6	3.08	off	< 0.02 ^x	2.4	51.36
	59	V3 - 7	4.16	20.0	3.09	off	< 0.02 ^x	2.3	46.14
	60	V3 - 8	4.53	15.0	3.12	off	< 0.02 ^x	2.3	43.73
	61	V3 - 9	4.83	10.0	3.12	off	< 0.02 ^x	2.3	42.96
	62	V3 - 10a	5.28	5.0	3.16	off	< 0.02 ^x	2.2	43.08
	63	V3 - 10b	5.28	5.0	3.16	off	< 0.02 ^x	2.2	42.04
	64	V3 - 10c	5.28	5.0	3.16	off	< 0.02 ^x	2.3	40.63

Appendix C-6. Cycle 6 (2/28/2015) Data Continued

	Sample No.	Sample Name	Elapsed time (hr)	Temp. ⁺ (°C)	pH ⁺	Light (on/off)	Fe ^{II} * (mg/L)	Fe(total)* (mg/L)	Se ^{IV} ** (µg/L)
Vessel 3	65	V3 - 11	6.00	10.2	3.13	off	< 0.02 ^x	2.4	38.62
	66	V3 - 12	6.45	15.1	3.08	off	< 0.02 ^x	2.4	37.21
	67	V3 - 13	6.65	20.2	3.06	off	< 0.02 ^x	2.4	37.89
	68	V3 - 14	6.85	25.0	3.05	off	< 0.02 ^x	2.4	23.87
	69	V3 - 15	7.18	30.0	3.05	off	< 0.02 ^x	2.4	35.64
	70	V3 - 16a	7.38	35.0	3.03	off	< 0.02 ^x	2.4	37.84
	71	V3 - 16b	7.38	35.0	3.03	off	< 0.02 ^x	2.3	37.27
	72	V3 - 16c	7.38	35.0	3.03	off	< 0.02 ^x	2.4	39.76
Vessel 4	73	V4 - 1a	0	18.1	3.36	off	< 0.02 ^x	0.35	57.20
	74	V4 - 1b	0	18.1	3.36	off	< 0.02 ^x	0.32	54.49
	75	V4 - 1c	0	18.1	3.36	off	< 0.02 ^x	0.33	59.77
	76	V4 - 2	1.00	25.0	3.33	off	< 0.02 ^x	0.33	35.67
	77	V4 - 3	1.50	30.0	3.29	off	< 0.02 ^x	0.30	36.62
	78	V4 - 4	1.57	35.8	3.30	off	< 0.02 ^x	0.22	35.92
	79	V4 - 5a	2.27	27.6	3.28	off	< 0.02 ^x	0.32	41.91
	80	V4 - 5b	2.27	27.6	3.28	off	< 0.02 ^x	0.32	38.66
	81	V4 - 5c	2.27	27.6	3.28	off	< 0.02 ^x	0.36	38.86
	82	V4 - 6	2.92	23.7	3.32	off	< 0.02 ^x	0.30	38.23
	83	V4 - 7	3.85	20.0	3.32	off	< 0.02 ^x	0.30	32.47
	84	V4 - 8	4.22	15.0	3.34	off	< 0.02 ^x	0.22	30.99
	85	V4 - 9	4.62	10.0	3.38	off	< 0.02 ^x	0.25	31.08
	86	V4 - 10a	5.22	6.1	3.43	off	< 0.02 ^x	0.22	30.45
	87	V4 - 10b	5.22	6.1	3.43	off	< 0.02 ^x	0.22	30.50
	88	V4 - 10c	5.22	6.1	3.43	off	< 0.02 ^x	0.23	30.69
	89	V4 - 11	5.82	10.4	3.37	off	< 0.02 ^x	0.20	26.87
	90	V4 - 12	6.02	15.1	3.36	off	< 0.02 ^x	0.22	48.13
	91	V4 - 13	6.42	20.1	3.36	off	< 0.02 ^x	0.20	47.75
	92	V4 - 14	6.64	25.4	3.32	off	< 0.02 ^x	0.20	45.91

Appendix C-6. Cycle 6 (2/28/2015) Data Continued

	Sample No.	Sample Name	Elapsed time (hr)	Temp. ⁺ (°C)	pH ⁺	Light (on/off)	Fe ^{II} * (mg/L)	Fe(total)* (mg/L)	Se ^{IV} ** (µg/L)
Vessel 4	93	V4 - 15	6.92	30.6	3.32	off	< 0.02 ^x	0.20	44.73
	94	V4 - 16a	7.05	35.1	3.32	off	< 0.02 ^x	0.19	45.47
	95	V4 - 16b	7.05	35.1	3.32	off	< 0.02 ^x	0.20	47.76
	96	V4 - 16c	7.05	35.1	3.32	off	< 0.02 ^x	0.20	47.05

⁺ Measured using DrDAQ PicoLog Recorder

* Samples analyzed using HACH DR2800 Spectrophotometer

** Samples analyzed using HG-ICP-OES

^x Sample below ferrozine MDL of 0.02 mg/L for Fe^{II} and Fe(total)

^{xx} Sample below HG-ICP-OES MDL of 5 µg/L for Se^{IV}

--- Sample not analyzed

Sample names including a,b,c are triplicate samples

Appendix C-7. Cycle 7 (4/26/2015) Data

	Sample No.	Sample Name	Elapsed time (hr)	Temp. ⁺ (°C)	pH ⁺	Light (on/off)	Light Intensity ⁺⁺ (Lux)	Se ^{IV**} (µg/L)
Vessel 1	1	V1 - 1a	0	24.1	2.83	on	118.4	338.6
	2	V1 - 1b	0	24.1	2.83	on	118.4	351.2
	3	V1 - 1c	0	24.1	2.83	on	118.4	351.1
	4	V1 - 2	0.50	29.9	2.83	on	118.4	350.6
	5	V1 - 3a	1.00	35.0	2.83	on	113.0	370.5
	6	V1 - 3b	1.00	35.0	2.83	on	113.0	376.5
	7	V1 - 3c	1.00	35.0	2.83	on	113.0	373.6
	8	V1 - 4	1.77	30.0	2.82	on	113.0	361.7
	9	V1 - 5a	2.25	25.0	2.82	on	113.0	363.9
	10	V1 - 5b	2.25	25.0	2.82	on	113.0	370.8
	11	V1 - 5c	2.25	25.0	2.82	on	113.0	355.5
	12	V1 - 6	2.63	20.0	2.83	on	113.0	358.4
	13	V1 - 7	3.21	15.0	2.83	on	107.7	357.3
	14	V1 - 8	3.91	10.0	2.84	on	107.7	349.3
	15	V1 - 9a	4.38	6.6	2.88	on	107.7	352.5
	16	V1 - 9b	4.38	6.6	2.88	on	107.7	337.2
	17	V1 - 9c	4.38	6.6	2.88	on	107.7	343.5
	18	V1 - 10	4.75	10.2	2.88	on	107.7	363.0
	19	V1 - 11	5.13	15.0	2.83	on	107.7	367.0
	20	V1 - 12	5.66	20.0	2.81	on	102.3	356.8
	21	V1 - 13a	6.09	25.0	2.81	on	102.3	374.0
	22	V1 - 13b	6.09	25.0	2.81	on	102.3	360.4
	23	V1 - 13c	6.09	25.0	2.81	on	102.3	361.9
	24	V1 - 14	6.64	30.0	2.80	on	102.3	374.6
	25	V1 - 15a	7.07	35.1	2.80	on	118.4	388.4
	26	V1 - 15b	7.07	35.1	2.80	on	50.6	375.2
	27	V1 - 15c	7.07	35.1	2.80	on	118.4	376.9
Vessel 2	28	V2 - 1a	0	24.1	2.86	on	118.4	351.0
	29	V2 - 1b	0	24.1	2.86	on	118.4	355.6
	30	V2 - 1c	0	24.1	2.86	on	118.4	358.7
	31	V2 - 2	0.50	30.0	2.86	on	118.4	365.4
	32	V2 - 3a	1.27	35.0	2.87	on	113.0	358.8

Appendix C-7. Cycle 7 (4/26/2015) Data Continued

	Sample No.	Sample Name	Elapsed time (hr)	Temp. ⁺ (°C)	pH ⁺	Light (on/off)	Light Intensity ⁺⁺ (Lux)	Se ^{IV**} (µg/L)
Vessel 2	33	V2 - 3b	1.27	35.0	2.87	on	113.0	362.1
	34	V2 - 3c	1.27	35.0	2.87	on	113.0	357.3
	35	V2 - 4	1.84	30.0	2.86	on	113.0	360.8
	36	V2 - 5a	2.26	25.1	2.87	on	113.0	368.3
	37	V2 - 5b	2.26	25.1	2.87	on	113.0	357.2
	38	V2 - 5c	2.26	25.1	2.87	on	113.0	362.3
	39	V2 - 6	2.76	20.0	2.87	on	113.0	361.7
	40	V2 - 7	3.28	15.0	2.86	on	107.7	349.1
	41	V2 - 8	3.98	10.0	2.87	on	107.7	344.4
	42	V2 - 9a	4.41	7.3	2.86	on	107.7	343.8
	43	V2 - 9b	4.41	7.3	2.86	on	107.7	346.6
	44	V2 - 9c	4.41	7.3	2.86	on	107.7	343.2
	45	V2 - 10	4.76	10.0	2.86	on	107.7	354.0
	46	V2 - 11	5.18	15.0	2.86	on	107.7	369.9
	47	V2 - 12	5.65	20.0	2.85	on	102.3	356.6
	48	V2 - 13a	6.10	25.0	2.86	on	102.3	370.1
	49	V2 - 13b	6.10	25.0	2.86	on	102.3	363.9
	50	V2 - 13c	6.10	25.0	2.86	on	102.3	365.7
	51	V2 - 14	6.72	30.0	2.86	on	102.3	365.6
	52	V2 - 15a	7.10	35.2	2.86	on	118.4	382.1
Vessel 3	53	V2 - 15b	7.10	35.2	2.86	on	50.6	377.2
	54	V2 - 15c	7.10	35.2	2.86	on	118.4	376.3
	55	V3 - 1a	0	24.3	2.87	on	118.4	364.2
	56	V3 - 1b	0	24.3	2.87	on	118.4	361.5
	57	V3 - 1c	0	24.3	2.87	on	118.4	368.0
	58	V3 - 2	0.50	30.5	2.86	on	118.4	361.1
	59	V3 - 3a	1.12	35.0	2.85	on	113.0	382.8
	60	V3 - 3b	1.12	35.0	2.85	on	113.0	386.4
	61	V3 - 3c	1.12	35.0	2.85	on	113.0	378.6
	62	V3 - 4	1.84	30.0	2.86	on	113.0	382.1
	63	V3 - 5a	2.26	25.1	2.86	on	113.0	371.8
	64	V3 - 5b	2.26	25.1	2.86	on	113.0	377.1

Appendix C-7. Cycle 7 (4/26/2015) Data Continued

	Sample No.	Sample Name	Elapsed time (hr)	Temp. ⁺ (°C)	pH ⁺	Light (on/off)	Light Intensity ⁺⁺ (Lux)	Se ^{IV**} (µg/L)
Vessel 3	65	V3 - 5c	2.26	25.1	2.86	on	113.0	386.1
	66	V3 - 6	2.73	20.0	2.86	on	113.0	364.1
	67	V3 - 7	3.26	15.0	2.87	on	107.7	357.1
	68	V3 - 8	3.96	10.0	2.90	on	107.7	364.2
	69	V3 - 9a	4.43	6.7	2.95	on	107.7	355.0
	70	V3 - 9b	4.43	6.7	2.95	on	107.7	352.7
	71	V3 - 9c	4.43	6.7	2.95	on	107.7	353.4
	72	V3 - 10	4.78	10.2	2.94	on	107.7	365.7
	73	V3 - 11	5.15	15.0	2.89	on	107.7	372.9
	74	V3 - 12	5.63	20.0	2.87	on	102.3	374.1
	75	V3 - 13a	6.08	25.0	2.87	on	102.3	376.8
	76	V3 - 13b	6.08	25.0	2.87	on	102.3	374.1
	77	V3 - 13c	6.08	25.0	2.87	on	102.3	368.4
	78	V3 - 14	6.66	30.0	2.87	on	102.3	374.7
	79	V3 - 15a	7.09	35.2	2.87	on	118.4	383.1
	80	V3 - 15b	7.09	35.2	2.87	on	50.6	389.8
	81	V3 - 15c	7.09	35.2	2.87	on	118.4	388.5
Vessel 4	82	V4 - 1a	0	24.1	2.79	on	118.4	378.5
	83	V4 - 1b	0	24.1	2.79	on	118.4	386.4
	84	V4 - 1c	0	24.1	2.79	on	118.4	374.9
	85	V4 - 2	0.50	30.0	2.79	on	118.4	381.0
	86	V4 - 3a	1.25	35.0	2.79	on	113.0	393.6
	87	V4 - 3b	1.25	35.0	2.79	on	113.0	---
	88	V4 - 3c	1.25	35.0	2.79	on	113.0	389.0
	89	V4 - 4	1.83	30.0	2.79	on	113.0	380.3
	90	V4 - 5a	2.26	25.0	2.79	on	113.0	383.4
	91	V4 - 5b	2.26	25.0	2.79	on	113.0	382.6
	92	V4 - 5c	2.26	25.0	2.79	on	113.0	396.0
	93	V4 - 6	2.69	20.0	2.80	on	113.0	387.3
	94	V4 - 7	3.26	15.0	2.84	on	107.7	375.5
	95	V4 - 8	3.98	10.0	2.87	on	107.7	380.6
	96	V4 - 9a	4.41	7.4	2.91	on	107.7	369.5

Appendix C-7. Cycle 7 (4/26/2015) Data Continued

	Sample No.	Sample Name	Elapsed time (hr)	Temp. ⁺ (°C)	pH ⁺	Light (on/off)	Light Intensity ⁺⁺ (Lux)	Se ^{IV**} (µg/L)
Vessel 4	97	V4 - 9b	4.41	7.4	2.91	on	107.7	363.9
	98	V4 - 9c	4.41	7.4	2.91	on	107.7	367.6
	99	V4 - 10	4.78	10.1	2.91	on	107.7	367.7
	100	V4 - 11	5.11	15.0	2.85	on	107.7	383.4
	101	V4 - 12	5.73	20.0	2.82	on	102.3	384.8
	102	V4 - 13a	6.08	25.0	2.80	on	102.3	382.4
	103	V4 - 13b	6.08	25.0	2.80	on	102.3	389.8
	104	V4 - 13c	6.08	25.0	2.80	on	102.3	385.9
	105	V4 - 14	6.66	30.0	2.79	on	102.3	390.3
	106	V4 - 15a	7.08	35.2	2.80	on	118.4	397.9
	107	V4 - 15b	7.08	35.2	2.80	on	50.6	412.5
	108	V4 - 15c	7.08	35.2	2.80	on	118.4	397.1

⁺ Measured using DrDAQ PicoLog Recorder

⁺⁺ Measured using HOBO Pendant Light/Temperature Loggers

^{**} Samples analyzed using HG-ICP-OES (MDL of 5 µg/L Se^{IV})

--- Sample not analyzed

Sample names including a,b,c are triplicate samples